Unsupported Small Metal Particles: Preparation, Reactivity, and Characterization

STEPHEN C. DAVIS and KENNETH J. KLABUNDE*

Department of Chemistry, Kansas State University, Manhattan, Kansas 66506

Contents

I. Introduction and Scope

The structure, properties, and methods of preparation of highly dispersed transition metals have been studied extensively for the past century and especially for the past 50 years in light of their role in catalysis. The catalytic usefulness of these types of materials has been exploited extensively by chemical engineers and chemists in petroleum and related fields. More recently (in the last 10 years), the unusual properties of very small metallic particles and their modes of formation and stabilization have attracted the attention of theoretical and experimental physicists. The interest in this area is accelerating rapidly. The unusual structural, magnetic, electrical, and chemical properties of very highly dispersed metals (compared with properties of bulk states) have brought cooperative work between physicists, chemists, engineers, and material scientists. Due

Stephen C. Davis was born in Fort Ord, CA, in 1953 and grew up in Virginia. He graduated Magna Cum Laude with a B.S. degree in Biology and Chemistry from the University of Tampa in 1975. During his undergraduate training, he developed a strong interest in catalysis chemistry. The opportunity to explore the application of the new field of metal atom chemistry toward heterogeneous catalysis brought him to Kenneth Klabunde's research group at the University of North Dakota. In 1979 he moved with Dr. Kabunde's research group to Kansas State University where he completed his graduate work for the University of North Dakota (Ph.D. 1980) and continued working for Dr. Klabunde doing postdoctoral research in matrix isolation chemistry of thermally unstable intermediates and transition-metal R–M–X compounds. His continued interest in heterogeneous catalysis brought him to his present position in catalysis research for Monsanto at Texas City, TX.

Kenneth J. Klabunde was born in Madison, WI, in 1943, and grew up in the Madison area and later Davenport, IA. He is married and has three children. Dr. Klabunde has always enjoyed chemical research in nontraditional areas, and thus was attracted to Donald Burton's fluorocarbon research group at the University of Iowa (Ph.D. 1969) and later to Phil Skell's carbon vapor research program at The Pennsylvania State University (Postdoctoral 1969–1970). He took a job at the University of North Dakota in 1970. There he established substantial research programs in "metal atom chemistry", studies of reactive intermediates on catalyst surfaces, and catalyst studies related to fuel technology. In 1979 he moved to Kansas State University as Chemistry Department Head and is continuing his research efforts. Recently he has become deeply involved in the enhancement of Industrial–Academic relations especially regarding cooperative research efforts.

to the different disciplines of science involved and rather poor communications between them, each field has developed its own methods for the characterization and use of small metal particles. Only very recently have these fields merged to a point where there is a realization of the complementary nature of the work by each discipline.

It is the goal of this review to make clear the important results obtained by the various scientific fields in the study of the preparations, properties, reactivities, and methods of characterization of very small metal particles as related to catalysis research. A description of the forms of highly dispersed metals for use in catalysis research will be presented along with their important structural features and examples of their use. Since the uniqueness of dispersed metals will be stressed, a section on massive metal catalysts will be presented for comparative purposes. In addition, the growth of small particles from single atoms will be considered, followed by discussions of the properties of the resultant clusters. Emphasis will be placed throughout on the unusual reactivities and catalytic abilities of small metal particles, especially with regard to reactions of simple hydrocarbons on metal surfaces. The forms of dispersed metals will be broken down into these general categories: (1) thin films, (2) small crystallites (supported, unsupported, and theoretical), (3) clusters ("naked", ligand stabilized, and theoretical). There will be many points of overlap of these categories, and comparisons between them will be frequent. And in order to limit the scope of the review somewhat, nickel will be primarily considered over other metals whenever possible. Also note that unsupported metal particles will be emphasized, and supported systems will only be discussed intermittantly. Thus, support effects will not be discussed.

II. Massive Metal Catalysts

Massive metals are characterized by having a well-ordered infinite lattice of metal atoms. The properties of massive metals are very different from those of highly dispersed metals, and the primary use of massive metals in catalysis research is as a model for determining the role of the metal type and the effect of surface cleanliness on catalytic activity. Surfaces of bulk metals can be scrupulously cleaned without causing drastic changes in the properties of the metal. Techniques are available to assess the cleanliness of the surface (LEED, AES, etc.). The advantage in the study of bulk metal surfaces lies in the control of variables, the most important of which are cleanliness and structural integrity. Various forms of bulk metals such as foils, wires, ribbons, pellets, etc. have been used as catalysts. The most important form, due to the control of variables, is the single crystal. Using single crystals, studies of catalytic reactions on specific crystallographic planes can be made. Controlled exposure of other crystallographic planes can be obtained as well as production of structures not present on "smooth" metal surfaces (i.e., steps, corners, terraces, kinks, etc.) by cutting these single crystals. The use of well crystallographically characterized single crystals has shed a great deal of light on the understanding of the catalytic abilities of metal atoms in various positions of a metallic lattice, and correlations with dispersed metal systems have been made. An example of this type of system is the selective dehy-

drogenation and hydrogenolysis of cyclohexane and cyclohexene on stepped platinum surfaces reported by Somorjai and Blakely.[1] These workers found atomic steps on the metal surface to be active sites for C–H and H–H bond breaking. Hydrogenolysis reactions increased but dehydrogenation reactions were unaffected by putting kinks in the steps. This work demonstrated the feasibility of etching a metal surface to control selectivity for a specific reaction type. Furthermore, an earlier study by Somorjai and co-workers showed that H–D exchange occurred readily on a single platinum crystal with a high Miller index [997] but not detectably on one with a low Miller index [111]. This difference in reactivity was ascribed to the large density of atomic steps present on the high-index surface.[2] The importance of low coordination metal atoms in such sites as edges and corners of crystallographic planes will be dealt with in some depth when electronic and catalytic properties of small metal crystallites are discussed later.

Another form of bulk metal used in catalysis research is that of thick films. These films, deposited on a wide variety of substrates (glasses, alkali halides, etc.), fall into the bulk metal category when the film has reached a film thickness of about 50 nm.[3] Thinner films have "islands" of isolated crystals which give rise to nonbulk properties.

The general methods of preparing metal films, thin or thick, are (a) thermal evaporation, (b) sputtering, and (c) chemical deposition. The first two categories are the most industrially important.[4] While continuous metal films exhibit properties very similar to those of massive metals, many differences can be present. The surface structure of evaporated films is very sensitive to the conditions of preparation, and these films may be rather porous, with densities varying from that of the bulk metal. This also affects the electrical resistivity which in turn is sensitive to adsorption of gases. The nature of the substrate and deposition conditions can greatly affect the crystallinity of evaporated metal films. Films can be grown epitaxially to the extreme of a single crystal film on some supports such as rock salt or polycrystalline with completely randomly oriented crystals (e.g., deposition on glass substrates). The most obvious property of thick films is the porosity which is evidenced by the ratio, R, of the actual surface area (as measured by gas adsorption techniques) to the geometric surface area. For a single metal crystal or massive metal R is unity, while for metal films values of R are greater than unity. This is due to the process by which films grow creating crystals, epitaxed or randomly oriented, which have small gaps between them. These gaps are small enough so that diffusion of reactants (for a catalytic reaction) into them is unimportant in the overall reaction kinetics. However, many types of crystal planes are exposed on the surface of polycrystalline films which should greatly affect catalytic properties.

Conditions employed for the deposition of metal films have a great influence on their topographical properties. In general, higher melting metals yield narrower crystals whereas thicker films have large crystal widths. Furthermore, higher substrate temperatures tend to cause a smoothing out of surface irregularities and larger crystal widths. An example of deposition parameter affects on the structure of thick films is given in Table

TABLE I. Nickel Film Catalysts Deposited on Glass at ~10^{-4} Pa[3]

specific film weight, $\mu g\ mm^{-2}$	substrate temperature during deposition, K	average crystal width, nm	R
0.65	273	46	7.9
0.65	273	~200	1.3

I. The gaps between crystals in films deposited at relatively low temperatures can be decreased in size or completely eliminated by annealing the film at elevated temperatures. For platinum, palladium, and nickel, R decreases toward unity up to ~470 K, above which little change occurs.[3] This reduction of gap size causes changes in electrical properties compared with those of bulk metal and ultimately leads to a featureless surface topography.

Epitaxy is an intensively studied phenomenon of film growth in which a metal is deposited on a substrate consisting of an exposed single crystal plane such as the [100] face of cleaved alkali halides. The influence of the substrate causes oriented growth of metal crystals. Thus, fccub metals grow with their crystals parallel to [100], [110], and [111] surfaces of NaCl, but on [001] mica cleavage planes they grow with a [111] plane parallel to the substrate forming a hexagonal arrangement of atoms.[5] It may be noted that the term epitaxy, meaning "arrangement on", was first introduced by Royer in 1928 and had been observed occurring naturally on minerals long before its use in oriented metal film growth.[6]

When epitaxed films were annealed at temperatures much higher than the deposition temperature, the crystal gaps were closed, which lead to an almost completely single, oriented crystal film. In order for epitaxed films to be useful in catalytic research large surface areas would be desirable. The use of metal deposition on single cleaved rock salt surfaces produces films of small surface area. So that larger surfaces could be obtained, a technique was developed by Anderson and Avery in which an evaporated layer of rock salt was used as the support.[7] This method is limited by the maximum substrate temperature which can be effectively used without causing problems of distorting the support surface which is ~520 K. In general, higher melting metals require higher substrate temperatures during deposition in order for epitaxy to be optimized. Due to this and the previously mentioned limitation, platinum could not be epitaxially grown in this manner, yet nickel could be grown epitaxially.

Metal films, oriented or not, have become useful in the study of surface reactions, but their correlations with structural and electronic properties of various catalytic metals have only become useful since the advent of tools necessary for characterization of the metal surfaces. The use of ultrahigh vacuum conditions was needed as well as surface structural and chemical composition determination methods. It is in fulfilling these needs that great technological improvements have been evolved. Pressures as low as 10^{-13} torr can now be achieved by using various pumping systems such as sputter-ion pumps, titanium sublimation pumps, turbo molecular pumps, titanium sublimation pumps, turbo molecular pumps, getter pumps, etc. Methods of

characterizing and cleaning film surfaces such as electron microscopy, low-energy electron diffraction (LEED), Auger electron spectroscopy, and ion sputter cleaning are available which allow very good control and knowledge of metal surface properties and changes in these properties upon chemisorption. Indeed, the use of films in catalysis research arose out of a need for unambiguously clean metal surfaces on which to study chemisorption. Chemisorption is one of the most fundamental steps in a catalytic reaction, and any kind of impurity present in a system designed to study this important process can only further (usually hopelessly) complicate an already complicated system and lead to uninterpretable results.

An example which illustrates the importance of the studies of massive metals and thick films discussed above is in order. Kishimoto studied the effect of annealing cold worked, bulk platinum, palladium, and nickel on the catalytic activity of formic acid decomposition.[8] He observed great changes in catalytic activity upon annealing the metals to temperatures at which dislocations (lattice misfits) disappeared (300–900 °C). The results were interpreted as showing that the presence of such dislocations at the surfaces of the catalysts plays a very important role in governing the activity.

Powders of bulk metals which are composed of very large particles (>1 μm) exhibit bulk properties and can be considered under the category of massive metal catalysts. These types of catalysts can be activated relative to the undivided bulk metal by various mechanical means. Schrader and co-workers studied the effect of mechanical activation of nickel (99.4% Ni) catalysts.[10] Methods of activation attempted were pressing, rolling, filing, disintegrating, milling, and attrition (grinding down by friction). Pressing, rolling, and filing had little effect on catalytic activity as measured by orthohydrogen–parahydrogen conversion. However, attrition increased the catalytic activity of the nickel.

The place of massive metals in basic catalysis research should be clarified in concluding this subsection. The fundamental interactions between molecules and the metal surface needs to be understood, and that is the purpose of studying clean metal surfaces. However, reactions of molecules on well-characterized, scrupulously clean metal surfaces at low pressures is far removed from the real world in which the catalyst must operate. This divergence is unavoidable and leads to a conflict between those who are concerned only with making their reaction proceed more economically and cannot wait for full (or even partial) understanding of the catalytic system and those who strive for an understanding of the catalyst. Venables classified these two groups as "technologists (Homo faber) and scientist (Homo sapiens?)".[9]

III. Basic Forms of Dispersed Metals

A. Thin Metal Films

As mentioned in the previous subsection, there are many different methods of depositing metals in the form of films on various substrates. At much lower deposition rates and times than those needed to produce the thick films, thin (actually ultrathin) films may

be formed. These films are characterized as being composed of very small isolated metal crystals (crystallites). These films are, therefore, discontinuous in contrast to the continuous thicker films that exhibit bulk properties. A great deal more catalytic work has been performed recently with ultrathin metal films than with the thick films. The reason for this is that when the film is thin enough (on the order of a monolayer of atoms) it can serve as a model for highly dispersed metal catalysts and yet retain the advantages of control of cleanliness and surface reproducibility. The main features of the ultrathin films are small crystallite sizes (several nm down to <0.5 nm) and high surface areas ($\sim$150 cm^2 to several m^2).[3,11] Due to conditions in which ultrathin films are usually prepared (evaporative or sputtering deposition) they have limited value. Films of all metals sinter (increase in crystallite sizes) to some extent when raised to some temperature above that at which they were deposited. Therefore, changes in the structures of films deposited at low temperatures will be unavoidable when they are to be used at the higher temperatures required for many catalytic reactions. The subject of sintering as well as initial particle growth of this type of highly dispersed metal will be treated in detail in the next section. Another limit to the advantages of ultrathin metal films is their inherent susceptibility toward contamination (poisoning). For example, mercury atoms (from manometers or Hg diffusion pumps) will irreversibly chemisorb to the surfaces of many metals, thereby displacing more weakly chemisorbed atoms or molecules such as hydrogen. Stopcock grease, CO, and sulfur compounds are other common poisons.

Methods of preparing ultrathin films commonly employed today are:[5] (1) thermal evaporation—(a) resistive heating, (b) flash evaporation, (c) arc evaporation, (d) exploding wire technique, (e) laser evaporation, (f) rf heating, (g) electron bombardment; (2) cathodic sputtering (positive ion bombardment); (3) chemical methods—(a) electrodeposition, (b) chemical vapor deposition (especially thermal decomposition). An excellent review of these methods is given by Chopra.[5] The best control and monitoring of deposition parameters are obtained by thermal evaporation and sputtering techniques. The literature of thin film use dates back as early as 1852 with the work of Bunsen and Grove. Interest in the uses of the optical properties of metal films and investigations into the nature of two-dimensional solids caused a great deal of effort to be put into the studies of these systems. This work was mainly the concern of mechanical engineers, physicists, and material scientists for nearly a century. The study of chemical interactions of gases with metallic films did not come about until 1935.[13]

The classical work of Beeck and co-workers in 1941 stimulated a fast growth in thin film catalysis research.[14] Beeck used a simple method for preparing the films. A thin metal wire was sealed in a glass tube, and impurities were desorbed by resistively heating the wire while pumping on the system. After degassing, film deposition onto the glass container walls was carried out by heating the wire to a temperature just below the metal melting point and condensing the vaporized metal atoms on the walls which were cooled to 0 °C. Beeck found the surface area to be proportional to the film

thickness, indicating a very porous framework with a large internal surface. Electrical conductivity was found to be about seven times less than that of the bulk metal.

Today, evaporated films are by far the most widely used forms of metal for fundamental catalysis research.

Instead of depositing a thin film by metal evaporation in vacuo, the evaporation can be carried out in the presence of a small residual pressure of an inert gas ($\sim$1 torr). This technique, gas evaporation technique (GET), has been used extensively by small particle physicists in order to obtain films with narrow crystallite size distributions, average sizes less than 10 nm, particles electrically insulated from one another, and large sample sizes (0.1–1.0 g).[15] There is evidence that the morphology of films can be altered by depositing them in the presence of low pressures of gases (10^{-5} torr) since they may chemisorb to the nucleating particles and change the rate of self-diffusion on the surface. At lower pressures (10^{-9} torr) changes would be expected to be insignificant since a film deposited in 100 s would contain a maximum of 0.1 of a monolayer. At high pressures (10^{-3} torr) of inert gas very noticeable changes in film structure occur.[16] Beeck and co-workers claimed to have obtained completely "oriented" films of nickel by evaporation in 1 torr of N$_2$ or Ar. These films, studied by electron diffraction, had the least dense plane [110] of nickel parallel to the glass substrate. Iron films deposited this way had their least dense plane [111] also parallel to the substrate. Pressures of inert gases of 0.5–2 torr produced the same orientation. However, pressures of 5 × 10^{-2} torr made the films less oriented, and under high vacuum (10^{-4}–10^5 torr) completely random orientation resulted. Furthermore, pressures over 2 torr resulted in less orientation until the orientation was completely random above 8 torr. Thus, film orientation is at a maximum using about 1-torr pressure.

The catalytic activities of the oriented and nonoriented films were measured by the rate of ethylene hydrogenation. The completely oriented films of nickel produced in 1 torr of N$_2$ had surface areas twice that of vacuum evaporated films but activities 10 times greater. This means a fivefold increase in activity for the oriented films over the nonoriented films. Since neither N$_2$ nor Ar was expected to adsorb significantly to the nickel, the orientation was postulated to be caused by a kinetic effect such as dissipation of condensation energy at the surface. The results could be attributed to a change in the energy distribution of the metal atoms before they reached the substrate surface, creating a preferred lattice formation upon condensation. The catalytic activity differences could not be accounted for since it was not known whether the adsorption process, reaction, or vaporization of product was reponsible for the observed enhancement of rate for oriented films.

In contrast, Logan and Kemball reported no evidence of orientation in nickel films produced by evaporation in the presence of 1 torr of nitrogen.[17] Their test for catalytic activity was the exchange reaction between NH$_3$ and D$_2$ at 50 °C. Three films evaporated in the presence of nitrogen had the same activity as normal vacuum deposited films. These films were of lighter weight than those of Beeck's, and in fact a fourth, heavier film, deposited in the same manner did have

twice the activity of the normal films, but no evidence of preferred orientation was found. These workers looked for orientation by use of X-ray diffraction, and it is likely that Beeck's interpretations of the electron diffraction patterns were incorrect.[16] The microstructures of these GET films are not clear, and much work is currently being carried out in this regard that will be treated in the following sections on particle growth. Films prepared by the GET are very porous as noted by many workers and originally by Beeck. He observed that the catalytic activity per unit weight of film was constant for various film weights, implying that the reacting gases (ethylene and hydrogen) must have had easy access to the interior of the film.

More recent GET studies have shown that metal evaporation at pressures greater than 1 torr result in gas-phase nucleation of the metal atoms, causing a precipitate in the form of a visible smoke to be deposited on the substrate. The deposits are in the form of a sponge of crystals.[16] Smoke was even observed as early as 1930 by Pfund when Bi was evaporated from a W wire in the presence of about 0.25 torr of air.[18] This smoke was in the form of a black Bi "soot" which he observed could be used to coat delicate surfaces for the formation of thermopiles used in the generation of thermoelectric currents.

B. Metal Powders, Blacks, and Colloids

Metal powders used as catalysts are most commonly prepared by hydrogen reduction of metal oxide powders.[3] The oxide power is usually prepared by precipitation of the metal as a hydroxide, carbonate, or basic carbonate. Thermal decomposition of nitrate, oxalate, or other salts of the metal can also be used to produce the metal oxide. Lower processing temperatures result in better metal dispersion than higher temperature treatments. This point is very important since a minimum particle size is desired in order to achieve a maximum metal surface area per unit weight of metal. Commonly, rather large particle sizes (micrometer range) and low surface areas (0.1-1.0 m^2 g^{-1}) of the metal powders result. Decomposition of iron, cobalt, and nickel carbonyls can be used to prepare metal powders with particle sizes in the micrometer range. There are, however, many methods available which enable better dispersions. It is very difficult to compare the dispersions obtained by the many varied preparative conditions used in the literature. Various methods found in the literature in which either surface areas or crystallite diameters of the resultant metals have been measured are given in Table II. Other methods of preparing nickel catalysts are included in Table II for comparison. The Urishibara and Raney nickels are skeletal metal catalysts and are discussed later. As can be seen, drastic differences in surface areas and crystallite diameters have been achieved not only by use of different methods but also with very similar methods. For example, Ru particles prepared by reduction of RuCl$_3$·3H$_2$O in aqueous NaBH$_4$ resulted in powder with a surface area of 26.4 m^2 g^{-1}; however, reduction of the same salt in aqueous formaldehyde resulted in surface areas of 4 and 33 m^2 g^{-1} by two different groups.[19-21] It is very important for catalysis researchers to characterize their catalysts as fully as possible since there are so many variables that can affect the nature of the final

TABLE II.   Effects of Preparative Methods on Dispersions of Metal Powders

A. Reduction Precipitation of Metal Salts in Aqueous Medium Followed by H$_2$ Reduction of Precipitate

metal	salt	reducing agent	H$_2$ redn. temp, °C	surface area, (m^2 g^{-1})	ref
Pd	(NH$_3$)$_2$-PdCl$_4$	NaBH$_4$	300	12.8	19
Pt	H$_2$PtCl$_6$·6H$_2$O	NaBH$_4$	300	3.7	19
Rh	RhCl$_3$	NaBH$_4$	300	30.5	19
Ru	RuCl$_3$·3H$_2$O	NaBH$_4$	300	26.4	19
Ru	RuCl$_3$·3H$_2$O	HCHO^a (in KOH soln)	200	4.0	20
Ru	RuCl$_3$·3H$_2$O	HCHO^a (in KOH soln)	200	33	21
Ir	IrCl$_4$	HCHO^a (in KOH soln)	200	11	21
Rh	RhCl$_3$	HCHO^a (in KOH soln)	200	7	21

B. Adam's Preparation:[24] Metal Halide Fused with Sodium Metal Nitrate Followed by H$_2$O Leaching and Then H$_2$ Reduction of the Metal Oxide

metal	salt	fusion temp, °C	H$_2$ redn temp, °C	ref
Pt	PtCl$_4$	500	200	23
Rh	RhCl$_3$	500	200	23
Ir	IrCl$_4$	500	200	23
Ru	RuCl$_3$	500	200	23

C. Thermal Decomposition of Nickel Salts Followed by H$_2$ Reduction Metal Oxide

salt	decompn temp, °C	H$_2$ redn temp, °C	surf area, m^2 g^{-1}	crystallite size, Å	ref
Ni(OH)$_2$	300	200		100-140	25
Ni(OH)$_2$	350	260-400	7.0	130	26
NiCO$_3$·Ni(OH)$_2$	300	200		130	25
NiCO$_3$·Ni(OH)$_2$	400	350	0.82		27
Ni(NO$_3$)$_2$·6H$_2$O	300	200		240	25
NiC$_2$O$_4$	300	200		230	25
NiCO$_3$·Ni(OH)$_2$^{b}	300	200		42	25

D. Thermal Decomposition of Ni(CO)$_4$

decompn temp, °C	surf area, m^2 g^{-1}	crystallite size, Å	ref
260	0.15	<1000	28
320	0.24	<1000	28
325	0.30	<1000	28
330	0.38	<1000	28
300		~600	29

E. Miscellaneous Preparations

catalyst	crystallite size, Å	ref
Urushibara^c		
U-Ni-A	37-41	29
U-Ni-B	66-88	29
Raney nickel	43	29
Raney nickel	25-150	30
Ni Vacuum Evaporation^d	30	31

^{a} Willstatter method.[22] ^{b} 5 at. % Al additive. ^{c} See text and Table V. ^{d} Particles collected in bis(diphenylphosphino)butane.

catalysts. The nucleation and growth of metal particles seem to be very sensitive to the preparative conditions. One example is a study performed in 1958 in which

TABLE III. Crystal Packing in Particles Produced by Thermal Decomposition of Organic Salts of Cobalt[32]

salt	% fccub	surface area, $m^2 g^{-1}$
formate	80	4
acetate	30	8
propionate	20	13
butanoate	15	24
pentanoate	50	6

TABLE IV. Variations of Surface Areas and Crystallite Sizes of Five Pd Blacks[33]

sample	A	B	C	D	E
surface area, $m^2 g^{-1}$	68	36	31	7.2	3.5
crystallite size, Å	70	140	160	690	1410

X-ray studies were used to show that Co can crystallize into a fccub close-packed form to a limited extent upon thermal decomposition of various organic salts in vacuo.[32] Table III illustrates the effect of the starting salt on the nature of the metal powder. Above 420 °C Co normally undergoes a change from cph to fccub packing. It appears that the change is rather slow so that fccub packing can exist metastably at lower temperatures.

Metallic sponges are forms of metals, usually referred to as "blacks", which are produced by the Willstätter method of metal salt reduction by formaldehyde under alkaline conditions.[11] The term "sponge" refers to the network of particle aggregates as seen under an electron microscope. Electron micrographs of palladium blacks are shown in a paper by Sermon.[33] Again, the conditions of preparation greatly affect the degree of aggregation. Table IV shows the wide variations in particle sizes and surface areas obtained for five different Pd black samples.

Colloidal metals are fine dispersions of metal particles with diameters in the range 10^3–10^4 Å that can be held in a colloidal suspension by addition of a stabilizer.[3] The colloids are usually formed in an aqueous medium, and a stabilizer is added such that a hydrophilic colloid is formed which is stable at concentrations up to 50 wt %. A typical stabilizer used is poly(vinyl alcohol) which adsorbs onto the surface of the metal particles. Colloids are generally very easily coagulated if the stabilizer is not present and difficult to separate from a reaction mixture when the stabilizer is present. There are three general methods used to prepare metal colloidal suspensions.[3] The first is the Bredig technique which involves striking an arc between two metal wires under a very dilute solution of sodium hydroxide.[11] The second method utilizes controlled reductive precipitation of metal salts to yield particles of colloidal dimensions. The third method uses metal hydroxide particles of colloidal dimensions which are precipitated and then reduced, the colloidal suspension being generated by addition of a stabilizer. Without stabilizers, as in metal blacks preparations, even particles with very small sizes (<100 Å average) will form aggregates above colloidal size and precipitate out of solution.

As mentioned previously there are many methods found in the literature for preparing active unsupported metals for use as catalysts. In addition to those methods already described, Table V shows variations which have appeared in the literature from 1947 to 1977 for preparation of active nickel suitable for gas or liquid phase hydrogenation reactions along with examples of

their uses. The Urushibara catalysts will be considered as skeletal metals along with Raney nickel in the next section. Most of the catalysts prepared by methods shown in Table V have not been structurally characterized and may contain many inorganic impurities. For example, Brown's P-2 nickel (part IA4 of Table V) is believed to contain Ni_2B (B = boron) as the active species. The degree of reduction obtained by H_2 treatment of metal salts as shown in Table V (part IC) were not indicated in most cases. Table V is, therefore, to be considered only as an indication of the many synthetic parameters which have been varied to produce useful catalysts.

C. Stabilized Porous and Skeletal Metals

Stabilized porous metals contain a minor component which serves as a structural promotor to prevent agglomeration of the metal particles. Iron, cobalt, and nickel are the primary metals used in this form. They are prepared by various methods, the most common of which for cobalt and nickel is coprecipitation.[3] In this method hydroxides of the metals and of the stabilizer (Mg, Th, etc.) are simultaneously precipitated from aqueous solution. The precipitate is then washed, filtered, dried, and reduced by hydrogen. Often a chemical promotor, such as a water-soluble potassium salt, which serves to alter the surface electronic properties of the metal, is added by impregnation prior to H_2 reduction. Addition of structural promotors allows production of catalysts with high surface areas which are much more thermally stable toward sintering. The amount of structural promotor added can vary so that there is no distinct separation between supported catalysts and structurally promoted catalysts. In fact, stabilized, porous metals are often placed on a support (such as kieselguhr) to improve reactant accessibility. Many variations in amounts and types of stabilizers have been used, but the understanding of these systems is at such a level that the variations are mainly empirical. An example of a stabilized porous metal is a typical Fischer–Tropsch catalyst with proportions of $Co:ThO_2:MgO:kieselguhr$ of about 100:5:10:200.[11] Such catalysts generally have surface areas of 50–80 $m^2 g^{-1}$.[3]

Skeletal metals are prepared by leaching out a nontransition-metal component from an alloy or precipitate. In the former case Raney metals are obtained by leaching aluminum from Ni–Al, Co–Al, or Fe–Al alloys with aqueous base, such as NaOH. Urishibara catalysts are prepared by precipitation of metal halides with zinc or aluminum followed by digestion of the Zn or Al with acid or alkali (cf. Tables II and V).

There is an extensive literature on uses and preparation variations of Raney nickel that has accumulated since its discovery in 1925.[3] Only recently, however, have structural and compositional characterizations of Raney nickel been made.[69–72] Raney nickel has been studied by N_2 adsorption surface are measurements, magnetic measurements, X-ray diffraction, small-angle X-ray scattering, and electron microscopy.

Before the structure and composition of Raney nickel are described, a brief summary of this preparation is in order. A Raney nickel alloy (Ni–Al) is added to a sodium hydroxide aqueous solution to digest the aluminum component. After digestion and washing by decanting, the sludge is placed in a washing tube in

TABLE V. Methods of Preparing Active Ni Catalysts (Unsupported) Suitable for Hydrogenation Reactions: General Survey 1947-1977

method of preparation	typical compounds used for hydrogenation (when cited in ref)	ref
I. reduction of Ni salts		
A. reduction by BH_4^-		
1, $NiCl_2 \cdot 6H_2O$ in DMF	unsaturated hydrocarbons under mild conditions	34
2, $NiCl_2 \cdot 6H_2O$ in H_2O or EtOH	olefins	35-37
3, $Ni(OAc)_2$ in H_2O	olefins in general	38
4, $Ni(OAc)_2$ in EtOH	olefins (high selectivity) unsaturated aldehydes (e.g., benzaldehyde → furfuryl alcohol)	
B. treatment of Ni salt with $BaSi_2O_5$ or $Na_2Si_2O_5$ followed by reduction of product with H_2 at 520 °C		41
C. reduction with H_2		
1, $Ni(HCO_2)_2$, 240-350 °C	benzene	42-44
2, Ni oxalate, 282 °C	benzene	45
3, $Ni(OAc)_2$		46
4, $NiCO_3$, cooled in CO_2 current	olefins (below room temp)	47
5, NiO, 240 °C	1,3-butadiene	48
310 °C	1,3-butadiene → 1-butene (major product)	49
	benzene	44
6, $NiO-Ni_2O_3 \geqslant 400$ °C	1,3-butadiene → trans-2-butene (major product)	49
7, $Ni(OH)_2$	benzene	44
D. reduction with alkali metal and Lewis base		
1, Ni(II), alkali metal in naphthalene-THF	cyclohexene	50
2, $Ni(NH_3)_6(NO_3)_2$, Ca in liq NH_3	benzene	51
3, $NiBr_2$, alkali metal in liq NH_3		52
E. addition of Ni salt to a support (e.g. silica gel) followed by reduction of Ni ions and removal of support		53
F. miscellaneous recutions		
1, $(acac)_2Ni$ reduced with $LiAlH_4$[b]	benzene, toluene	54
2, $(acac)_2Ni$ reduced with $(i\text{-}Bu)_3Al$ in heptane	cyclohexene	55
3, Urushibara type (activation of pptd Ni formed by $NiCl_2$ precipitation with Zn dust)		
method of activation type		
acid digested[a] (U-Ni-A)	cyclohexene, cyclopentene	56
base digested[a] (U-Ni-B)	cyclooctene	56
neutral digestion with alcohol refluxing[a] (U-Ni-N)	1-octene	56, 57
II. thermal decomposition of Ni co compounds (Ni may be powder or supported)		
A. $Ni(HCO_2)_2$, Ph_2O-biphenyl	dinitrotoluene	58
B. $Ni(HCO_2)_2$ CO_2 (gas		59
C. $Ni(HCO_2)_2$	benzene, toluene	60, 61
D. $Ni(HCO_2)_2$ inert gas 180-300 °C		62
E. Ni^{ll} oxalate (partial decomposition)	benzene	63, 64
F. Ni amalgam		65
III. atomization-decomposition		
A. particles activated with NaOCl + dilute HCl followed by H_2 reduction at 350 °		66
B. Ni vacuum depostied and powder collected in bis(diphenylphosphino)butane		67
C. Ni vacuum deposited at low temperature with hydrocarbons followed by warming		75
IV. Treatment of $Ni(CO)_4$ with nearly saturated solution of $Al(NO_3)_3$ containing 10% AcOH followed by digestion and reduction in H_2 at 450°		68

[a] Method of activation (type). [b] acac, acetylacetonato.

TABLE VI. Typical Chemical Compositions (%) of Raney Nickel Catalysts

Ni	Al	Al$_2$O$_3$	NiO	ref
95.4 ± 0.2	3.5 ± 0.1	0.03 ± 0.01	0.5 ± 0.1	71
75-80	10	5		72
92-93	3.6-4.1	0.1		72
77.9-90.4	0-5	3.1-5.9		72

TABLE VII. Effects of Heat Treatments on Nickel Crystallite Size of Raney Nickel Catalysts

treatment temp, °C	average diameter of crystallites, Å	method	ref
25	93	magnetic	71
112	112	magnetic	71
176	125	magnetic	71
350	140	magnetic	71
600	150	magnetic	71
25	36	X-ray	72
310	40	X-ray	72
400	57	X-ray	72
25	52	X-ray	72
130	57	X-ray	72
25	50	X-ray	72
130	61	X-ray	72
300	75	X-ray	72
490	104	X-ray	72

which the suspended catalyst is flushed with copious amounts of water under a hydrogen atmosphere. The catalyst is then washed with 95% ethanol and finally absolute ethanol and stored in the latter. The hydrogen atmosphere is present to maintain the reduced state of the catalyst. During digestion there is a constant evolution of hydrogen from the reaction

$$2Al + 20H^- + 6H_2O \rightarrow 2[Al(OH)_4]^- + 3H_2\uparrow$$
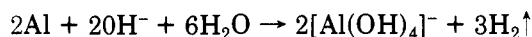
which causes a self-reduction of the catalyst. Raney nickel alloys in the 40-50 wt % nickel range, as normally used, have been shown not to be homogeneous but to contain several phases.[69] The main phases present are β(NiAl$_3$), γ(Ni$_2$Al$_3$), and a lesser amount of a eutectic containing about 5 wt % nickel. Alloys with higher nickel content contain significant amounts of NiAl which is unreactive toward alkali. Alloys containing lesser amounts (<40 wt %) of nickel yield less catalyst so the 40-50 wt % nickel range is considered optimal.

After digestion and washing, the final catalyst so produced is not pure nickel, as Table VI illustrates. All of the aluminum could not be removed even by leaching with boiling 6N NaOH.[71] One study, in which NiO content was determined, showed that the nickel is well reduced in the preparation of Raney nickel.[71]

The "impurities" in Raney nickel, especially aluminum oxide (in the form of bayerite), do not have an adverse effect on its catalytic usefulness. The aluminum oxide serves as a structural promoter to make the catalyst resistant to sintering. Table VII shows results of nickel crystallite size determinations by X-ray diffraction and magnetic methods for various heat-treated Raney nickel samples. As can be seen in Table VII, initial crystallite size is dependent upon preparative details, and all samples were very resistant to sintering. Scanning electron micrographs were very resistant to sintering. Scanning electron micrographs have shown that crystallites of bayerite occur over much of the

nickel surfaces, and this is the reason for the thermal stabilities of the catalysts.[3] Furthermore, it has been shown that samples containing as little as 1 wt % aluminum oxide underwent a reduction in surface area of only a factor of two upon heating to 750 K. A sample with 20 wt % aluminum oxide content underwent only a 20% reduction in surface area upon heating to 770 K. It seems remarkable that only 1 wt % of this structural promotor can significantly maintain the particle size and surface area integrity.

The skeletal nature of Raney nickel becomes apparent upon observation under an electron microscope. The catalysts appear as a sponge with grains of sizes larger than 1000 Å which consist of collections of crystallites ranging in size from 25 to 150 Å.[71] Average pore radius is about 35 Å, with smaller pores of 7-8 Å in radius also present. The nickel is fccub-packed crystallites with an appreciable amount of defects. The concentration of lattice defects decreases with increasing treatment temperature.

A final feature of Raney nickel is an evolution of varying amounts of hydrogen which occurs upon heating the "dry" catalyst. Much more H$_2$ is released than can be accounted for by adsorption or solution in the metal phases as sources. It is believed that the major source of the hydrogen is from a reaction between residual metallic aluminum and water bound in the bayerite.[3]

Another type of catalyst which can be considered as a skeletal metal is the Urushibara catalyst, discovered by Urushibara in 1951.[29] There are several types of Urushibara catalysts, such as U–Ni–A and U–Ni–B, which differ in their preparative details. The catalysts are prepared in two steps: (1) precipitation of nickel metal from solutions of nickel salts (e.g., NiCl$_2$) by more electropositive metals (e.g., Zn or Al) and (2) digestion of the Zn or Al with acid or alkali. The catalysts are very active and easy to prepare, making them competitive with Raney nickel catalysts. In fact, it was a property of Raney nickel, the release of nascent hydrogen during its preparation, that led Urushibara to the discovery of his catalyst. Urushibara thought that a common metal powder, not as active as Raney nickel, could be used to reduce estrone to estradiol if combined with nascent hydrogen.

$$\text{estrone} \xrightarrow{2H} 17\beta\text{-estradiol} \qquad (1)$$
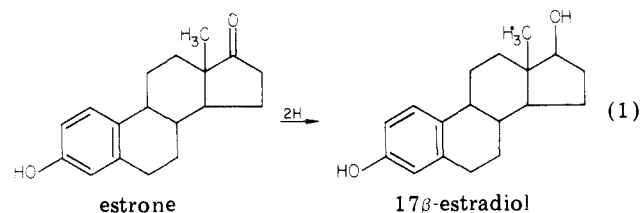
He obtained "precipitated nickel" by adding zinc dust to a solution of nickel chloride. This precipitated nickel was then added to an alkaline solution of estrone, and aluminum powder was added to reduce the estrone with the nascent hydrogen generated and the nickel as a catalyst. This method worked very well. Urishibara next tried the same procedure but without adding aluminum granules. Instead H$_2$ was bubbled through the solution. This method also worked well. However, without the alkalis the reduction failed. This was later shown to be due to large amounts of zinc hydroxide chloride produced during the precipitation process

which is insoluble in water but soluble in alkali and acid. The leaching process by base or acid removes all of the Zn(OH)Cl and produces a highly active catalyst.[29]

X-ray diffraction studies have revealed that inactive U–Ni–B (prepared by digestion with base) contains no Zn(OH)Cl but does contain substantial amounts of zinc and zinc oxide.[29] Table II shows nickel crystallite sizes obtained in Urushibara catalysts. The similarities between Urushibara and Raney catalysts seem obvious. Both catalysts contain structural promotors and have a spongelike appearance. However, there are significant differences between the two. In Raney nickel preparation, nickel crystallization or particle growth occurs when the aluminum component of the Ni–Al alloy is dissolved by alkali. In contrast, nucleation and particle growth of nickel occur on the surface of zinc or aluminum grains during the precipitation step in Urishibara catalyst preparations. Thus, the nickel particles are already formed before the zinc or aluminum is leached. In the preparation of Urushibara catalysts, the catalyst activity is a function of the conditions under which the precipitated metal is prepared. Conditions for the digestion step have little effect upon activity of the catalysts.

It has been suggested that nucleation and growth of nickel on the surfaces of zinc grains may occur epitaxially (discussed later) to force the nickel to crystallize in a cph structure.[29] This epitaxy would be expected to be accompanied by a large amount of lattice defects which could be sites of catalytic activity.

Abbreviations used for different Urushibara catalysts should be noted. U–Ni–A means a preparation involving zinc as a reducing agent and acid digestion (acetic acid) of the precipitated nickel. U–Ni–B is prepared by digestion with base. U–Ni–CA and U–Ni–CB preparations involve low temperature precipitation followed by acid and base leaching, respectively. U–Ni–AA and U–Ni–BA are similar to U–Ni–A and U–Ni–B except aluminum is used as the reducing agent.

D. Pseudoorganometallic Powders

Recently a new form of skeletal metal was reported, which was obtainable due to the surprising reaction of small "naked" Ni clusters with alkanes.[73,74] When Ni atoms (vapor) were codeposited with pentane vapor at –196 °C (77 K), a black matrix resulted. The color of the frozen matrix was undoubtedly due to the presence of Ni clusters formed by Ni atom migration. Upon warming to –130 °C (pentane melting point) a slurry of tiny Ni clusters/particles in pentane was formed. When this mixture was aged for 2 h, the Ni particles reacted extensively with the pentane (at –130 °C). The pentane was cleaved mainly into C_1 species (proposed to be C, CH, CH_2, and CH_3, not carbides) which remained bound to the Ni particle surfaces. Thus, a $N_xC_yH_z$ "pseudoorganometallic" powder formed which was quite thermally stable (>200 °C) and released CH_4 and other fragments of the pentane upon treatment with H_2O or H_2.[73,74]

This remarkable activity of naked Ni particles for alkane cleavage at –130 °C was shown to be general for a variety of alkanes. Stable $N_xC_yH_z$ formulations were those where the ratios of Ni:C:H were approximately (2–5):1:2. The carbonaceous species attached to the Ni surfaces were mainly C_1 species, although large alkane

SCHEME I
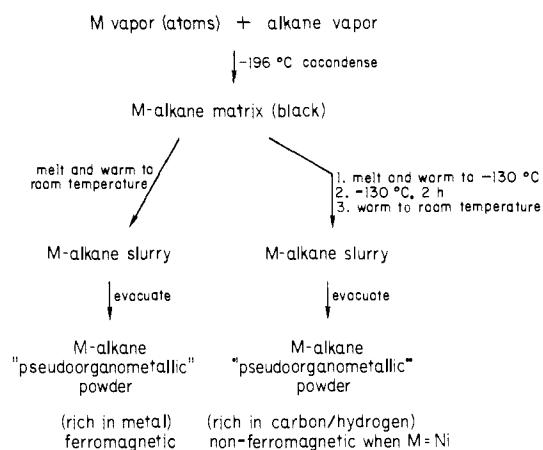
fragments were also present along with CO_2, which was formed by C_1 species scavenging oxygen.

These pseudoorganometallic powders proved to be extremely active catalysts in a variety of hydrogenation schemes.[75] Furthermore, the concept of "clustering of metal atoms in organic media" has led to the production of a range of active/selective catalysts, supported and unsupported, in hydrogenation, hydrogenolysis, dehydrogenation, and methanation.[76] In addition, these powders have exhibited unusual magnetic properties, and for example, Ni powders could be prepared as stable nonferromagnetic or ferromagnetic materials at will, depending on experimental conditions.[73,74,77] The magnetic behavior was apparently not due to crystallite size or long range ordering of the Ni atoms but instead was due to the thickness of carbonaceous layers on the crystallites (which were always <35 Å).[74,77] Thick layers (powders rich in C, H) prevented coupling between crystallites, thereby precluding ferromagnetism.[77]

The metals Fe, Co, and Ni behaved similarly (see Scheme I).

Three significant conclusions resulted from these studies: (1) "naked" metal clusters have extremely high activity with alkanes as evidenced by extensive reaction taking place at –130 °C, (2) there is a competition set up in an alkane matrix between metal atom/cluster recombination vs. alkane reaction, and (3) at least for the group 8 metals, clusters are apparently more active with alkanes than atoms are.

These topics will be touched upon again in later discussions. In the present context the most important point is that by the clustering of metal atoms in organic media, a new type of active skeletal metals are now available, which are actually pseudoorganometallic materials.

IV. Nucleation and Growth of Small Metal Particles

This section will deal in more detail with the initial aggregation of metal atoms to form embryonic clusters which serve as nucleation or condensation centers in the earliest stages of metal particle formation or film growth. Theoretical as well as experimental studies of the modes of formation, geometry, and stabilization of very small particles will be discussed. The growth of the small particles up to an "equilibration" point at which they remain until thermally or chemically disturbed will also be included. Finally, the process of

sintering, which is a reinduced growth of the "equilibrated" metal particles, will be considered. The terms cluster, particle, crystal, and crystallite will be rather arbitrarily used. In general, the term "crystal" will be used when the order of an array of metal atoms, even though finite on an atomic scale, is to be emphasized. "Crystallite" is technically to be considered as a small crystal, but the two terms may be interchanged without losing significance. "Clusters" generally refer to the smallest particles which will be described by geometric shapes rather than crystallographic lattice and long range order. The term "particle" will be used very arbitrarily such that a small particle may be a cluster and a large particle may be a crystallite. The meaning of these terms will be clear by context.

Most studies on nucleation have involved the use of evaporated metal films. Growth and sintering studies have been concerned with films, supported metal catalysts, and to a much lesser extent metal powders and other forms of dispersed metals mentioned previously. The depth into which these topics will be discussed depends upon the interest of the scientific community as reflected in the literature. It should be pointed out that a great amount of work in this area has dealt with clean films because of their relative ease of study and control of variables. Also, much work has been done with supported metal catalysts due to their industrial importance.

A. Formation and Growth of Thin Metal Films

In the early studies of film deposition, when modern tools such as electron microscopy and diffraction were not available, it was tacitly assumed that film growth occurred by simply coating the substrate surface with a continuous layer of atoms. It is now known that thin evaporated films are discontinuous consisting of "islands" of metal particles. The formation and growth of these islands have been studied intensively. Discrete stages are recognized which characterize film formation. These are (a) nucleation and growth, (b) coalescence, and (c) the filling-in stage. The earliest stages of nucleation and growth are the most difficult to study due to the small size of the clusters or particles present. Reproducible data on this stage of growth were obtained only after the advent of ultrahigh vacuum (UHV) conditions ($<10^{-10}$ torr) in the 1950s. Later growth stages depend very sensitively upon the initial stage so it is very important to have a well-characterized and very clean substrate surface on which to commence deposition. The use of LEED and Auger electron spectroscopy attached to the UHV systems can be used to check for contamination *before* deposition. In order to fully understand and predict the initial nucleation and growth process, physicists would like to perform the film deposition on a perfectly flat, clean surface. If this could be achieved, the use of statistical homogeneous nucleation theories could be directly applied. However, ideality seems to rarely be the case. Low energy electron bombardment of the substrate surface for structural characterization can induce severe defects which may act as sites of preferred nucleation so that the statistical nucleation would not be detected.[78] Experimental problems such as this make film nucleation and growth investigations very challenging and necessitates much tedious work.

1. Condensation and Nucleation

a. **Theory.** Chopra gives an excellent review of the birth of discontinuous films which will be summarized in a concise form.[5]

Consider metal atoms in the vapor state striking normal to the surface of a substrate. An individual atom, upon hitting the surface, rapidly loses kinetic and thermal energy. The loss of kinetic energy is a result of an inelastic collision of the atom with the surface. It loses most of its kinetic energy normal to the surface but may have some kinetic energy parallel to the surface. Depending upon how "hot" the impinging atom and how effective the substrate is toward dissipating the heat of the atom, it loses a certain amount of thermal energy. The efficiency of the substrate to thermally stabilize an atom striking its surface is influenced by the heat of desorption Q_{des}. This is the energy that a thermally equilibrated atom on the surface must acquire in order to escape to the vapor phase. The degree of thermal equilibration actually achieved is also dependent on many other parameters as well. A measure of this equilibration efficiency is given by the accommodations coefficient, α_T, as

$$\alpha_T = \frac{T_I - T_R}{T_I - T_S} = \frac{E_I - E_R}{E_i - E_S}$$

where T_I, T_S, and T_R are the temperatures of the incident atoms, the substrate, and the desorbed atoms, respectively, and E refers to their kinetic energies. Since Q_{des} depends upon the interaction between an impinged atom and the surface, its value is very sensitive toward the condition of the surface such as cleanliness. If Q_{des} is much greater than kT, where T is the temperature of an incident atom, an atom rapidly becomes thermally equilibrated and its mean stay time on the surface, before being desorbed, is long. During its stay time on the surface an atom is considered to be adsorbed and is called an "adatom". If $Q_{des} \sim RT$, thermal equilibration is approached slowly and an adatom remains "hot". This "hot" atom has a very short stay time. The thermally equilibrated atom spends its stay time diffusing about on the substrate surface. The distances $\bar{X}$ that an equilibrated adatom diffuses over the surface are given by the Einstein relation for Brownian movement:

$$\bar{X} = \sqrt{2a} \, \exp \frac{Q_{des} - Q_d}{2kT}$$

where a is the distance between adsorption sites on the surface and Q_d is the activation energy for a surface diffusion jump. This theory assumes that the adatom migrates in the form of jumps between potential energy wells on the surface. Q_d is therefore another parameter which is sensitive to the surface condition. If there are other adatoms within $\bar{X}$ of a given adatom, two of these may form a pair which may or may not be stable depending mainly upon the substrate temperature. The pairing of two adatoms marks the beginning of the nucleation process. Nucleation theories can now be used to evaluate the clustering or nucleation of adatoms. Two nucleation theories, yielding the same qualitative results, will be used. The first is the *capillarity* theory which shows the relationship between the size of a spherical cluster and its total free energy. The total free energy, ΔG_O, needed to form a spherical cluster of ra-
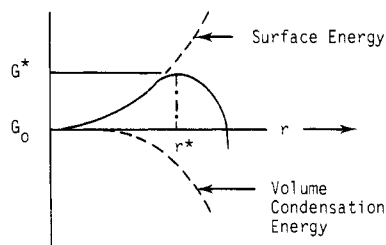
Figure 1. Total free energy of clustering vs. nucleus size (r).[2]

dius r is taken as the sum of the energy needed to create a surface (surface energy) and the volume energy of condensation. The variation of ΔG_O vs. r is shown in Figure 1. As can be seen, subcritical nuclei $(r < r^*)$, formed by collisions of thermally equilibrated adatoms jumping around on the surface, grow with an initial increase in free energy until a critical size is reached, greater than which growth continues with a decrease in free energy. Clusters smaller than r^*, the radius of the critical nucleus, are unstable and decompose, while larger clusters spontaneously grow to form stable particles. It can be seen now that an incident atom that instantaneously thermally equilibrates upon striking the surface can hop around on the surface for a finite length of time. If it collides with a critical nucleus or larger cluster it becomes stabilized on the surface in that cluster. If this atom collides with a subcritical nucleus the resultant cluster may become stable if the critical size results or if other adatoms collide with this subcritical nucleus before dissociation occurs. The final fate of a migrating atom which fails to become part of a stable nucleus is to desorb. If an incident atom becomes incorporated into a stable cluster it is considered to be condensed. The probability that an impinging atom will condense is called the condensation coefficient. The second nucleation theory, the *atomistic* theory, supports the capillarity theory. The main difference between the two theories is that the capillarity theory treats a continuously varying cluster size in terms of a continuously varying free energy while the atomistic theory considers the change in the number of atoms in a cluster in terms of discontinuous changes in the binding energy of the adatoms comprising the cluster. Both theories define the nucleation rate, I, as being proportional to the product of the concentrations of critical and nuclei and the rate at which adatoms join these critical nuclei by diffusion. It is important to note an adatom within an area $\sim \pi \bar{X}^2$ of a critical nucleus will diffuse to that nucleus. Since $\pi \bar{X}^2$ is much larger than the physical area of the critical nucleus, there is a much greater probability for the nucleus to capture atoms by diffusion than by direct impingement.

The size of a critical nucleus of Ag, for example, can be roughly estimated by using the capillarity theory with bulk parameters and a typical deposition rate of 0.1 nm/s at 300 K, yielding $r^* = 2.2$ Å.[5] This suggests that critical nuclei are of atomic dimensions.

b. Experimental Observations. Support for critical nuclei of atomic dimensions is found in the work of Hamilton involving the nucleation of zinc.[79] Zinc does not self-nucleate on the substrates used. However, when very small amounts of Au, Pd, or Ag were deposited on amorphous carbon or SiO_2 substrates followed by zinc deposition, islands were observed due to nucleation of the zinc on the predeposited nucleation

centers. The nucleation centers (clusters of Au, Pd, or Ag) could not be observed with high resolution electron microscopy. The nucleation of zinc on these clusters resulted in an enlargement of these centers to within resolution of the electron microscope. This technique was suggested as a versatile method of obtaining information on the initial stages of film growth. On the basis of the amount of Au, Pd, or Ag deposited and the number of islands of Zn observed, it was determined that even a single atom can act as a nucleation center for the zinc vapor. It is interesting to note the importance of critical nuclei to the photographic industry. Hamilton's work with zinc nucleation was carried out to determine the size of so-called "latent-image centers" formed on photographic films. These centers are photolytically produced silver clusters which catalyze the reduction $Ag^+ \rightarrow Ag^0$ on the film. Photons of light strike the photographic plate, causing the reduction of silver ions to produce silver atoms which then form small clusters that catalyze the deposition of silver atoms on these nuclei. The silver particles formed constitute the grain seen in photographs. The minimum silver cluster size found to catalyze the reduction was 3-4 atoms. Behrndt used Cd as well as Zn in a similar study.[80]

Unusual nuclei distributions on some substrates have led to the proposal of " active sites" present on some surfaces which are responsible for preferred locations of nucleation centers. This proposal, which can be supported by simple capillarity theory predictions, has as its greatest support a phenomenon called "decoration" which has very useful applications. Surface features of substrates, such as rock salt, which are difficult to see by electron microscopy may be made visible after a light vapor deposition of gold. The gold preferentially nucleates along the edges of defects present in the surface, thus highlighting (decorating) these features, rendering them visible to the electron microscope.[5] In light of this, it would seem evident that nuclei can form and reside at special structural features of the substrate surface preferentially. However, in most studies the nuclei appear to be randomly oriented, indicating a homogeneous nucleation process. The role of defects in surfaces as possible places for preferred nucleation is not understood or well documented. The isolation of nuclei seems to be related more to the free energy barrier (Figure 1) of nuclei formation and lower mobility of these nuclei relative to adatoms than to special surface sites. The phenomenon of decoration has been suggested by Chopra to be the result of a shadowing effect by ledges on the surface creating virgin regions in the shadows. The random distribution of isolated nuclei suggests a reason for the discontinuities observed in thin films assuming that each "patch" originated from a discrete nucleus. The question now arises as to how additional atoms are added to these nucleation centers. Two possibilities exist for the early growth of small metal clusters. The clusters may grow by direct impingement of atoms from the vapor phase or by diffusion of adatoms over the surface. The presence of "agglomerates" in thin metal films separated by interstices of various widths or "amorphous" patches observed in early film studies of Au, Sb, Bi, Zn, In, Cd, Cu, Au, and Mg was attributed to metal atoms on the substrate migrating to the nucleation centers.[81,82] This

conclusion has been agreed upon and supported by many other workers since that time. The fact that three-dimensional clusters are formed supports a predominant role of growth by surface diffusion mechanisms rather than direct capture of vapor atoms. Indeed, if each adatom were held stationary by the support, then further deposition of atoms onto a surface covered by a random distribution of adatoms would lead to a continuous film at very low coverages. This is assuming a growth mechanism by direct capture of vapor atoms. Thus, the presence of "patches" or discontinuities observed in electron micrographs of thin films provides strong support for the presence of isolated nucleation centers to which impinged adatoms migrate. Chopra observed that the island ("island" referring to observable three-dimensional clusters of perhaps 20 atoms) density increases in the early stages of film growth until a saturation is obtained.[5] For a number of metals with comparable melting points deposited on a variety of substrates such as ionic, amorphous, or single crystals at room temperature, once the saturation density is reached the islands are separated by 10–100 nm. Vapor atoms condensing between these islands move to the nearest island since this will reduce the free energy of the system. Further deposition beyond the point of saturation creates a decrease in the island density by coalescence of islands. The smoother the substrate, the more rapid the decrease in island density will be. These observations are in accord with the predictions of the nucleation theories discussed earlier.

Modifications of the atomistic theory of nucleation have been made to treat the case of "extreme incomplete condensation" which is characterized by a condensation coefficient much less than unity.[83] This situation is a result of a low desorption energy for adatoms or a short mean stay time such that short average migration distances result. In this extreme case island growth is predicted to be by direct impingement of vapor atoms with growth due to diffusion of adatoms negligible. Recently experimental evidence for this "extreme incomplete condensation" has been submitted.[84] A linear increase in average particle size with coverage for the deposition of Ag, Cu, Au, or Pd on amorphous C or SiO_2 was observed as well as an apparent sticking coefficient of 0.1 or less. Furthermore, this linear relationship between particle size and coverage was independent of deposition rate. If island growth was caused predominantly by adatom diffusion, nucleation kinetics predict cluster size distributions to be shifted toward a greater density of larger clusters due to their larger effective "capture" areas.[85] Impinging atoms, whose fates are determined by diffusion kinetics, near various sized clusters are more likely to be incorporated into the larger clusters present. This change in size distribution yields a nonlinear increase in average particle size with coverage. However, if growth is by direct impingement a linear increase in average particle size with coverage is observed.

The low condensation coefficient observed is in accord with theory when growth is by direct impingement. However, when Auger spectroscopy and sputter sticking of the substrate surface were carried out it was found that metal atoms had diffused throughout the support. When this amount of metal was taken into account, the condensation coefficient was found to be close to unity. Thus, surface migration of adatoms was impeded by diffusion *into* the substrate surface. This apparently has the same effect on particle growth as a low condensation coefficient. Low condensation coefficients do not necessarily imply that growth will be by direct impingement; however, direct impingement growth predominance may be due to low condensation coefficients. Baetzold also reported that a large fraction of the Ag, Cu, Au, or Ni evaporated onto predeposited carbon films diffused into the carbon substrate.[86]

The mobility of adatoms across the surfaces of substrates is very important in determining the shapes of the nuclei formed, the density of nuclei, the mean thickness at which coherent films are obtained, and mean crystallite size of the resulting film.[87] The mobility of atoms within crystallites also plays a very important role in determining the ultimate film structure and geometries of particles in early stages of growth. The temperature and nature of the substrate have a pronounced effect on these migration abilities. Low substrate temperatures are generally used for preparation of thin metal films for use in adsorption experiments. The reason for this is that at lower substrate temperatures smaller migration distances of adatoms results in a higher saturation nuclei density. This higher saturation density results in a coherent film with low electrical resistance being formed. This is a later stage of growth than that under consideration at the moment and will be subsequently discussed.

In the early stages of nucleation and cluster growth, as mentioned, adatoms migrate rapidly and cluster nucleation and growth are diffusion controlled. The interaction of the adatoms with nonmetallic substrates is probably of a van der Waals type. The binding energy of metal atoms attached to a cluster is much higher than that of atoms attached to the substrate. Therefore, surface diffusion of atoms on a metal cluster is expected to be much less than diffusion of atoms on the substrate surface. This results in a temperature dependence on the geometries of the small metal particles on the support. At low temperatures where metal atom migration on a metal particle is low compared to migration of adatoms to a growing particle, the particles mainly grow sideways. This results in "flattened out" particles and more of a two-dimensional type of growth. If the deposition rate is high enough so that these flattened particles which are growing sideways do not have time to "round" out, their coalescences (discussed later) will occur at thin film thicknesses. Individual atom migration on nonmetallic substrates is hard to study so little experimental data on ease of migration have been obtained.[87] The relative rates of atom migrations on the support and on particle surfaces are only important in determining the later stages of film growth. Although isolated cluster shapes may be influenced by these parameters during their growth, it is difficult to directly observe these geometries since a dynamic process is involved. Anderson obtained an electron micrograph of an ultrathin film of palladium deposited on air-cleaved mica at 545 K in UHV. The average diameter of the crystallites was 20 Å, with average heights of 14 Å.[3] Although this flattening may be real, errors in measurements create uncertainty. It is important to note the effect of impurities on the mica
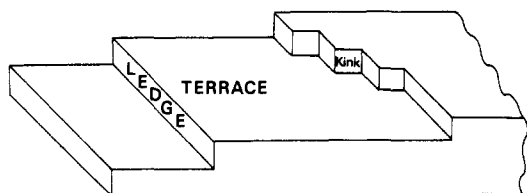
Figure 2. TLK model of "curvature" of a closed packed surface (simplified representation).

Figure 3. Removal of grain boundary between two coalescing particles (cross section).

substrate on the distribution of the particles on the surface. A nonuniform distribution of particles on the air-cleaved mica was observed while a random distribution resulted from deposition on vacuum-cleaved mica. The role of contaminants as culprits for preferred nucleation sites is well documented, yet not understood. Examples may be found in Geus's review.[87]

2. Coalescence and Later Stages of Film Growth

In this section the fate of the discrete isolated clusters formed in the earlier stages of nucleation and growth will be discussed. These stages are marked by coalescence of crystallites and then filling in gaps to produce a continuous film. The changes in structure of the isolated crystallites before coalescence and in the presence or absence of impinging vapor atoms or migrating adatoms over the substrate will be discussed first.

A model showing changes in geometries of isolated crystallites and the process of coalescence will be described as given by Geus.[87] It is to be expected that crystallites formed during film deposition deviate from ideal crystallographic shapes (discussed later). Instead there should be roughened edges and imperfections resulting in the curved surfaces seen in electron microscope photographs (cf. ref 3). If the particles are formed by close packing which is most likely for transition-metal atoms, curvature can result by the presence of terraces, ledges, and kinks (cf. Figure 2). This is referred to as the terrace–ledge–kink model (TLK) of a curved surface. Surface atoms in areas of high curvature (frequent ledges with many kinks) have a higher chemical potential than atoms in flatter areas. Therefore, there is a driving force for migration of surface atoms from areas of high curvature to flat areas or areas of negative curvature (valleys). Migration such as this results in a lowering of the energy of the surface, producing a smoother surface. Migrating atoms used to smooth out a surface can either come from *in* the surface or *on* the surface. If a crystallite with rough edges has just been formed and deposition of metal atoms on the substrate has ceased, migrating atoms must come from *in* the surface. If deposition is in progress, migrating adatoms present on the particle surface are present. In this case migrating atoms may come from *in* the surface or *on* the surface. In the former case (deposition ceased) transport of atoms over the surface to change the profile of the surface occurs by (1) formation of kinks in ledges and (2) mobility of dissociated kink atoms. These dissociated atoms are considered as mobile adatoms. Fewer intermetallic bonds need to be broken for migration of an adatom over a plane surface than for removal of an atom from a ledge to generate an adatom. Therefore, the activation energy determining migration of metal atoms from sites *in* the surface corresponds to the energy needed
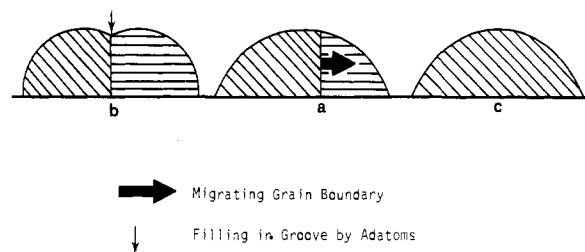
to take an atom out of a ledge and put it on a flat surface. This activation energy is much larger than that for migration of an adatom over the flat surface.

From energetic considerations it turns out that at very low temperatures, only atoms in regions where the surface is very strongly curved can desorb from a ledge to a terrace. These dissociated atoms are captured in the steps of these strongly curved parts of the surface. This filling in of the steps creates a partially faceted surface. This process continues until an equilibrium shape is reached which still contains areas of rather high curvature.

Due to the energetic barrier mentioned earlier, the concentration of adatoms on flat terraces near areas of high curvature is low for the equilibrated particle. If deposition is carried out during this particle structural change a somewhat different means of smoothing occurs. When new atoms are added directly or by surface migration to the particle, mobile adatoms on the particle surface are present. The high mobility of these adatoms on flat surfaces has already been explained. The addition of new atoms creates a high concentration of adatoms on the flat terraces near areas of high curvature. The high mobility of these adatoms results in their migration to and filling in the areas of high curvature (steps) to reduce the energy of the particle surface. The migration may be rapid enough so that they reach the step areas before colliding with each other which would result in two-dimensional nucleation. This filling-in process continues until the concentrations of adatoms on the edges approaches the concentration of adatoms on the flat planes. Due to the lower concentration gradient at this point, migration of atoms to the areas of steeper curvature is slower and two-dimensional nucleation starts to occur on the flat surfaces.

An interpretation of coalescence of crystallites during deposition will now be described. When two crystallites come into contact (by lateral growth), a very steep negative curvature ("valley") between the two is generated. This results in a lower concentration of adatoms in the flat planes in this "valley". Due to the concentration gradient, atoms from less steep regions of the crystallites are transported to and fill in the region between the particles. The "seam" or grain boundary caused by this filling in results in a groove at the surface which impedes surface migration of atoms from one particle to the other (cf. Figure 3). This grain boundary is filled in slowly by vapor metal atoms for large particle coalescence but rapidly migrates through one of the particles if they are small (Figure 3b,c). The grain boundary can only migrate through a particle if the surface is smooth (Figure 3b) since only in this case is there a continuous decrease in surface area of the grain boundary with migration.
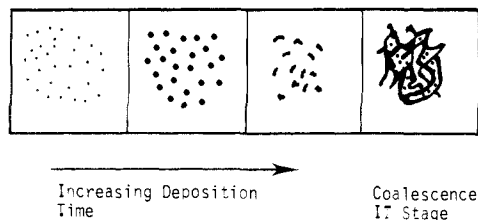
Figure 4. Film growth leading to the coalescence II stage.

The effect of impurities on coalescence can be pronounced. Tin films laid down in UHV on Pyrex covered with evaporated SiO consisted of very large crystallites, meaning that much coalescence occurred during deposition. The same result was obtained when the deposition was carried out in 10^{-5} torr of N_2, CO, H_2, Ar, methane, propane, and pentane. However, films deposited in 10^{-5} torr of oxygen contained poorly crystallized grains, showing that oxygen hindered the coalescence.

The coalescence stage of film growth commences once the deposition is carried out beyond the point of saturation of nuclei density (providing the temperature is high enough). The first observable change is a decrease in the island density due to mutual coalescence of neighboring islands by lateral growth. These larger islands continue to grow, at first, in a predominantly lateral direction due to diffusion of adatoms across the substrate surface. When the islands have reached a size such that the capture area of atoms directly from the vapor phase is large compared to the areas of naked substrate, growth normal to the surface accelerates. The islands thus grow outward from the substrate by direct capture of metal atoms and sideways by accumulation of atoms adsorbed on the substrate. This growth is commonly referred to as the coalescence I stage and involves considerable mass transfer by diffusion of adatoms between the islands. As the atoms touch, further coalescence occurs depending upon the substrate temperature. At sufficiently high temperatures this coalescence leads to the formation of an interconnected network surrounding vacant channels (Figure 4). This is referred to as the coalescence II stage. These stages of film growth are rapid when atom mobility and (at elevated temperatures) small island mobility are high. Upon formation of the network in the coalescence II stage the process is slowed down. The final stage to produce a continuous film (no naked areas of substrate surface) is the slow process of filling in vacant channels and requires a considerable amount of deposit for deposition on room temperature substrates. During this filling-in process secondary nucleation and slow growth of these nuclei occur wherever large areas of the substrate are exposed due to coalescence. This can be seen in transmission electron micrographs of a 100 Å thick Au film on NaCl at 300 °C.[5]

The kinetics of each stage may vary drastically depending mainly upon substrate temperature, smoothness of the surface, deposition rate, and the metal used. The stages of film growth reached for a given deposition and substrate at a certain temperature depend largely upon the very general features of agglomeration (coalescence) and mobility of species in the film. The dynamics of the coalescence process is not very well understood; however, general morphological changes in film structure at various substrate temperatures have

led to some understanding of this growth process. Chopra points out that once the coalescence II stage is initiated it proceeds very rapidly and requires little additional deposit to complete. This stage is recognized by a change from an electrically discontinuous structure to a continuous network. For example, Ag films on glass at 100 °C decrease in electrical resistance by many orders of magnitude with an addition of only about 10 Å of deposit beyond the critical thickness ($\sim$100 Å). This critical thickness is the maximum thickness of the film in which electrical discontinuity is observed (i.e., very high resistance). If deposition is ceased as soon as the coalescence II stage is initiated, the resistance decreases much more slowly than if deposition was not interrupted. This shows that even in the absence of deposition after this stage commences, coalescence continues. In the presence of deposition the stage is complete in a fraction of a second. In the absence of deposition the process is slower, yet still rather rapid. It has been observed to last several seconds for noble-metal films even at 77 K.[5]

By comparison of various metals deposited on a given substrate at different substrate temperatures correlations have been made between these parameters and the resultant film growth process. These correlations are brought about by using a temperature ratio τ which is the ratio of the temperature of the substrate (T) to the melting point of the metal (T_M). The dependence of film structure τ as discussed by Sanders will now be summarized.[16]

Five ranges of τ are considered which have approximate upper limits given by τ_{sd}, τ_r, τ_m, and τ_c, respectively. τ_{sd} ($\sim$0.1) is the temperature ratio at which surface diffusion of atoms just becomes noticeable. T_r ($\sim$0.3) is the value of T at which recrystallization commences. τ_m is the melting point of the bulk metal so it is equal to unity. τ_c is the value above which atoms reevaporate at such a high rate that renucleation does not occur.

The first range considered is when $\tau \leq \tau_{sd}$. The growth process under these conditions is described as follows: Impinging metal vapor atoms cool rapidly as they strike the surface so there is a high accommodation coefficient. Due to the low temperature, the mean migration distance of adatoms ($\bar{X}$) is small, resulting in very closely spaced nuclei. The nuclei grow laterally by capture of adatoms and also vertically by direct capture of vapor atoms. Thus, a high saturation nuclei density is reached at an early stage of deposition. The small crystallites formed are randomly oriented. For the reasons discussed earlier, surface self-diffusion is not significant. This results in gaps formed between touching or overlapping crystallites which are not filled in. Therefore, the structure of thin films prepared under these conditions consist of randomly oriented grains propagating outwards in the form of small columns as the thickness increases. Due to lack of surface self-diffusion and random orientation of the crystals the gaps between the columns are large enough to be accessible to gases. The effective surface area of these films is larger than the geometric surface area and increases linearly with increasing film thickness. As expected, the columns formed have very atomically rough surface features. The gaps present cause a high electrical resistance of the film. These gaps have been

observed by electron microscopy for W films deposited on glass at 273 K.[88]

The second range considered is $\tau_{sd} < \tau < \tau_r$. In this range surface self-diffusion is an important process resulting in filling in the gaps between touching crystals. This occurs because it lowers the surface energy as predicted in the previous theoretical discussion. The size of the crystals obtained is determined by the initial separation of the nuclei. At a higher temperature a lower saturation density results so crystals formed under the conditions in this range are larger than in range 1.[87] Due to the filling in of the gap between crystals, normal grain boundaries are formed which are inaccessible to gases. Therefore, the effective surface area is close to the geometric surface area.

The third range is $\tau_r < \tau < \tau_m$. Under these conditions the surface self-diffusion is more rapid and grain boundaries are mobile. Recrystallization occurs which results in a growth of grain size with thickness. The process of coalescence discussed previously occurs in this range by (1) particles touching, (2) formation of grain boundaries, and (3) migration of the grain boundary out of the resultant particle. Repetition of this process is recrystallization. Electron micrographs of these stages are given in Sander's review. It should be noted that due to recrystallization columns are not formed and the saturation density of nuclei does not determine the grain size. As a result continuous films are obtained at a relatively low thickness.

The fourth range is $\tau_m < \tau < \tau_c$. In this range the film deposits as a liquid on the substrate. It is interesting to note that small clusters of a metal may be liquid on the substrate even when the temperature is below the melting point of the bulk. This is due to the melting point depression in small particles. Thus Sn clusters of 60-Å diameter melt 60 °C below that of the bulk.

The fifth and final range is $\tau < \tau_c$. In this case the saturation density increases with increasing temperature due to rapid desorption of atoms having short mean stay times.

The above discussion which is based on experimental observations is in marked agreement with the theoretical discussions presented earlier.

In a few cases found in the literature amorphous forms of various metals have been obtained. Chopra reviews some of the conditions which may lead to amorphous structures.[5]

(a) Impurity Stabilization. Fine-grained and in some cases amorphous deposits are obtained when deposition is carried out in the presence of certain gaseous impurities. As mentioned earlier oxygen impurity can effectively inhibit grain growth even at pressures of 10^{-4}–10^{-5} torr. The "amorphous" patches of Au reported by Levinstein were present only when slow deposition was carried out.[81] Poor vacuum ($\sim 10^{-4}$ torr) was undoubtedly responsible for the amorphous structures.

(b) Vapor Quenching (VQ). Amorphous structures may be obtained by condensation onto very cold substrates so as to reduce thermal diffusion of adatoms. This technique is specially applicable to nonmetallic atoms or molecules which have tendencies toward covalent bond formation. Due to the relatively small coordination number of these species, large displacements of individual atoms are necessary for a change from a random to ordered arrangement. In contrast,

pure metals which crystallize in close-packed structures require very little displacement from a random to an ordered arrangement. Thus, pure metal deposits are usually crystalline when deposited at temperatures as low as liquid helium, although crystallite size is reduced.

(c) Codeposit Quenching. The most effective method of inhibiting mobility is the codeposition of two incompatable systems onto a cold substrate. This method has been used to obtain amorphous systems by codeposition of a metal and a nonmetal (e.g., Ag + 16% SiO).

The observable difference used to distinguish a fine-grained structure (<20 Å) and an amorphous structure is recrystallization. A fine-grained structure upon heating will yield a continuous recrystallization and, therefore, crystallite growth. An amorphous structure is characterized by a sharp transition from the amorphous to a crystalline structure at a definite temperature.

B. Low Temperature Clustering of Metal Atoms in Inert Gas and Alkane Matrices

The study of aggregation of metal atoms at low temperatures by matrix isolation techniques is a very new area involving only a few workers. Reactions of small metal aggregates (two or three atoms) with various ligands have recently been reported, and the use of the method for comparisons with heterogeneous catalysts has been suggested.[89-94]

Ozin and co-workers have studied diffusion of vanadium atoms in argon and alkane matrices by monitoring changes in atomic optical spectra during warmup and concentration studies.[89] Decrease in optical absorptions were taken to indicate the formation of "large" (>3 atoms) clusters via bulk diffusion through the matrix. Bulk diffusion generally occurred at temperatures of about one-third of the melting point of the matrix material. For example, diffusion of vanadium atoms through a normal pentane matrix became significant at about 50 K (mp = 143.5 K). Concentration studies were interpreted as diffusion of vanadium atoms on the matrix surface during deposition at 10–12 K. Higher concentrations (V/alkane $\sim 1/10^3$) resulted in the formation of dimers while lower concentrations ($1/10^4$) favored monomer isolation. The influence of different alkanes on surface diffusion was observed but not adequately interpreted. Longer n-alkanes inhibited surface diffusions better than shorter alkanes. In argon surface diffusion was much greater. Perhaps morphological (trapping sites) and accommodation coefficient differences are responsible for these observations.

As might be expected, temperature is critical when M atoms are dispersed in alkanes. While Ozin and co-workers find that V atoms easily clustered in alkane matrices upon approaching 50 K, reaction with the alkane did not take place. However, Davis, Severson, and Klabunde[73,74] have shown that Fe, Co, and Ni atoms *do react* with alkanes, but at temperatures >77 K, most efficiently near 140 K. Clustering took place readily in the 77–140 K range, however. Thus, available evidence indicates that M atom clustering is facile in the 50–140 K range whereas reaction with the alkane is facile in the >140 K range (some overlap of these ranges is evident, but further work is needed in order to define them more precisely). Many other metals and

alkanes need study, however.

Studies of aggregation in noble gas matrices of a variety of first row transition metal atoms (V, Cr, Mn, Co, Ni, Cu) have shown that mobility, and hence dimerization, is reduced with more polarizable matrices. Under identical conditions use of Ne matrices yielded more dimerization than Xe matrices.[91] Using the clustering of nickel atoms as an example, Moskovits compared theoretical models with experimental results to interpret the clustering kinetics.[92] Best fit with experimental results was obtained by use of a model which assumes a short-lived surface condition in which impinged matrix atoms and metal atoms are mobile. The reactions occurring (e.g., aggregation) are suddenly stopped (quenched) after a certain amount of time τ_q. The concentration of dimer was adequately accounted for when dependence on two inseparable quantities τ_q and K_M was assumed, where K_M is a rate constant for $M_n \rightarrow M_{n+1}$.

A study of silver atom aggregation in noble gas matrices was reported.[93] In this study it was found that a quantitative yield of isolated silver atoms could be obtained only if the noble gas deposition rate was above a critical value and the substrate temperature was below a critical value (e.g., Xe 21 K, Kr 15 K, Ar 11 K). The yield of isolated atoms decreased rapidly with a slight increase in temperature and was zero at temperatures corresponding to roughly one-third the triple point of the matrix material (e.g., Xe 38 K, Kr 30 K, Ar 22 K). Absorption spectra of matrices in which Ag isolation was not quantitative were used to assign bands for Ag_2–Ag_6 aggregates. Spectral features led to the conclusion that two processes were in operation. The first is isolation of atoms and formation of aggregates. The second is immediate formation of larger aggregates. No explanations were submitted.

C. Particle Formation in Dispersed Metal Catalysts Prepared by Reduction of Metal Compounds in Nonzero Oxidation States

In the previous section on particle formation in metal films the metal remained in a zerovalent oxidation state for very clean systems. The effect of impurities such as oxygen on the distribution, coalescence, and grain size of metal particles in thin films was mentioned. Due to the cleanliness that can be achieved in film deposition processes under UHV conditions, much has been learned about the interactions of metal atoms in the formation and growth of small particles as discussed. Furthermore, chemisorption studies which are very impurity sensitive can be carried out with excellent reproducibility by using films of the most catalytically important metals such as iron, cobalt, and nickel (especially epitaxial films). However, all other forms of dispersed metals are prepared from compounds of the metal and must be subsequently cleaned. This necessitates the use of elevated temperatures above the temperatures of preparation. As a result structural changes such as coalescence or sintering of particles occur. Even with the use of elevated temperatures the cleaning is extremely difficult, if not impossible. The most difficult to clean and hence characterize form of dispersed metals is pure metal powders due to their sensitivity toward sintering.[13] This sensitivity is a result of the particles readily coming into direct contact with

each other. If structural promotors are included to reduce sintering of metal particles, an even more complex and difficult to characterize system is formed. Supported metal catalysts can be more vigorously cleaned without great morphological changes. In the case of supported catalysts nucleation and growth processes are difficult to study due to the complex nature of the support surface as well as the effect of impurities. Substrates used in film studies are generally well characterized.

Metal particles formed in the early stages of film growth that can be studied by depositing ultrathin films can be considered as ideal forms of particles present in most other types of dispersed catalysts. As will be subsequently shown, comparison of particles produced in these vastly different systems can reveal important similarities as well as differences in structure.

The nucleation and growth of metal particles in metal powder preparation will be discussed followed by a brief description of supported metal preparation. Nickel dispersion will be treated predominantly.

The detailed process of nucleation and particle formation will vary depending upon the preparation method used. As discussed in the section on forms of dispersed metals, particles of nickel are most commonly prepared by formation and subsequent reduction of metal oxides. The preparation of nickel powders, for example, usually involves precipitation of a nickel hydroxide, carbonate, or basic carbonate from soluble nickel salts. Thermal decomposition of these leads to precipitation of NiO which crystallizes in the rock salt structure. Upon reduction with hydrogen, the $O^-_{(s)}$ ions at the oxide surface react with hydrogen molecules and are converted to $OH^-_{(s)}$, with electrons being trapped at sites in or near the surface. At sufficiently high temperatures $OH^-_{(s)}$ groups are desorbed in the form of water. The electrons released by these reactions are eventually taken up by the Ni^{2+} ions, forming Ni^0, which form clusters which nucleate a metallic phase. This is a relatively slow process at lower temperatures. The key to this reduction seems to lie in the structure of the nickel oxide precipitate. The initial stage of the reduction is greatly affected by the defect structure of the nickel oxide since this dictates the nature of the H_2 chemisorption process. Precipitated nickel compounds are usually imperfectly crystalline, with stacking disorders in the layered lattices. Rapid precipitation should lead to structures containing a higher concentration of lattice defects. A higher concentration of defects should lead to more rapid initial nucleation. In practice it is found that the lower the temperature at which precipitation and reduction are carried out the better is the dispersion of the resultant nickel particles. Once nucleation has started, the effect of the hydrogen atmosphere is pronounced. Hydrogen can dissociatively chemisorb on the nickel clusters that are formed. These hydrogen atoms are mobile, so they can migrate to the nickel particle/nickel oxide interface and be used in reduction of the oxide. This process causes a much more rapid reduction since hydrogen atoms react with the oxide more readily than does molecular hydrogen.[3]

The above nucleation and growth process for a typical metal powder preparation raises the question: what determines the final crystallite size obtained at the preparation temperature? In order to suggest an an-

swer to this fundamental question, comparisons with other types of systems will be made. In the discussions of nucleation and film growth, crystallite size was determined by the saturation density of nuclei. The saturation density by the saturation density of nuclei. The saturation density was found to increase with decreasing substrate temperature due to shorter adatom migration distances. In the case of nucleation in metal oxide reduction an opposite trend is found. Higher temperatures will favor more rapid initial reduction of the metal oxide and higher density of nuclei. However, a higher temperature also favors coalescence or sintering of particles which results in larger particles. Therefore, a compromise must be made so that a temperature is used at which the nuclei concentration is a maximum without appreciable coalescence. Problems affecting this balance are the presence of nucleation sites, which may be defect structures in the metal oxide particle surface, and generation or presence of water vapor. Water vapor retards the initial reduction process while defects accelerate the process. Maximum dispersion should be obtained by (1) using starting materials which will maximize the defect concentration in precipitated metal oxides, (2) drying the metal oxide thoroughly at low temperatures, and (3) using a high flow rate of hydrogen in the reduction process while keeping the temperature low. The high flow of hydrogen serves two purposes: (1) it lowers the partial pressure of water vapor, and (2) it increases the rate of reduction at lower temperatures.[3]

The process of particle growth described does not need to be treated in further detail. The mechanisms of coalescence of metal particles described for films can be applied, and mechanisms of sintering will be discussed shortly.

With all other factors taken to be equal, the dependency of the type of metal on the dispersion resulting from metal oxide reduction depends upon the thermodynamics of the process. The nucleation rate determining step is assumed to be the initial reduction by molecular hydrogen as

$$MO_{x(s)} + xH_{2(g)} \rightleftharpoons M_{(s)} + xH_2O_{(g)}$$
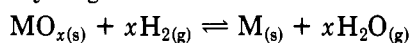
The more thermodynamically favorable this process is to form $M_{(o)}$, the more rapid is the initial reduction and hence nucleation. Equilibrium data show the following trend for the ease of reduction at 673 K:[3] $Ag_2O > PdO > IrO_2 \sim RhO > RuO_2 \gg ReO_2 > NiO > CoO > FeO$.

Another factor arises which may play an important role in determining the final particle size. Observations by a number of workers show that the presence of chemisorbed hydrogen can inhibit sintering of nickel films.[14,17,95] However, McKee observed a very significant decrease in surface area upon reducing an oxidized sample of Pt-black with hydrogen at the same temperature at which the oxidized sample area was measured.[96] It was pointed out that for the reaction

$$PtO_{(s)} + H_{2(g)} \rightarrow Pt + H_2O_{(ads)}$$
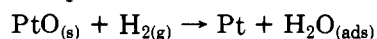
42 kcal/mol is evolved. If this heat is not dissipated rapidly it would be capable of producing high local temperatures at the points of contact of the metal particles even when the powder is cooled to temperatures as low as 0 °C. From these observations it seems likely that the presence of chemisorbed hydrogen can inhibit the coalescence of metal particles formed by

metal oxide reduction providing that the metal oxide dissipates the heat of reduction.

Nucleation and particle growth during the preparation of supported catalysts are even more complex than that described for powders. There may be many different nucleation processes occurring which may vary markedly under different preparation conditions and materials. The chief culprit for the differences in this process as compared with powder preparation is the presence or formation of a porous support on which metal particle precursors can be trapped or react. Reactions between the metal compounds (salts or complexes) and the support surface can occur, such as ion exchange. The support can occlude the precursor (e.g., $Ni(NO_3)_2$) compound which is then oxidized to the metal oxide and subsequently reduced or it can adsorb the metal oxide and subsequently reduced or it can adsorb the metal cations and undergo exchange with cations in the support (e.g., H_3O^+). Also, ligand exchange usually occurs at elevated temperatures such that H_2O ligands are exchanged for anionic groups attached to the support surface. When this occurs, the metal cation may or may not have the same coordination symmetry. An example of the variety of species that can be present even after extensive reduction is given by Coenen and Linsen.[97] After extended hydrogen reduction at 770 K, nickel–silica catalysts prepared by various methods of precipitation and coprecipitation had the following variable compositions: metallic nickel 25–81 mol %, nickel oxide 3–29 mol %, and nickel silicate 8–66 mol %.

V. Physical Properties of Small Metal Particles

Only recently have studies aided in advancing understanding and determination of properties of small metal particles by theoretical methods. Several groups have been interested in very small particles, for example, those involved in nucleation theory, photographic processes, and catalysis. The interest by the latter group was indicated early in the literature, especially by Russian scientists who were the first to actively pursue the relationship between particle size and catalytic activity.[98] Boreskov was the first to complete a systematic investigation of this relationship.[99]

It has been realized for the past 50 years that electronic and structural properties of metal surfaces are much different than those of the bulk metal, which is adequately characterized by the band theory, valence bond theory, and X-ray studies.[111] The importance of lattice spacings, arrangements of atoms, and electronic features of small metal particles in catalysis are difficult to determine. In 1967 Thomas and Thomas pointed out that "recent" advancements in technology had yielded extremely powerful tools for the study of structure and reactions on catalyst surfaces.[100] Furthermore they predicted that in the future heterogeneous catalysis would be brought closer to homogeneous catalysis in understanding. The merging of the two areas is being vigorously pursued today as recent reviews indicate.[101,102]

From a structural standpoint there have been four general approaches toward characterizing very small metal particles present in dispersed catalysts. The first is the oldest and most general and involves making structural implications from catalytic activity observa-

tions. The oldest example of this approach can be found in a report by Kobozev in 1938.[103] Kobozev studied reactions such as benzene and ethylene hydrogenation which showed structure sensitivity on extremely highly dispersed iron on carbon catalysts. As a result of many studies he envisioned a catalyst as a solid consisting of a well-defined crystalline phase and a so-called amorphous phase. In the amorphous phase there exists an "ensemble" of metal atoms which is responsible for catalytic activity. The crystalline phase was assumed to act only as a kind of catalyst support.

The second approach to the structural determination of very small metallic particles is direct observation using electron microscopy or other sensitive tools and comparison of the results with theoretical calculations. This has been done to a certain extent, but only with difficulty. As will be seen shortly, many contradictory results have emerged, especially for supported catalysts which are very dependent on preparation conditions. Despite these variables significant reproducibility is beginning to emerge.

A third approach is the correlation of reactions on very well defined metal surfaces (e.g., single crystals) which are structure sensitive and which can be studied in enough detail to provide a reasonable mechanistic understanding, assuming the results are applicable to dispersed metal catalysts and then study "homogeneous" catalytic reactions on these clusters. However, this has proven to be very difficult to do. Through the use of all of these approaches homogeneous and heterogeneous catalysis will hopefully merge.

A. Structure and Stability

If the shape and size of small metal particles present in a dispersed catalyst affect its catalytic activity and selectivity it is important to know what possible geometries are stable and likely to exist. Many theoretical studies have been reported, and these will be dealt with first.

Allpress and Sanders calculated that upon building a cluster by adding atoms one at a time such that each is placed in a site where there are the maximum number of nearest neighbors, no fccub structure is obtained up to 13 atoms.[104] The geometries calculated are three atoms, triangle; four atoms, tetrahedron; seven atoms, pentagonal bipyramid; thirteen atoms, icosahedron. Since atoms of various fccub metals were used in the calculations, they assumed that departure from this structure upon decreasing the cluster size is due to the influence of surface atoms which have less than the maximum number (12) of nearest neighbors. The curve in a plot of percent surface atoms vs. total number of atoms in a tetrahedral cluster rises sharply for clusters <1000 atoms. Also, the proportion of atoms in the surface decreases in the order tetrahedron > pentagonal bipyramid > octahedron > icosahedron.

Total energy calculations were also made for clusters of various sizes and symmetries. Initial calculations were made which dealt only with ideal crystals with close-packed faces and complete shells of atoms. The reason for this was that a crystal with an incomplete shell would have atomic roughness on the surface and increase the energy per atom. A different program was then used which let the computer add atoms to sites of maximum binding energy. Plots of energy per atom

vs. number of atoms showed curves of decreasing energy per atom as cluster size increased. Small cusps in the curve appeared at 13 and 55 atoms for the icosahedral clusters. These are the points where the shells are completed. There was not much decrease in total energy due to shell completion. From these calculations it was found that for large clusters of about 2000 atoms (40-Å edge length for an icosahedron) the order of stability was icosahedron > octahedron > tetrahedron > pentagonal bipyramid. For small clusters (< 100 atoms) the icosahedron was again the most stable.

Calculations of lattice dilations showed that the average nearest-neighbor distance for an icosahedron is slightly larger than the bulk fccub distance.

These calculations predict that a crystal less than 40-Å diameter should be most stable in the form of a multiply twinned icosahedron with close-packed faces.

Hoare and Pal used optimization of potential energy surfaces to search for minimum energy configurations for 3–60 atom clusters.[105] The improvement in these calculations over those of Allpress and Sanders was the use of potential energy surfaces instead of sums of pairwise potentials. It was determined by these calculations that the lowest energies were for polytetrahedral packings (for 1–70 atoms). Of these packings the tetrahedral, pentagonal (D_{5h}), and icosahedral symmetries were the most compact. These packings revealed a local symmetry around a growth center, and it was concluded that the symmetries of these growth centers could be preserved for two full shells of atoms but not for three or more. Larger (>147 atoms for icosahedron) clusters should have irregular arrangements and enhanced mobility of surface atoms.

Quantum mechanical calculations of cohesive energy of particles up to 147 atoms using a tight binding model for the s, p, and d bands were made.[106] Clusters of fccub and close-packed icosahedral structures were studied. The icosahedron is the most stable in this size range according to these calculations. This is attributed by these authors to the larger average atomic coordination number for the icosahedron.

Friedel pointed out that due to symmetry considerations maintenance of a fivefold symmetry axis from adding tetrahedrons cannot be maintained for macroscopic crystals.[107] It is the large surface to volume ratio that leads to specific properties in smaller crystals. A 13-atom icosahedron was analyzed, and it was shown that its stability arises because at the expense of slight elastic distortion the 12 surface atoms have 5 nearest neighbors each instead of 4 as in the nucleus of hcp or fccub phases. It was concluded that fccub or hcp nuclei would be unlikely to form for this small size.

Due to evidence that catalytic activity of metals may depend in part on the nearest-neighbor distances of surface atoms, Burton and Briant calculated these distances for microclusters of 13–147 atoms.[108] From these calculations Burton and Briant concluded that calculations of nearest-neighbor distances directly from interference functions, which is the standard practice, is incorrect if bulk symmetry is assumed. Nearest-neighbor distances of small clusters calculated in this manner are from 2% to 3% lower than bulk values. Icosahedral packing should be used for icosahedral clusters. Using radial distribution functions nearest-neighbor distances greater than bulk were obtained, and

these were considered "physically correct" results. However, it was pointed out that other experimental results such as Mössbauer studies support lower nearest-neighbor distances with decreasing particle size. It was concluded that it is not known if nearest-neighbor distances are or are not decreased from bulk values.

Experimental studies of small metal particle structure usually lack the resolution necessary to observe differences between various geometries. In most cases only average particle sizes or size distributions are obtained, and these usually assume simple cubic or spherical geometries (e.g., see ref 3, 109–111). The technology is not present such that local surface disorders on an ordered core of a small metal particle can be detected. Detection of this detail is by inference or speculation only, and usually by extrapolation from macroscopic systems. However, some structural differences between small metal particles produced in different ways have been directly observed. These may be compared to large cluster compounds whose detailed structure can be determined by X-ray crystallographic methods.

Ino reported studies of epitaxial growth of Ni, Cu, Ag, Au, and Al vacuum deposited on a cleaved NaCl face.[112] Using dark and light field electron microscopy and electron diffraction, Ino observed no epitaxy in very early stages of the film growth of Au. The particles of random orientation had the appearance of "butterfly-like" images and were multiply twinned with nearly a fivefold symmetry as determined by electron diffraction. Since these structures were present in the earliest stage of nucleation, before coalescence of nuclei became appreciable, it was concluded that the multiple twinning was not due to coalescence of nuclei. No other explanations were given. It should be added that further deposition leads to preferred orientations. Two orientations have been observed, depending on the metal. These are the [001] plane parallel to the [100] NaCl plane and the [111] plane parallel to the [100] NaCl plane. The preference for [001] orientation was in the following order: Ni > Cu > Ag > Au > Al. In these early stages of growth of Au, [001] orientation was present as well as the randomly oriented multiply twinned structures. With greater deposition these forms disappeared and the [111] orientation grew exclusively.

Komoda confirmed Ino's results in a study of ultrathin gold films on cleaved NaCl.[113] When high resolution microscopy was used, multiply twinned particles with external shapes of either decahedron or icosahedron were observed. No gaps or dislocations were observed. Slightly diverging lines in the lattice images were interpreted as suggesting that the particles were formed from a nucleus of several atoms forming the smallest unit of either a decahedron or icosahedron. Growth proceeds layer by layer of atoms on the nucleus in a most closely packed form. These structures are present for particles even less than 20 Å in diameter. The particles no longer keep their initial structures when they grow beyond 150 Å in size.

Harris later observed a gap in icosahedral Au particles beyond ~80 Å in size.[114] This gap is proof that these icosahedrons are formed from multiply twinned particles (cf. Figure 5).

Particle shapes observed in GET deposits of Au "smoke" during the pioneering days of the technique
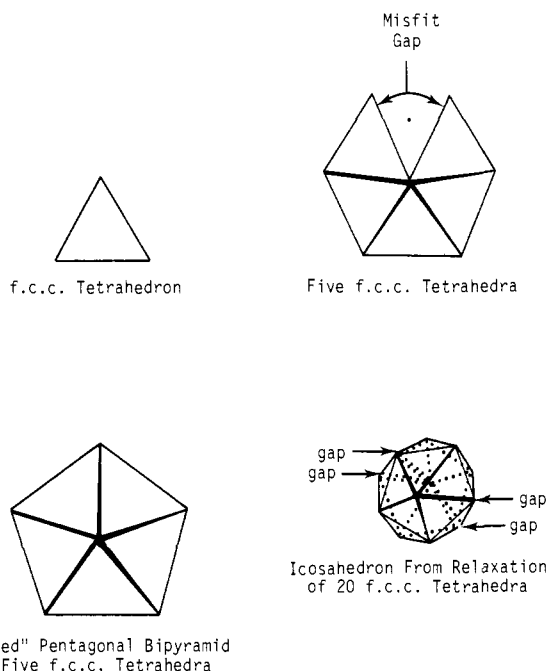
Figure 5. Multiple twinning of tetrahedra on [111] faces.

were spherical.[114] Poor resolution and possibly an unclean system were undoubtedly responsible for these observations. In a more recent study, multiply twinned particles of Ag deposited in Ar on NaCl at 300 °C were observed.[115] No misfit gap was observed so it was concluded that the five tetrahedra share the misfit angle evenly. The multiple twinning was attributed to properties of the metal and not interaction with the support.

Recently Yokozeki and Stein studied microcrystals formed in the gas phase in a supersonic free jet mixture of the metal in argon by gas-phase electron diffraction.[116] Since this GET study was carried out in the gas phase, no support interactions or crystallite formation by coalescence of initial microcrystallites was involved. Particles of Bi, Pb, and In of 40–95 Å diameters were measured. Changes in crystal structure from that of bulk metal were observed for clusters in the 50–60 Å diameter range (2000–4000 atoms per cluster). For example, In changes from tetragonal to fccub as the cluster size decreases. Lattice parameters of the microcrystals were found to decrease as the cluster size decreased. A reason for the change was proposed. The high proportion of surface atoms in small clusters favors crystal defects in surface regions of high curvature. These defects such as vacancies may play an important role with regard to cluster stability in dictating a change from tetrahedral to fccub In.

Avery and Sanders used the technique of light and dark field electron microscopy to search for multiply twinned particles in Ni, Au, Pt, and Pd dispersed on silica catalysts.[117] In the dark field image, multiply twinned icosahedral particles appear as two white spots, each spot having the shape of a rhombus. Au particles 100–350 Å in diameter were examined and only a few were multiply twinned; the remainder had fccub structures. Of the Pt particles of 10–80 Å and Pd particles of 20–100 Å studied, less than 2% were multiply twinned, with most being of the cubic close packed structure. Nickel provided too poor a contrast for any conclusions to be made.

It should be noted that the rhombus shaped spots in the dark field images are due to reflections from internal planes formed as a consequence of multiple twinning. The remainder of the icosahedron (hexagonal external shape) cannot be seen in the dark field. In the light field the rhombi are lighter than the remainder of the particle. When these light and dark field differences are seen, it means that the geometry arose from multiple twinning. Sanders and Allpress give an excellent illustration of multiple twinning and particle growth leading to this phenomenon.[118] These authors also point out that these studies were carried out at elevated temperatures in the 370–770 K range. At low temperatures particles usually do not grow to well-defined shapes. As a consequence of this, there may be an increased proportion of multiply twinned crystals among the smallest particles.

Recently an X-ray diffraction method for determining strain as well as particle size distribution was reported.[119a] Appreciable strain was observed in particles prepared by coprecipitation of NiO with alumina or silica followed by reduction. The strain was attributed to either internal pressure buildup in small particles to counter the surface tension or deformation of fccub structure in a manner similar to multiple twinning. The average particle size for the Ni particles was 21 Å. Up to 25% error could be introduced in these particle size distribution measurements by assuming zero strain.

A very unique direct study of a supported rhodium on silica catalyst was reported by Prestridge and Yates.[119b] By use of a high resolution scanning electron microscope clusters of five Rh atoms on the support were resolved. Each atom can be seen and measured. The "spots" measured 2.7 ± 0.2 Å in diameter (compare with atomic diameter of Rh 2.74 Å), and spacings between the spots measured 3.5–4.0 Å, which is in good agreement with the lattice spacing given for the fccub structure of Rh of 3.8 Å.

Many transition-metal cluster compounds have been synthesized and structurally characterized. The symmetries of many cluster compounds of various sizes have been similar to those predicted during the lowest energy growth process from 1 to 13 atoms.[120] Many unusual symmetries have been obtained in cluster compounds, mostly due to the nature of the stabilizing ligands and formal charge of the cluster unit. However, a general trend in the geometry of these clusters is toward that of a polytetrahedral icosahedron. The geometries found in cluster compounds are compared with theoretical stages of most stable growth in a review by Basset and Ugo.[102] The problem in using cluster compounds as models for small particles in dispersed catalysts is chiefly synthetic in nature. The larger the cluster of metal atoms is the more difficult it is to stabilize in the form of a discrete cluster compound. It has not been possible to synthesize a cluster compound large enough such that it would be stable with or without ligands (e.g., reversible ligand exchange with a support surface). At the time of this writing synthesis of "large" cluster compounds is in the "spotlight" of inorganic chemistry. The leaders in the field have been Chini, who very recently reported the $[Pt_{19}(CO)_{22}]^{4-}$ synthesis,[121] and Dahl,[121] who determined the crystal structure. Synthesis of the dimer of the Pt_{19} cluster $[Pt_{38}(CO)_{44}]$ has also been mentioned.[122] The potential of this work in
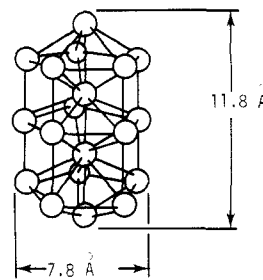
Figure 6. Idealized symmetry D_{5h} of the pseudofivefold symmetry of $[Pt_{19}(CO)_{12}(\mu_2\text{-}CO)_{10}]^{4-}$ cluster (CO ligands omitted).[121]

lending understanding to catalysis cannot be over emphasized. The $[Pt_{19}(CO)_{22}]^{4-}$ tetranion as shown in Figure 6 has a pseudofivefold symmetry, which, as Burton points out, seems to be the natural structure of small microcrystals of many materials that are macroscopically fccub.[120,121]

In the previous discussions it was pointed out that this fivefold symmetry has often been observed and theoretically predicted. The $[Pt_{38}(CO)_{44}]$ cluster, however, exhibits the cubic close packed structure found in bulk platinum! Catalysis researchers are anxious to receive reports on the chemistry of these excellent models of particles found in dispersed metal catalysts. Work such as this is bringing homogeneous and heterogeneous catalysis much close together.

Use of transition-metal cluster compounds for preparation of supported catalysts was reported by Waters and co-workers and by Ichikawa.[123,124] Decomposition of cluster compounds on refractory supports was studied by these researchers in hopes of obtaining very well characterized (size and geometry of the metal particles) supported metal catalysts for use in catalytic studies. In most cases it could not be proven whether the metal centers remained intact after ligand removal by pyrolysis. Excellent metal dispersion on the supports was obtained in all reports. Ichikawa provided good evidence that a Ni_3 cluster on silica gel from decomposition of $[Cp_3Ni_3(CO)_2]$ remained intact (Cp = cyclopentadienyl).[124a] Catalytic studies by Ichikawa will be discussed in a subsequent section.

The importance of shortened nearest-neighbor distances in small metal particles reported in the literature is difficult to assess. When fivefold symmetry exists, there is necessarily a deviation from cubic close-packed lattice parameters, and a decrease in average lattice parameters would be expected to close the "gap" in such structures built from twinning of, say, fccub units. If an icosahedron could be formed instead of a "spherical" fccub structure, the increase in the number of bonds would more than make up for the strain created by lattice shrinkage.[120] The decrease in lattice parameters with particle size decrease is only about 3% for a decrease in size from 10^3 to 10 Å as reported in the literature.[102] This decrease in lattice parameters, if it exists, is difficult to prove since comparison with cluster compounds is invalid due to ligand and formal charge effects, and furthermore, theoretical studies are contradictory.[102,104,108]

B. Sintering

Sintering will be defined as any increase in particle size in dispersed metal catalysts above the equilibrium size obtained during preparation. The causes of sin-

TABLE VIII. Thermal Treatment of Nickel Films[88]

film weight, mg	treatment conditions	average crystallite size, Å[a]	film area, cm² before[b]	after
11.6	none	460	1430	
14.2	500 K, 2 min, vacuum	460	1590	440
5.1	670 K, 60 min, vacuum	2000-3000		400
9.3	470 K, 5 min, hydrogen	460		
7.6	470 K, 75 min, hydrogen	1000-1500	1300	600
11.4	670 K, 60 min, hydrogen	2000-3000		
8.8	420 K, 120 min, hydrogen		1120	635

[a] After treatment. [b] Films deposited at 273 K.

tering may be thermal, chemical, or mechanical in nature. Only thermal sintering will be considered. Chemical interactions will be treated as effects on thermal sintering. As Anderson points out, sintering of metal particles can be expected to occur at any temperature above the preparation temperature.[3] The purpose of this section is to highlight the important morphological changes which occur during the sintering process and discuss briefly mechanisms of the process in supported metal catalysts. Catalytic consequences resulting from sintering will be treated in a later section concerning the theory of active sites. The effects of chemisorbed molecules on the sintering process will be shown.

The sintering of dispersed metals can occur by two different mechanisms: (1) migration and then coalescence of particles; (2) dissociation of individual metal atoms from a particle followed by migration of the atoms across a support or in the vapor phase to another particle.[3] As discussed previously, an increase in temperature leads to higher mobility of surface atoms in a particle so when particles contact each other at elevated temperatures coalescence can occur.

The degree of sintering is normally determined by measurements of changes in surface area and average particle size. More important, from a catalytic standpoint, is the change in particle size distribution upon sintering. This was not realized until rather recently. However, reporting particle size distributions is now a standard practice.[109,125,126]

Morphological changes in thin metal films at various substrate temperatures have been treated in some detail. Some specific examples are in order. Table VIII shows the changes in surface areas and crystallite sizes of nickel films of various thicknesses and the effect of hydrogen chemisorption on the sintering process.[88]

From these data it was suggested that two stages occur during film sintering. The first stage is closure of gaps, which is rather rapid and leads to a rapid decrease in surface area without changing the crystallite size. The second stage is coalescence of crystallites and removal of asperities. The removal of asperities was observed by EM during heating for 60 min at 670 K and resulted in the production of a mostly featureless surface. From Table VIII it can also be seen that the presence of hydrogen markedly reduces the rate of sintering of Ni films. It was suggested that the presence of H₂ reduces the surface mobility of Ni atoms.[95] In

contrast, it was reported that H₂ accelerated sintering of a 1000-Å Ni film at 600 °C.[127]

Sintering of metal powders needs little discussion since coalescence and interparticle transport of surface atoms can easily be envisioned. The ease of thermal sintering of powders has already been mentioned. Of main concern is the prevention or inhibition of sintering in metal powders. McKee reported much greater resistance to sintering of oxidized platinum black relative to the reduced form.[96] The average size of Pt particles in McKee's Pt-black was ~100 Å in diameter. A mechanism for sintering of metal powders was suggested by McKee. Lattice vacancies could migrate away from the contact area between two spherical particles and be discharged at the surface or at grain boundaries if they exist. This would result in a net transfer of material to the contact zone and cause growth of "necks" between the particles. The sintering, whatever the detailed mechanism is, would lead to an elimination of surface defects.

A pertinent study was reported by Wada and Ichikawa.[128,129] Ni was evaporated, in vacuo or in a low pressure of inert gas, into a tetrahydrofuran matrix at −196 °C. The matrix was allowed to melt, and fine particles of Ni slowly settled out of solution. When the solution was stirred, the particles were redispersed. They concluded that the particles were covered with solvent, which prevented them from "sticking together". Thus, this work as well as the work on pseudoorganometallic particles (section IIID)[73-77] is related to the sintering phenomenon.

The sintering of supported metal catalysts has been studied in much detail due to its direct industrial importance. Two main theories have emerged. One is the interparticle transport model, which results in a two-dimensional "ripening" of particles by migration of atoms or molecules on the surface or in the vapor phase from smaller crystallites to large crystallites. The other model uses particle movement over the surface followed by collision and coalescence. In this latter category two cases emerge. If migration is slow compared to coalescence, the growth process is said to be diffusion controlled. If the coalescence stage is slow compared to migration, the process is sintering controlled. Particle size distributions can be used to distinguish these process.[130]

Flynn and Wanke reported a model for sintering based on dissociation of individual atoms from a particle followed by their migration and capture by another particle.[131] It was determined that, if this is the only sintering process occurring, the broader the particle size distribution (PSD) the faster the sintering. The ultimate condition would be for a completely unisized distribution. In this extreme case no sintering should occur. This is because the model assumes transfer of mass from smaller particles to larger particles.

Ruckenstein and Pulvermacher reported a model based on migration of crystallites upon the support surface and sintering of the colliding particles.[132] Their theory predicts an exponential rate of surface area decay. The rate of decay was formulated as

$$\frac{dS}{dt} = -KS^n$$

where S is the total surface area of the metal, K is a constant, and n is an exponent which is very sensitive

to the mechanism of the decay process. For diffusion-controlled processes $n < 3$. Possible effects of the atmosphere on surface area decay were also suggested.

At high temperatures the mobility of crystallites on the support is rather great, and the sintering process is rate determining. At lower temperatures the process is diffusion controlled.[133] This latter condition, which occurs at room temperature, is called "aging".

A decrease in strain in coalesced Ni particles observed in a Ni–alumina catalyst upon sintering led to the suggestion that a driving force for sintering is the reduction of internal strain.[119]

C. Magnetic Properties

One of the most pronounced differences between small particles and bulk ferromagnetic metals is their magnetic properties. In 1896 Leick reported unusual magnetic properties of Ni and Fe films deposited under the influence of weak magnetic fields in the plane of the film.[134] In 1930 Frenkel and Dorfman predicted that a ferromagnetic crystal of moderate size consisted of smaller units referred to as "magnetic drops".[135] These "magnetic drops" were predicted to be the smallest units which displayed normal ferromagnetism and were a minimum of 10^{-4} cm in diameter. In 1938 Elmore obtained "positive" evidence that small particles behave as permanent magnets.[136] Kittle, in 1946, calculated the size of the smallest domain structure of ferromagnetic bodies to be about 2×10^{-6} cm and smaller particles should exhibit quite different magnetic properties from bulk specimens.[137]

Eventually theories developed on the nature of the magnetic properties of small particles of ferromagnetic metals. Particles smaller than the ferromagnetic domain size (~ 300 Å) require much higher magnetic field strengths to saturate the particles than the bulk metal.[138,139] When these small metal particles are subjected to a large external field they act like paramagnetic atoms with a very large magnetic moment. This phenomenon has been termed "superparamagnetism" or "collective paramagnetism" by Bean and Selwood, respectively.[140,144]

This unique property of small metal particles of normally ferromagnetic metals was exploited by Selwood and Bean in 1955 and 1956 in a sensitive method for the determination of particle sizes of less than 50 Å.[140-145] Prior to these reports the most sensitive method available for particle size determinations was X-ray diffraction line broadening, which had a practical lower limit of 100 Å at the time. The problem with X-ray diffraction is that the best accuracy is 50% for small particle sizes.[125] In order for magnetic measurements to be utilized in the determination of particle size, the presence of superparamagnetism must be proven.[142] The method of particle size calculations by the magnetic method is discussed in a later section covering methods of characterizing physical properties of dispersed metals.

It was observed in the pioneering days of the magnetic method for particle size determinations that chemisorbed hydrogen caused a decrease in the magnetization of small metal particles at a given field strength from values obtained in vacuo.[141] The presence of N_2 produced an increase in magnetization, as did O_2. It was believed that Ni has 0.6 electron hole per atom

in its d band, and parallel coupling of unpaired electrons resulting from the deficit causes ferromagnetism. The decrease in magnetization due to H_2 chemisorption was postulated to be due to electron donation to the metal d band. O_2 may withdraw electrons, creating more holes. The effect of chemisorbed gases on magnetic properties is not observed for large particles or bulk samples due to the low ratio of surface atoms/total atoms. In small particles there is a high percentage of surface atoms, so the effect is pronounced. This decrease in magnetization upon H_2 chemisorption led Selwood to the development of a method for determination of the mechanism of H_2 chemisorption on nickel.[145]

In Selwood's original work it was reported that the Curie temperature of small metal particles varies with particle size.[141] However, recently it was reported that the Curie temperature is independent of particle size but strongly dependent on the degree of reduction of the metal particles.[146] Thus, if a Curie temperature the same as the bulk value is obtained, one can be reassured that the sample is essentially completely reduced. The saturation magnetization of completely reduced metal particles is also identical with that of the bulk. Indications were made in this report that much information on particle size distributions, degree of reduction, and support interactions can be obtained by careful analysis of superparamagnetism behavior and ferromagnetic resonance data. Care must be made in interpretation of magnetic data to be sure particle size effects are responsible for the observations. Derouane and co-workers[146] seriously questioned conclusions, based on magnetic measurements, concerning catalytic activity variations with particle size as reported by Carter and Sinfelt.[147,148] The latter workers used magnetic measurements to obtain information on nickel particle size and support effects on catalytic activity. It was observed that a large increase in magnetization occurred upon sintering which approached that of the bulk value. Also, in unsintered samples the specific magnetization did not approach that of the bulk as the field strength was increased. Since the saturation magnetization of completely reduced particles is the same as the bulk metal value, Sinfelt and Carter's results were due to incompletely reduced nickel particles. Sintering creates larger particles with a lower percentage of surface atoms. Therefore, the effect of incomplete oxidation on the saturation magnetization is less for larger particles than for smaller ones. This would explain the approach of the specific magnetization toward the bulk value for the sintered catalyst.

The effect of chemisorption on magnetic properties was recently used to support a postulate that hydrogen is the principal solute in the nickel component of Raney nickel catalysts.[149]

D. Electronic Properties

The electronic properties of small particles has received much attention since catalytic processes would be expected to be very sensitive to any unusual perturbations in transition-metal d bands. Many theoretical treatments of the effects of particle size on the metal band width and Fermi level have been made.[150,151] Density of states calculations have been reported for model clusters exhibiting special surface features such
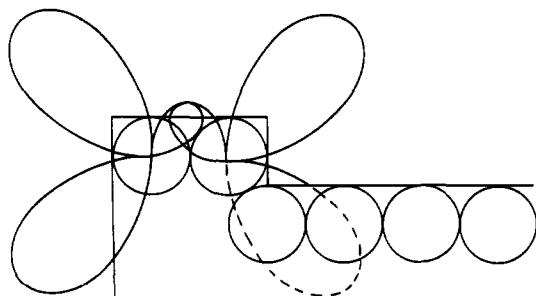
Figure 7. Idealized representation of orbital charge densities of states near the Fermi level at step sites on a nickel cluster surface.[152]

as edge and corner atoms and steps.[152-154] Experimentally, the techniques of AES and PES have been used in attempts to determine the density of occupied states in clusters of various sizes.[86] X-ray photoelectron spectra have been used to determine the effects of cluster size on the d band width and ionization threshold.[155]

Calculations reported by Kubo showed that the average spacing (δ) between energy levels in a statistical collection of small metal particles is inversely proportional to the size of the particles.[150] In bulk metals δ is smaller than any of the relevant energy parameters such as kT. In small particles, however, δ may no longer be considered small compared with kT. Thermal properties, heat capacity, and magnetic susceptibilities, for example, may be very different for small particles relative to the bulk due to the increase in δ. This would be expected to be especially relevant at a low temperature where $\delta \geq kT$. Kubo predicted that, as a result of the larger δ in small particles, each one may have either an odd or even number of electrons in the electronic states. Electrons in the highest occupied states need more than the kT available at low temperature to change state. The properties mentioned due to the presence of an energy gap are called "quantum size effects". The existence of an energy gap in real samples is not experimentally well established, as pointed out in a review by Marzke.[151] The presence of odd or even numbers of electrons in small particles is difficult to determine due to the statistical distribution of these particles in a real sample.

Theoretical calculations of density of states at the Fermi level in 13-atom clusters of Fe, Ni, and Cu was reported.[152] The density was largest in the case of Fe clusters. The d band width for the case of a 13-atom Ni cluster was much smaller than that of the bulk. The model used in these calculations was varied to include special surface features such as steps. Plotting orbital charge densities for states near the Fermi level revealed strong charge lobes extending above the step atoms and terminating in the plane below the step (see Figure 7) for the Ni case. In general stepped surfaces show a variety of bonding orbitals not present on flat surfaces. It was concluded that increased catalytic activity of stepped surfaces may be related to the increased diversity of bonding possibilities induced by the presence of the step.

Further calculations of charge densities on corner and edge atoms of stepped surfaces of Fe, Ni, and Cu were reported.[153] It was found that there is a general charge buildup on the corner and edge atoms of the cluster with a corresponding increase of the orbital densities

directed out from the cluster. At corners of steps nickel has a tendency to concentrate charge near the center of each step side.

Quantum mechanical calculations of state densities for various corner, edge, and step sites of different size Ni clusters up to 1280 atoms were reported.[154] The conclusion drawn was that the electronic structure of clusters follows, upon size increase, a general trend toward that of bulk for surface sites that have the same nearest-neighbor environment.

Experimental evidence has been reported that changes from a discrete set of electronic levels to a spectrum characteristic of bulk metal are continuous and the bulk spectrum is reached when the particle contains about 100 atoms.[86,156] As a result of this, Auger electron spectra reveal no changes due to particle size variations for Ag-, Cu-, Au-, and Ni-evaporated ultrathin films on amorphous carbon.[86]

Calculations by Hamilton and Baetzold of bonding in Pd clusters were reviewed.[156] The atomic electron configuration for Pd is $4d^{10}5s^0$. Bonding in Pd clusters is due to the 5s orbitals, mainly, which overlap to form a stronger bonding molecular orbital than would be obtained with the 4d molecular orbitals. This leads to a $4d^9 5s^1$ configuration for Pd_2. Pd_8–Pd_{10} have configurations of about $4d^{9.4}5s^{0.6}$ and bulk Pd has the $4d^{9.6}5s^{0.4}$ configuration. The effect of particle size changes on catalytic activity due to electron configuration changes should be nonexistent in real systems, with particles containing hundreds of atoms according to these theoretical studies.

Rhodin and Adams give a review of theoretical and experimental approaches to chemisorption as related to electronic properties of clean and chemisorbed metal surfaces.[157] Techniques discussed include (1) field emission energy distribution (FEED), (2) ultraviolet photoelectron emission spectroscopy (UPS), and (3) ion neutralization spectroscopy (INS). The use of these and other techniques in the study of metal surface interaction with atoms and molecules will be covered in a later section that covers reactions on single metal crystals.

A general introduction to the determination of work function and surface charge transfer of metal particles is given by Rhodin and Adams.[158] Charge transfer between W[100] and Ni[100] surfaces and first row diatomic molecules were calculated by using extended Hückel molecular orbital theory by Anderson and Hoffmann.[159] From these calculations it was determined that metal atoms at steps and corners of metal clusters gain extra electronic charge as a result of orbital orthogonality. As a result they form stronger bonds with electrophilic adsorbates. There is a trend toward development of negative charge on corner and step atoms. Charge transfer can occur between the adsorbate and the surface, the direction of which depends upon orbital overlaps and relative orbital energies.

VI. H–H, C–H, C–C, and C–O Bond Breaking by Transition-Metal Surfaces

Since breaking of bonds in a hydrocarbon (or oxygenated hydrocarbon) during catalytic reactions is necessary, conditions which optimize such processes are of great interest. The following discussion treats the effects of properties of various metal surfaces and ad-

sorbates on conditions necessary to break H–H, C–H, C–C, and C–O bonds. The types of properties to be considered are generally (1) the form of the metal, (2) the metal used, and (3) the structure of the adsorbates. The correlation between these properties and the presence and nature of "active sites" is stressed. Following a short historical review of the term "active site", the discussion is divided into sections corresponding to the form of metal used in the studies. These subdivisions include single crystals, films, powders, supported metals, and metal clusters.

In 1925 Taylor proposed that adsorption would take place preferentially on surface metal atoms situated at special structural features such as peaks, fissures, and other crystalline discontinuities.[160] It was inferred that the greatest catalytic activity occurs at such special surface sites. This led to the terminology "active sites" or "active centers". The term "active site" was used to explain many aspects of heterogeneous catalysis at the microscopic level for interpretation of macroscopic results (e.g., activity, products, and product distributions). At the time that the term was first used, all that was known about surface reactions was the nature of the reactants and products. Intermediates on the metal surface and mechanisms of the reactions were determined only implicitly. Since structural details of the surface of a small metal particle are not known, the term "active site" remains implicit in nature. However, a degree of understanding of surface reactions has been achieved such that direct evidence for some active sites on surfaces has been elucidated.

After Taylor proposed special structural features as centers of enhanced catalytic activity, many studies were performed to support the theory. Many types of bulk defects that intersect the surface were proposed as active sites. Dislocations and point defects were proposed as active sites in reactions such as formic acid decomposition or ethylene hydrogenation on cold-rolled nickel catalysts in the 1930s.[100] Further support of the role of surface defects in catalytic activity was accumulated by the late 1950s. For example, Woodcock and Farnsworth reported an enhanced activity for the hydrogenation of ethylene on clean platinum and nickel catalysts after ion bombardment.[161]

Work of Sosnovsky in 1959 as described by Thomas seemed to provide strong evidence for dislocations as active sites.[100] Sosnovsky studied the decomposition of formic acid on well-characterized single silver crystals exposing [111], [110], and [100] faces. Reactions on each surface were studied after bombardment by positive argon ions at varying potentials. The ion bombardment was expected to produce surface defects, and it was observed that the catalytic activity was altered by such treatment. Arrhenius plots were made for reactions, and it was seen that the preexponential factor, A, changed by several orders of magnitude, as shown in Table IX. The changes in A were attributed to changes in the number of active sites. The change in activation energy accompanying the change in A was attributed to a compensation effect brought about by the effect of temperature on the distribution of active sites.

It has been pointed out that Sovsnovsky's work was repeated in 1963 with evaporated silver films with surface dislocations and no important effect of these

TABLE IX. Effect of Ion Bombardment of Silver Crystals on Their Catalytic Activity for Formic Acid Decomposition on [111] Planes[100]

maximum ion energy, eV	log A	E, kcal mol^{-1}
13	2.3 ± 0.6	12.2 ± 1.2
38	6.1 ± 0.5	17.6 ± 0.9
77	7.3 ± 0.4	20.4 ± 0.8
118	6.9 ± 0.7	19.9 ± 1.5
280	6.7 ± 0.9	19.7 ± 1.8
3000	7.7 ± 1.1	22.5 ± 2.3

defects on catalytic activity was observed.[100] Impurities were suggested to be responsible for the discrepancies. Thomas emphasized the importance of surface cleanliness in studies to suggest the role of defects in catalysis. There are about 10^{15} lattice sites per cm^2 on close-packed surfaces of metals. If there is one-millionth of a monolayer of impurity present on a surface, this corresponds to about 10^9 "impurity sites" per cm^2. This value is comparable in magnitude to the density of dislocations in typical surfaces studied. Therefore it would be difficult to distinguish between activity changes due to defects and contamination. Recently very careful studies of reactions on single metal crystals have provided strong support for the role of surface features in catalysis. These studies will be reviewed in the following section.

It would be expected that changes in particle size are accompanied by changes in surface structure. Therefore many studies were carried out to demonstrate the effect of particle size changes on specific catalytic activity (i.e., activity per unit of metal surface area). Bond reported in 1962 that no such attempts had been successful.[11] This was not good for the "active site" advocates. Clark reviews the work of Boreskov, who published studies of specific catalytic activities for a variety of reactions and catalysts in the early 1950s.[162] In one study, Boreskov reported a sensitivity of specific activity to surface area of a platinum catalyst. This was H_2–D_2 exchange at low temperature.

The confusion created by the seemingly conflicting results from specific activity studies was partially cleared up in 1968 when Boudart provided data suggesting that some reactions are insensitive to surface structure and some are sensitive.[163] Boudart termed the structure-insensitive reactions as "facile" and structure-sensitive reactions as "demanding". In 1966 Boudart and co-workers reported a remarkable lack of sensitivity of the activity (expressed as a turnover number which is the number of reactant molecules converted per minute per catalytic site) to crystallite size for hydrogenation of cyclopropane at 0 °C on Pt/Al_2O_3 catalysts.[164] For dispersed samples the specific catalytic activity was independent of the Pt loading on various supports. Dorling and Moss reported that the hydrogenation of benzene on Pt/SiO_2 catalysts was facile, as indicated by their data given in Table X.[165]

In 1968 Boudart and co-workers reported a study of neopentane hydrogenolysis on supported Pt and Pt powder.[163] Two parallel reactions were observed:

$$C(CH_3)_4 + H_2 \xrightarrow[\text{catalyst}]{\text{Pt}} \xrightarrow{1} (CH_3)_2CHCH_2CH_3$$

$$\xrightarrow{2} (CH_3)_2CHCH_3 + CH_4$$
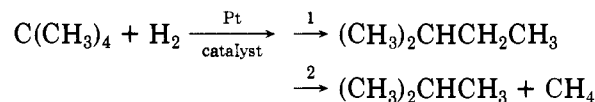
These are (1) isomerization and (2) hydrogenolysis. It

TABLE X. Activity of Pt/SiO₂ Catalysts for Benzene Hydrogenation at 25 °C[165]

treatment temp, °C	crystal- lite size, Å	metal surface area m² g⁻¹	benzene con- verted, molecules cm⁻² of Pt s⁻¹
120	45	2.00	2.8 × 10¹³
250	220	1.32	2.7 × 10¹³
300	210	1.52	3.2 × 10¹³
400	360	3.00	1.4 × 10¹³
500	640	1.53	1.3 × 10¹³
600	980	0.20	inactive
800	890	0.04	inactive

TABLE XI. Effect of Catalyst Heat Treatment on Selectivity for Isomerization of Neopentane over 1% Pt on Spheron[163]

treatment	% dis- persion	% selec- tivity(s)
(1) H₂ at 500 °C	35	2.5
(2) Above + heat to 900 °C in vacuo	35	13

was found that the selectivity(s), defined as the ratio of rate of isomerization to rate of hydrogenolysis, was (were) very structure sensitive, as shown in Table XI.

In 1975 Bond stated that only three well-established categories of demanding reactions existed.[166] These are (1) reactions involving C–C bond breaking (hydrogen-olysis and skeletal isomerization) and formation (deh-ydrocyclization), (2) D₂ exchange with C₆H₆, and (3) various oxidation reactions. Reasons for the existence of demanding and facile reactions will be treated from a mechanistic standpoint in subsequent subsections.

Reactions on metal surfaces of various forms involving H–H, C–H, C–C, or C–O bond cleavage will be treated in the following subsections in order to determine possible causes of activity and selectivity variations.

A. Single Metal Crystals

The study of catalytic reactions on well crystallo-graphically characterized single metal crystals has been pioneered by Somorjai and has been the subject of numerous reviews.[167–174] The evolution of the present day role of surface science in catalysis studies has been described by Somorjai.[167] In the 1940s little progress in surface science was made due to technical problems such as low signal to noise ratios in molecular beam scattering techniques and surface cleanliness. In the 1950s semiconductor technology placed a demand on surface science, which responded with developments of less expensive and faster electronics. These advancements led to developments of many highly sensitive techniques for structural and compositional charac-terization of solid surfaces. The rapid developments in space technology led to the production of ultrahigh vacuum systems which cured the problem of surface cleanliness. Due to these technological advancements many important results from the study of reactions on metal surfaces have emerged.

In 1948 carbon deposition on a spherical nickel crystal exposing [111], [110], and [100] crystal faces from CO disproportionation at 550 °C was reported (cf. Figure 8).[175] Black patches due to carbon deposition grew to cover the [111] faces only, indicating preferred dispro-portionation due to geometrical requirements. In 1957 Cunningham and Gwathmey studied the hydrogenation
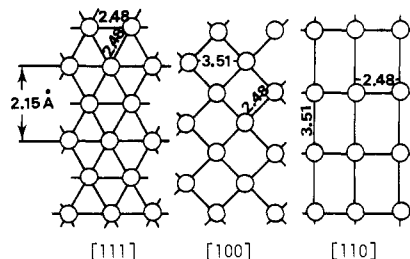
Figure 8. Crystallographic planes of nickel.

of ethylene on [100], [111], [110], and [321] faces of nickel at 50–200 °C.[176] It was found that the [321] face had the highest rate and the [100] face the slowest. The relative rates could not be explained in terms of dif-ferences in crystal geometries of the surfaces. Electronic differences were suggested.

A flood of articles published since 1972 have con-firmed and suggested reasonable causes for the obser-vations of the early workers. Chemisorption of satu-rated hydrocarbons on Ni [111], [100], and [110] sur-faces at 20 °C was reported in 1970.[177] An ordered residue structure was observed when CH₄, C₂H₆, or neopentane was adsorbed. This "carbonaceous" layer had a 2 × 2 array on the surface that was proposed to be built by C₁ units (CH₂). LEED and work function measurements were interpreted as indicating that CH₂ fragments were most likely present, with each species producing a surface dipole of 0.2–0.3 D on the [100] face and 0.7–0.8 D on the [110] and [111] faces. These au-thors further pointed out that reports in the literature reveal no chemisorption of CH₄ on polycrystalline films of Ni in the temperature range –70 to 100 °C, in con-trast to the observations on the single Ni crystals.

Further studies of saturated hydrocarbon chemi-sorption were reported in 1971 by Maire and Legare.[178] Ni [111] surfaces were studied by LEED and work function studies of propane and neopentane adsorption. The adsorption of these hydrocarbons always resulted in a decrease in the metal work function. It was con-cluded that hydrocarbon chemisorption on clean Ni surfaces is probably dissociative, resulting in the for-mation of residues of the type (CH)ₓ.

A basic review of the surface techniques LEED, field ionization microscopy (FIM), and field emission (FEM) was published by Gasser in 1971.[179]

Unsaturated hydrocarbon chemisorption on Pt [100] surfaces was studied in 1972 with LEED and AES techniques.[180] CO was determined to be bound to the surface in the form of terminal and bridging carbonyl species. The terminal carbonyl had Pt–C bond lengths of 1.6 Å and the bridging species had Pt–C distances of 2.4 Å. The hydrocarbons C₂H₄, C₂H₃Cl, and C₂H₃F formed 2 × 2 C surface arrays upon chemisorption at room temperature, due, presumably, to acetylenic species.

In 1972 a study of the dehydrocyclization reaction of n-heptane (1) on platinum surfaces was reported.[181]
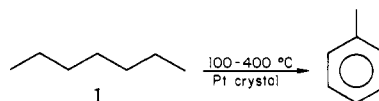
The crystal surfaces used were well characterized by cleaning under UHV conditions and studies by LEED and AES techniques. The surfaces studied had the
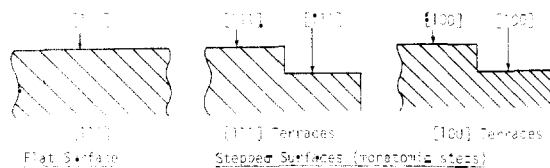
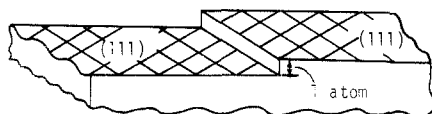**Figure 9.** Representations of flat and stepped surfaces of platinum.

Figure 10. Representation of Pt [997] surface.

orientations shown in Figure 9. It was found that the initial rate of formation of toluene was twice as high on the stepped surface with [111] terraces as the one with [100] terraces. Furthermore, the [111] flat surface was an order of magnitude less reactive than the stepped surface with [111] terraces. Another interesting observation was that the reaction could be sustained in the presence of H₂ for more than 1 h. In the absence of H₂ a layer of "carbon" was deposited during the reaction due to hydrocarbon cracking. The most reactive surface (stepped [111] terraces) became covered by an ordered "carbon" layer. The less reactive surfaces had a disordered cover. The presence of H_2 during the reaction seems to reduce the rate of dissociative chemisorption of n-heptane so that dehydrocyclization can compete successfully.

In 1973 H_2/D_2 exchange was studied on low and high Miller index surfaces of Pt single crystals.[182] The [997] and [111] surfaces were studied, and it was found that H–D exchange takes place readily on the stepped surface [997] (Figure 10) but not detectably on the [111] crystal surface. The difference in reactivity was ascribed to the large density of atomic steps present on the high-index surface that are responsible for the dissociation of the diatomic molecules.

McAllister and Hansen studied the decomposition of NH_3 on tungsten single crystal faces and found the order of activities [111] ≫ [100] > [110].[183]

$$2NH_3 \xrightarrow[W]{800-970\ K} N_2 + 3H_2$$
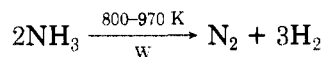
In a study of hydrocarbon adsorption on tungsten and platinum single crystals, dissociation products were shown by field ionization mass spectrometry to migrate on the surface and form deposits at favorable sites.[184]

Cartier and Rye used single crystal studies to yield support for a geometric factor in catalysis.[185] These researchers used a flash desorption technique to study ethylene hydrogenation on W single crystals. H_2 and C_2H_4 were sequentially adsorbed on the metal at a low enough temperature such that no reaction occurred. This was followed by rapid heating and the appearance of ethane in the gas phase measured by mass spectrometry. The amount of ethane produced was actually small since ~99% of the chemisorbed ethylene decomposed, yielding H_2 in the gas phase. Ethane, however, desorbed at a lower temperature than H_2, 170 and 210 K, respectively, on the [110] surface and at lower temperatures on the [111] surface. The Horiuti–Polanyi mechanism, originally proposed in 1934, was invoked to explain the observations. This mechanism where * indicates the metal surface. This mechanism is in

$$\underset{*}{H} + CH_2{-}CH_2 \underset{k_{-1}}{\overset{k_1}{\rightleftharpoons}} \underset{*}{CH_2}{-}CH_3 \qquad (2)$$

$$\underset{*}{CH_2}{-}CH_3 + \underset{*}{H} \xrightarrow{k_2} CH_3{-}CH_{3(g)} \qquad (3)$$
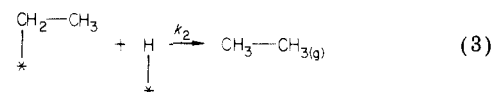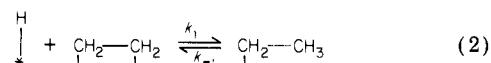
agreement with the crystallographic dependence for the flash hydrogenation. For hydrogenation to occur it was postulated that a transition state

$$\left[\underset{* \longleftarrow r \longrightarrow *}{\overset{CH_2-CH_3}{\diagup \quad \diagdown}} \right]$$
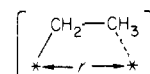
was formed in reaction 2. The probability of this transition state decreases with increasing W–W distance. Shorter W–W distances favor a k_{-1} reverse reaction and lower chance for hydrogenation via reaction 3.

The [111] surface was more active (mass 30 peak appeared at a lower temperature) than the [110] surface. Indeed the W–W distance in a [111] plane is 4.47 Å while in a [110] plane W–W distances of 2.78 and 3.14 Å are present.

A W [110] surface was used for studies of C_2H_4 decomposition by UPS, LEED, and work function methods.[186] In this work features of photoelectron spectra obtained were attributed to C–H, C–C, and C–W bonds in adsorbed species of the form C_2H_2. These measurements were made at room temperature. The work function of the metal surface decreased by 1.2 eV at saturation coverage. When the W [110] was heated with chemisorbed ethylene to about 500 K, C–H bonds were broken with evolution of H_2 gas. However, the C–C and C–M bonds remained intact, and the work function increased by about 0.6 eV. The C–C bonds, according to the UPS studies, were not broken until about 1100 K.

A more detailed study of olefin chemisorption and decomposition by UPS was reported by Demuth and Eastman for a Ni [111] surface.[187] This work was done to determine the importance of πd bonding in hydrocarbon chemisorption. Photoemission valence orbital energy levels for condensed (weakly bound) and chemisorbed hydrocarbons were obtained. Emission intensity (electrons/eV) vs. electron binding energies (eV) plots were made for adsorbed and gas-phase hydrocarbons and comparisons made to determine π and σ orbital levels. Unsaturated hydrocarbons (C_6H_6, C_2H_2, and C_2H_4) upon chemisorption had a slight shift of binding energy of the low-lying σ orbital to a lower value of relative ionization potential. However, upper π orbitals showed a rather large increase in binding energy upon chemisorption, a shift of about 0.9–1.5 eV. Saturated hydrocarbons showed no shifts and were observed to adsorb physically on Ni [111] at temperatures less than 150 K. The spectra of C_2H_4 chemisorbed at 100 K changed upon warming to 230 K to the identical spectra of C_2H_2 chemisorbed. This indicated a thermal activation for dehydrogenation of ethylene. C_2H_2 and C_6H_6 chemisorbed species were stable up to 470 K, above which they completely dehydrogenated to form a carbonaceous layer. From the data obtained it was predicted that the surface reaction
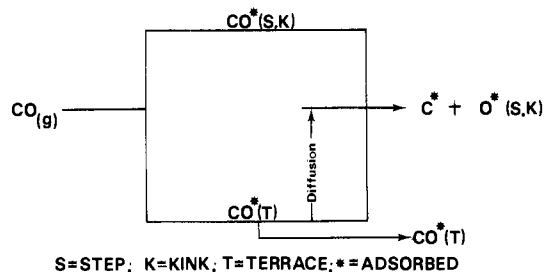
$$C_2H_{4(ads)} \rightarrow C_2H_{2(ads)}$$
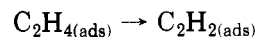
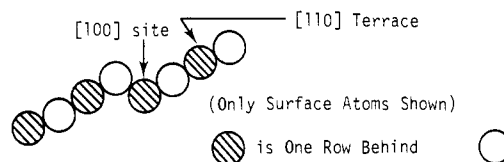**Figure 11.** Adsorption of CO on a Pt surface.[190]

Figure 12. W stepped surface showing N_2 dissociation site (cross section).

**Figure 13.** Side view of stepped Pt(s) [5[111] × [111]] surface.

becomes exothermic because of πd bonding.

Further chemisorption studies were reported by Demuth and Rhodin using LEED, AES, and work function techniques.[188] H_2, O_2, CO, S, Se, and Te adsorption on Ni [111], [110], and [001] surfaces were compared. Three types of adsorption, based on interaction strength with the surface, were categorized. The first is molecular-like adsorption in which the molecule is adsorbed associatively as exemplified by CO on Ni [001], [110], and [111] surfaces at 77 K. The second type of interaction is atomic-like adsorption in which there is strong bonding between adsorbate and substrate but no disruption of the latter. The third type of adsorption is disruptive adsorption in which the surface of the metal is changed by distortion or penetration of adsorbate into the lattice. This phenomenon is characteristic of adsorption above room temperature or at high coverages as, for example, H_2 on Ni [001] or [110] surfaces. It is clear from these studies that the adsorbate, surface crystallography, adsorption temperature, and coverage are specific factors on which the nature of chemisorption of reactive gases depends.

Further studies of CO chemisorption were reported for Pd single crystals.[189] Flash desorption spectroscopy and contact potential measurements were made for adsorption of CO and Pd [111] and [100] surfaces. It was observed that CO formed "close-packed" layers on the surface with an initial activation energy of 34–40 kcal/mol. Adsorption was also studied on stepped surfaces, and it was found that the presence of steps had no effect on the distribution or heats of adsorption of CO. The CO was determined to be located at sites where it can have six or nine nearest neighbors.

In contrast to this report, Somorjai reported a definite effect of steps on the chemisorption of CO on Pt.[190] In a careful UPS study it was found that dissociative adsorption of CO occurs at steps and kinks on Pt surfaces (Figure 2) while associative adsorption occurs at terrace sites. Furthermore, associatively adsorbed CO was found to be able to migrate to a step site and dissociate. The adsorption process can be summarized as shown in Figure 11.

Somorjai's observations supported observations reported in 1974 for adsorption of N_2 on W surfaces.[191] LEED, AES, and UPS studies showed that N_2 on W surfaces exhibiting steps can (1) dissociate at a step site, (2) migrate, or (3) desorb. Steps serve as sites for N_2 dissociation and the atoms produced can migrate out on a terrace. The site of N_2 dissociation was proposed to be at a vacant pair of [100] atoms (step atoms, Figure 12). The dissociatively adsorbed N_2 dissociation was proposed to be at a vacant pair of (100) atoms (step atoms, Figure 12). The dissociatively adsorbed and associatively adsorbed states were observed as low as
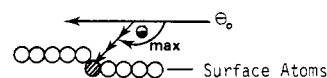
90 K, and desorption energies for the two types of adsorbed states were 320 and 80 kJ mol^{-1}, respectively.

A possible reason for the differences in the CO adsorption studies discussed lies in the results of McCabe and Schmidt reported in 1977.[192] From FDS and AES studies of CO on low Miller index Pt surfaces, activation energies for desorption were determined. The activation energies varied from 26 to 36 kcal mol^{-1}, and impurities were found to have a pronounced effect on the values. Surface oxides altered the desorption temperature significantly but differently on each plane. Impurities may therefore have been responsible for the observations of CO on Pt planes in 1974.[189]

Much more experimental support for the function of special surface features such as steps and kinks was reported during 1974–1979. Chemisorption studies included saturated and unsaturated hydrocarbons and several diatomic molecules. Studies with diatomic molecules will be discussed, followed by hydrocarbon adsorption and reactions.

In 1976 H_2 adsorption on a Pt [111] surface at 150 K was reported.[193] By LEED, ELS, FDS, and contact potential studies it was determined that H_2 adsorbs dissociatively on the low index Pt [111] surface without any measurable activation energy. It was concluded that the role of atomic steps in controlling dissociation is questionable.

In contrast, a strong step influence on H_2–D_2 exchange on Pt surfaces was reported in 1977.[194,195] The reaction

$$H_2 + D_2 \rightarrow 2HD$$
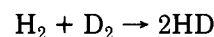
was studied on Pt [111] and Pt (s) [5[111] × [111]] surfaces as a function of incident angle for a molecular beam of H_2/D_2. HD production rate was maximum when the beam was incident on the face of a step (Figure 13, θ_{max}). Steps were found to be seven times more active for HD production than terraces. H_2 dissociated immediately upon impact with the surface so the variations in activity for HD production was attributed to the geometry of the step structure and not an activation energy barrier for adsorption.

Important effects of adsorbed oxygen on high Miller index crystal surfaces were reported in 1976 by Blakely and Somorjai.[1] It was found that chemisorption of C or O_2 can stimulate surface reconstruction. Twenty-two high Miller index planes of Pt were studied. Certain kinked step surfaces were stable when clean and in the presence of adsorbed oxygen but reconstructed to a lower Miller index structure when exposed to carbon. Some surfaces were stable in UHV or a carbon layer but not in the presence of O_2. Many surfaces were surprisingly stable. The implications of these results to
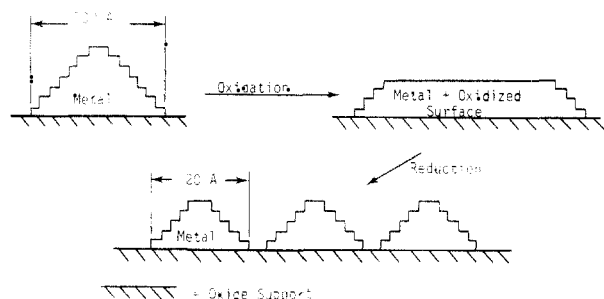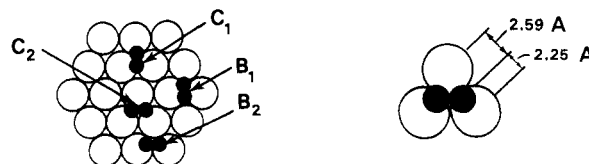
Figure 14. Redispersion of a metal particle.[1]


Figure 15. Adsorption sites of C_2H_2 on Pt [111].[198]

TABLE XII. Structural Parameters of Surface Ethylidyne Complex and Ethylidyne Cluster Compounds[200]

	C-C, Å	C-M, Å	M-M, Å	MCM, deg
Pt [111] ethylidyne surface complex	1.5	2.0	2.77	88
$CH_3CCo_3(CO)_9$	1.53	1.90	2.47	81
$CH_3CRu_3(CO)_9H_3$	1.51	2.08	2.84	86

heterogeneous catalysis must be discussed. Few surfaces were stable under oxidizing, reducing, and UHV conditions employed; rather, most faces changed their surface structures with change in environment. This suggests that "stable" surface structures play an important role in catalysis since these retain activity under a variety of drastic environmental changes such as O_2/H_2 cycles. In dispersed catalysts, changes in the surface structure of the metal particles may alter reaction rates and product distributions of surface reactions. Changes in catalytic specific activity with particle size, as has been observed for certain reactions, may be due to changes in the surface structure of the particles with size. In view of the effects of environment on surface reconstruction it was proposed that the nature of the support used in a catalyst may influence the type of surface features that are stable. Oxidation had been observed to decrease catalytic activity in most systems and was generally attributed to site blockage by oxygen. In light of these studies, in addition to site blockage, reconstruction of particle shapes may be a significant effect. This surface reconstruction phenomenon can be used to explain another important process in catalysis. It has been demonstrated that oxidation–reduction cycles at high temperatures can be used to redisperse large metal particles (e.g., Pt on Al_2O_3) $\geq$ 100 Å into small particles $\leq$20 Å on high surface area supports.[196] Somorjai suggested that the lower surface tension of a metal oxide than that of a metal causes a flattened structure to be formed from a semispherical particle of the reduced metal which is readily reconstructed into smaller semispherical structures upon reduction of the oxidized structures, as shown in Figure 14.[1] An additional fact supporting the effects of oxidizing and reducing atmospheres on reconstruction is that the presence of a small amount (~1%) of HCl or Cl_2 in the reducing gas speeds the dispersion.

Somorjai further pointed out that the surfaces which were stable toward reconstruction were those that had either a high density of periodic one-atom-high steps or a complete lack of steps.[168] Also, most of the observed reconstruction processes were reversible. The main lesson to be learned from these studies is that the atomic surface structure of a freshly prepared catalyst is drastically changed under reaction conditions.

Studies dealing with the effect of surface structures on chemisorption of saturated and unsaturated hydrocarbons were first reported in 1974.[197] The following surfaces were studied: (1) Pt(s) [9[111] × [100]], (2) Pt(s) [6[111] × [100]], (3) Pt(s) [7[111] × [310]], and (4) Pt(s) [4[111] × [100]]. Surfaces 1–3 were stable toward reconstruction in H_2 and hydrocarbon atmospheres at 25–1000 °C. Chemisorption of ethylene,

benzene, and toluene produced carbonaceous deposits. On surfaces 1 and 2 the deposits had ordered structures while on surface 3 a disordered structure resulted. The [310] plane of surface 3 results in a high concentration of kinks in the steps. From these and other results it was postulated that upon chemisorption of a hydrocarbon, saturated or unsaturated, on the Pt surfaces any of four processes can occur: (a) nucleation and growth of an ordered "carbon" surface structure, (b) dehydrogenation, (c) decomposition of organic molecules (e.g., C-C bond breaking), and (d) rearrangement of the substrate (reconstruction). On surfaces 1 and 2 processes a and b predominated; on surface 3 process c and on surface 4 process d predominated.

Prior to 1976 the only information obtainable about adsorbed hydrocarbons on metal surfaces by the LEED technique was the order of the molecules. No information could be obtained about the atomic geometry of the adsorbed molecule. In 1976 Somorjai reported that "surface crystallography" could be achieved with LEED.[198,199] Diffraction spots vs. incident beam energy profiles can be used to calculate interatomic distances normal to the surface of the two dimensional unit cells. This is possible because the I-V profiles are very sensitive to geometric spacings so that computer simulation can be achieved, resulting in accuracies up to 0.1 Å in atomic positions. Somorjai exploited this feature of the LEED technique by studying, in more detail than previously possible, the chemisorption of C_2H_2 on a Pt surface.[198] In addition to observing an ordered 2 × 2 chemisorbed layer of acetylene on Pt [111], the relative geometries of adsorption sites were predicted. A Pt [111] surface was exposed to C_2H_2 at 300 K followed by gentle heating to 400 K for 1 h. With I-V profiles of the adsorbed layer it was determined that the molecules adsorbed in either a threefold position or a twofold bridge position (Figure 15) at a distance 1.95 ± 0.1 Å above the topmost plane of Pt atoms.

Further detail of C_2H_2 chemisorbed species was elucidated in 1978 by LEED, UPS, and ELS methods.[200] By use of LEED I-V profiles from experimental data and those calculated by assuming geometries, best fit was obtained for an ethylidyne surface complex.
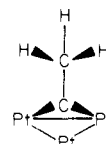
Comparison of structural data for the ethylidyne surface complex with similar species in cluster compounds was made as shown in Table XII. These data and vibrational frequencies obtained by ELS strongly support the existence of ethylidyne surface complexes.

Ethylene and acetylene chemisorption was studied on Ni [111] and Fe [100] surfaces by UPS, LEED, and AES methods.[201-203] C_2H_4 chemisorbed on Fe [100] surfaces was studied by UPS, LEED, and AES, and no evidence for C_2H_2 adsorbed species was obtained.[202] Spectral features obtained at 123 K indicated the presence of mainly CH_2 fragments. Weakly bound C_2H_2 was observed to be bonded to a layer of dissociated acetylene fragments on the Fe [100] surface. The ease of C–C cleavage was attributed to πd bonding interactions, resulting in "stretching" of the adsorbate molecule to the extent of breakage. This multilayer structure was observed even at the low temperature of 98 K. C_2H_2, C_2H_4, and C_2H_3F chemisorption studies on Ni [100] surfaces at 77–423 K were reported.[203] Ethylene chemisorbed on Ni [100] had the same UPS spectra as acetylene on this surface. Support was drawn from the literature for dissociative chemisorption. It was pointed out that UPS studies of C_2H_4 chemisorption on Ni [111] surfaces and polycrystalline Ni revealed that C_2H_4, physisorbed at 77 K, dissociated to C_2H_2 adsorbed species upon warming to 230 K. C_2H_3F formed acetylenic residues on Ni [100] by elimination of HF. CH_4 chemisorbed dissociatively on Ni [110] at 473–579 K, forming an ordered 2 × 3 surface layer.[204]

Support for Boudart's categorization of "demanding" and "facile" reactions on metal surfaces was reported for studies of reactions on single crystal surfaces. In 1974 Somorjai and co-workers showed that similar results could be obtained for catalytic studies on dispersed supported metal catalysts and single crystal surfaces.[205] The hydrogenolysis of cyclopropane

$$c\text{-}C_3H_6 + H_2 \xrightarrow[\text{catalyst}]{} C_3H_8$$
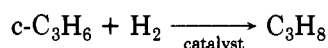
was studied on stepped Pt surfaces at 1 atm of pressure by using a special apparatus allowing high pressure and UHV conditions on the sample without its movement or contamination. An activation energy for the reaction on a Pt(s) [6[111] × [200]] stepped surface was found to be 12.2 ± 1.0 kcal mol^{-1}. Values obtained for the reaction on dispersed Pt catalysts were reported as 8.0–12.2 kcal mol^{-1}. By converting initial rate data reported in the literature for the reaction on dispersed Pt catalysts to the conditions of 75 °C and 135 torr of cyclopropane pressure agreement within 20% was obtained. This provided support that single crystals may be excellent models for polycrystalline supported metal catalysts. It was assumed that cyclopropane hydrogenolysis was a facile reaction which resulted in similar rates for very different surfaces. Structure insensitive and structure sensitive reactions reported in the literature were summarized by Somorjai and are shown in Table XIII.

In 1976 Somorjai reported that some reactions are sensitive to the structure of carbonaceous layers on the surface.[206] Sensitivity to structure was indicated by the effect of kink density in a stepped surface on reaction rates. The influence of a carbonaceous overlayer on activity was determined by studying surfaces with ordered and disordered layers. The reactions shown in

TABLE XIII. Reaction Structure Sensitivity[205]

Structure-Insensitive Reactions
(a) benzene hydrogenation on Pt/SiO$_2$
(b) dehydrogenation of cyclohexane, hydrogenation of cyclopentane, H$_2$–D$_2$ exchange on Pt/SiO$_2$
(c) cyclopropane hydrogenolysis on Pt/Al$_2$O$_3$, Pt/SiO$_2$ and Pt powder
(d) ethylene hydrogenation on Pt/SiO$_2$

Structure-Sensitive Reactions
(a) ethane hydrogenolysis on Ni/SiO$_2$–Al$_2$O$_3$ and Rh/SiO$_2$
(b) neopentane hydrogenolysis and isomerization on Pt/Al$_2$O$_3$, Pt/SiO$_2$, and Pt powder
(c) hydrogenolysis of methylcyclopentane on Pt/Al$_2$O$_3$ and Pt/SiO$_2$
(d) hydrogenation of 1,2- and 1,3-butadiene on Ni/Al$_2$O$_3$, Ni/SiO$_2$, and Ni powder
(e) hydrogenation of benzene on Ni/SiO$_2$

TABLE XIV. Classification of Reactions by Step Density and Carbonaceous Overlayer Dependence[206]
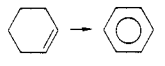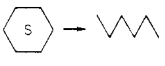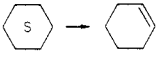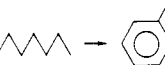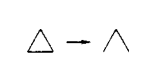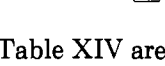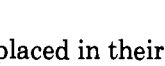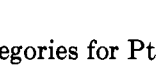
step structure sensitive		step structure insensitive	
overlayer structure sensitive	overlayer structure insensitive	overlayer structure sensitive	overlayer structure insensitive
⬡ → ⬡	⬡(s) → ∕∖∕∖	–	⬡(s) → ⬡
∕∖∕∖ → ⬡		–	△ → ∧

Table XIV are placed in their proper categories for Pt single crystal surfaces. It was pointed out that structure sensitivity may not be observed for dispersed catalysts since particles of any size will always contain many steplike atoms of low coordination so structure insensitivity may be observed.

Falicov reported theoretical studies of stepped surface structures of Pt.[207] Corner and step "ledge" atoms were shown to have a variety of charge lobes (only angular distributions considered) not present on terrace atoms. This enhanced variety of available orbital symmetries was postulated as the major cause for the enhanced reactivity of these features.

In summary, the general implications of these single crystal studies should be pointed out. Structural features which allow atoms to be in low coordination states provide enhanced reactivity for C–H and C–C bond-breaking processes over higher coordination sites such as terraces. Some reactions may occur with low activation energies or little geometric requirements and thus show structure insensitivity. Other reactions may be more difficult and require special surface features such as steps and kinks. Adsorbed impurities or carbonaceous layers may affect catalytic activity or selectivity by acting as promotors, inhibitors, or creating sites where desorption of products may occur readily (e.g., carbonaceous covered terrace site). Single crystal catalytic studies can be carried out at low pressures or high pressures of reactant gases, which minimize the extrapolation necessary to the conditions employed in industry.

B. Metal Films

Metal films have been used, for reasons already discussed, to obtain information about heats of adsorption of hydrocarbons in addition to probing mechanisms of chemisorptive and catalytic processes. Anderson and

TABLE XV. Heat of Chemisorption of H_2 on Nickel Films and Single Ni Crystal Faces[173]

surface	temp, K	ΔH_{ads}, kcal mol^{-1}	method
film	298	16–30^a	calorimetry
film	77	18	calorimetry
[100]	298	23.1	thermal desorption
[110]	282	20.3	thermal desorption
[111]	298	21.4	isothermal
filament	279	52.6	calorimetry
filament	86	38.2	calorimetry

^{a} Range of several studies.

TABLE XVI. Heat of Chemisorption of O_2 on Ni Films

temp, K	ΔH_{ads},^{a} kcal mol^{-1}	method
298	120–130	calorimetry
298	115	calorimetry
298	107	calorimetry
273	76–89	
90	71	
77	70	

^{a} Each entry represents a separate study.

Baker reviewed catalytic reactions on metal films in 1971.[208] In this section the subject is treated with discussions of chemisorption of a variety of molecules followed by surface reactions such as cracking, hydrogenolysis, skeletal isomerization and exchange reactions. Unsaturated hydrocarbon reactions are discussed first, followed by reactions of saturated hydrocarbons. Highlights from the literature of the period of ~1940 to 1979 are presented.

A few inorganic molecules chemisorbed on metal films warrant discussion due to their presence under the conditions employed in this research.

Somorjai and Toyoshima presented a recent comprehensive review of chemisorption data obtained for H_2, O_2, CO, and CO_2 on a variety of metal surfaces.[173] Due to the presence of many possible "binding states" of an adsorbed molecule on a metal surface, heats of adsorption (ΔH_{ads}) may vary by 20 kcal mol^{-1}. Therefore it is difficult to assess a single value for the heat of chemisorption of an adsorbate on a given transition metal. Nevertheless, remarkable agreement of ΔH_{ads} values for H_2 chemisorption on Ni films and single crystals arises upon data comparison, as shown in Table XV. Agreement in ΔH_{ads} of H_2 is found by using different methods as well as for different surfaces. Table XVI shows data for O_2 chemisorption on Ni films. The variation in the values is much more pronounced than in the case of H_2 chemisorption. ΔH_{ads} of CO and CO_2 on Ni films of 17–42 and 44–54 kcal mol^{-1}, respectively, were reported.[173]

Many studies of CO chemisorption on transition metals have been reported due to the importance of reaction 4. Identification of intermediates in this reaction have been pursued for many decades. Two likely species of adsorbed CO have been the subject of intense debates. These are a linearly bound CO or a bridged structure.

$$CO + H_2 \rightarrow CH_4 + H_2O + >C_1 \text{ hydrocarbons} \quad (4)$$
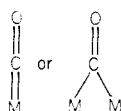
TABLE XVII. CH_4 Adsorption on Ni Films[208]

| film preparation conditions^b	temp, °C	surface occupation^a	relative adsorption rate	E_{act}, kcal mol^{-1}
0 °C deposition (HV)	−78–70	no adsorption		
0 °C deposition (HV)	140–260	0–10%	slow	~11
0 °C deposition (HV)	140–200	0–9%	slow	~10
250 °C deposition (UHV)	50–250	0–0.1%	slow	~1

^{a} Percentages give number of adsorbed molecules per 100 surface metal atoms. ^{b} HV = high vacuum; UHV = ultrahigh vacuum.

Presently there is support for both species on metal surfaces along with dissociative forms and even formation of gaseous carbonyl compounds such as Ni(CO)$_4$.[209] A recent study of reaction 4 on Rh foil at 300 °C was reported which yielded results in terms of product distributions that agreed well with data obtained on dispersed Rh catalysts.[210] Under all conditions (250–350 °C, H_2/CO ≥ 3:1) methane was the major product (>80%) isolated; small amounts of C_2–C_3 hydrocarbons were also obtained. The apparent activation energy for the reaction on Rh foil is 24 ± 3 kcal mol^{-1}. Hydrogenation of CO_2 was found to yield 100% CH_4 over Rh foil with an activation energy of 16 ± 2 kcal mol^{-1}.

Mercury vapor has created many problems in catalysis research through its role as a poison.[11] The importance of isolating a metal catalyst from mercury sources can be stressed by citing an investigation of Hg adsorption on a Ni film at room temperature.[211] It was found that a Ni film with prior exposure to Hg vapor could not adsorb H_2. Furthermore when Hg was exposed to a film containing preadsorbed hydrogen, 88% of the H_2 was displaced.

The last inorganic molecule to be considered here is H_2O. A study in 1975 revealed that H_2O adsorbs on Ni and V films at 77 K without dissociation.[212] Upon warming to 273 K, however, H_2O decomposition occurs which can be aided by addition of a Lewis acid coadsorbate such as BF_3.

The adsorption of methane on metal films has been reviewed.[208] Data obtained from this review for CH_4 adsorption on Ni films is presented in Table XVII. It has been observed that a low activation energy process which is rapid for methane adsorption occurs on many metals (W, Mo, Cr, Ir, Rh, and Ti) at low coverages (<10%) followed by an activated process at higher coverages.[208] The "fast" process is probably the reaction
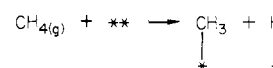

in which * indicates a surface adsorption site. The activated process involves more extensive dehydrogenation to $CH_{2(ads)}$, $CH_{(ads)}$, and ultimate $C_{(ads)}$. These secondary processes make thermodynamic studies very difficult since gas–surface equilibrium and equilibrium distribution of the various dehydrogenated states are difficult to assess.

Ethane adsorption on Ni films at −78 to 70 °C showed an initially low energy process at coverages up to 2% followed by an activated process at higher coverages.[208] In general it has been observed that ethane adsorbs more readily than methane on most metals, presumably due to the lower C–H bond strength in ethane vs. methane. In the case of ethane as well as other saturated hydrocarbons, C–H cleavage can be followed by C–C cleavage on metal films, as will be shown when hydrogenolysis is considered. Saturated hydrocarbons with three or more carbons all have nearly the same ΔH_{ads}.

Unsaturated hydrocarbons such as ethylene strongly adsorb on transition metals.[208] Upon chemisorption, ethylene dehydrogenates rapidly to acetylenic type surface species, as was shown for chemisorption on single metal surfaces. At low coverage the reaction
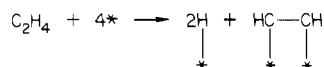
occurs. At higher coverages ethane appears in the gas phase due to self-hydrogenation. Beeck showed by ethylene hydrogenation studies that the reaction

$$H_{(ads)} + C_2H_{4(ads)} \rightarrow C_2H_{6(g)}$$
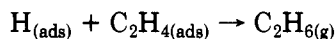
is slow.[213] The reaction

$$H_{(ads)} + C_2H_{4(g)} \rightarrow C_2H_{6(g)}$$
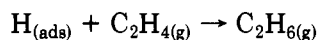
is, however, nearly instantaneous. Jenkins and Rideal used Beeck's observations to support a mechanism for the self-hydrogenation of ethylene on Ni films at 20 °C.[214]

They concluded that ethane formation at higher coverages resulted from reaction between gas-phase ethylene and adsorbed hydrogen atoms (from dehydrogenation of initially adsorbed ethylene). The lack of ethane formation at low coverages suggests that adsorbed hydrogen and adsorbed acetylenic type "surface complexes" can coexist. Ethylene was shown to exclusively chemisorb by dissociation of C–H bonds in an irreversible process.

At high coverages of C_2H_4 there is evidence for a concomitant nondissociative adsorption occurring.[208] This is implied by a decrease in ΔH_{ads} with an increase in coverage. This decrease results from a greater contribution of the nondissociative adsorption to the observed ΔH_{ads} at the higher coverages. The relative reactivities of transition metals toward olefin adsorption can be seen by comparing ΔH_{ads} at low coverages of ethylene: (Ta, W, Cr) > 100 kcal mol⁻¹, (Fe, Ni, Rh) 50–70 kcal mol⁻¹, and (Cu, Au) ∼ 20 kcal mol⁻¹.

Studies of benzene adsorption on metal films have shown that initial ΔH_{ads} is about one-half of the corresponding value for olefin adsorption.[208] Dissociative chemisorption has been observed on Fe, Ni, and Pt, but the loss of hydrogen is much less for benzene than ethylene. The nondissociative adsorption of benzene is thought to result in a πd metal bonding complex on the surface. This type of bonding may also occur in nondissociatively adsorbed olefins.

Butane and higher hydrocarbons in addition to ethane have been observed in the gas phase following hydrogenation of surface complexes of chemisorbed ethylene.[208] This observation, in addition to the observation of reduction in hydrogenation rates with time,

has led to the conclusion that surface polymerization of the acetylenic-type species can occur. Poilblanc and co-workers showed that ethylene could be adsorbed and then hydrogenated to release all of the surface species in the form of ethane when the surface (Ni film) was precovered with CO.[215] Without the CO pretreatment a significant amount of "carbon" remained on the surface after hydrogenation of the adsorbed ethylene. It was suggested that CO acts as an inhibitor to polymerization. Pretreatment of the surface with hydrogen was postulated to promote a nondissociative form for chemisorbed olefins.
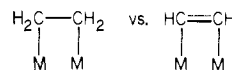

Evidence for C–C bond cleavages of adsorbed olefins at elevated temperatures will be considered in the next section on metal powders.

The practical implication of the above studies is that by adsorbing H_2 or CO on a metal catalyst prior to hydrogenation of an olefin, fouling of the catalyst by carbonaceous deposits is hindered. This is not the case, however, for the methanation reaction (eq 4). In this reaction adsorbed carbon is a likely intermediate, as shown by Araki and Ponec.[216] A nickel catalyst, which was precarbided, had a higher initial methanation rate than one without this pretreatment.

The exchange reaction between saturated hydrocarbons and deuterium on metal films has been reviewed by Bond and discussed by Anderson and Baker.[11,208] In this discussion correlations made by Anderson and Baker in 1971 and results from some more recent studies will be used.

From the work of Kemball and co-workers in the late 1950s mechanisms for the exchange reaction between deuterium and methane on transition metals were suggested that were in accord with product distributions obtained experimentally.[208] On polycrystalline films of Rh, Ni, Pt, W, and Pd the reaction

$$CH_4 + D_2 \xrightarrow{\text{metal}} CH_xD_y$$
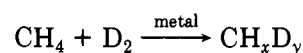
$$x = 1, 2, 3, \text{ or } 4; y = 4 - x$$

gave CH_3D and CD_4 as major products, with lesser amounts of CH_2D_2 and CHD_3 obtained. The activation energy for the formation of CH_3D was found to be significantly lower than that for CH_2D_2, CHD_3, and CD_4, which had similar activation energies. Since the surface species $CH_{2(ads)}$, $CH_{(ads)}$, and $C_{(ads)}$ have much different stabilities, formation of CH_2D_2, CHD_3, and CD_4 directly from these species is improbable. The predominance of CH_3D in the reaction products seems to be due to a lower activation energy for monodeuteration and a higher activation energy for $CH_{3(ads)} \rightarrow CH_{2(ads)}$ than CH_4(physically adsorbed) $\rightarrow CH_{3(ads)}$. The higher deuterated products may arise by an "interresidue hydrogen transfer" reaction:

$$2CH_{2(ads)} \rightarrow CH_{(ads)} + CH_{3(ads)}$$

which passes through an intermediate such as
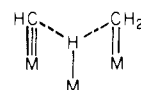
Ethane undergoes exchange much more readily than methane on all metals studied. Differences in exchange product distributions and rates among higher hydrocarbons are less, and trends cannot be detected due to interfering factors such as residue buildups which mask these subtle changes. Polycrystalline Ni films deposited at 0 °C were used for C_2H_6/D_2 exchange reactions at 0 °C. The products obtained were 98% C_2H_5D and 2% $C_2H_4D_2$. On other metals different results have been observed, but no trends could be given due to the reasons just mentioned. Multiple exchange to produce more highly deuterated products was proposed to occur by repeated processes of the type

$$C_2H_6(g) \rightleftharpoons \underset{M}{C_2H_5} \rightleftharpoons \underset{M}{H_2C} - \underset{M}{CH_2}$$
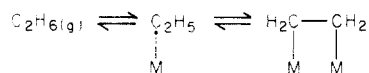
Support for this type of interconversion process comes from the observations that the formation of highly deuterated products is inhibited by high D_2/C_2H_6 ratios (D_2 acts as an inhibitor), and an increase in monodeuterated products occurs upon surface poisoning by carbonaceous residues.[208] Mechanistic conclusions for D_2 exchange with $\leq C_3$ hydrocarbons are supported in large part by agreement with theoretical product distribution calculations that take into account the various equilibria involved. For hydrocarbons with more than three carbons the theoretical treatment is too complicated due to an increase in variables.

Propane–deuterium exchange was observed as low as −47 °C on nickel films, with propane-d being the major product at this temperature.[217] The secondary hydrogens were found to exchange about 10 times faster than primary hydrogens. A few mechanistic intermediates have been proposed for the active surface species in these reactions. The first intermediate is a residue bound to the surface by more than two carbons such as
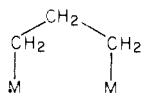
$$\underset{M}{CH_2} - \underset{M}{CH} - \underset{M}{CH_2}$$
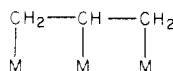
The second is a π-allyl type intermediate of the type

$$CH_2 \overset{CH}{\diagdown} \underset{M}{|} CH_2$$
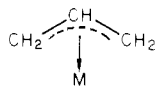
The third is the already mentioned 1,2-diadsorbed species

$$\underset{M}{CH_2} - \underset{M}{CH} \diagdown^{CH_3}$$
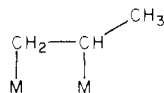
The fourth possibility is a 1,3-diadsorbed species of the type

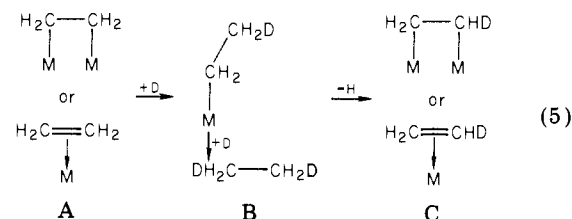$$\overset{CH_2}{\diagdown} \underset{M}{CH_2} \overset{\diagup}{\diagdown} \underset{M}{CH_2}$$

This latter intermediate is not likely, at least on Ni/kieselguhr catalysts, since exchange between D_2 and 3,3-dimethylhexane resulted in negligible exchange in the quaternary methyl groups.[208] There is support for all three of the other intermediates on various metals and under various conditions. It is difficult to prove the existence of any of the possible intermediates.

However, there seems to be support shifting toward π-bonded type intermediates in more recent studies, especially at elevated temperatures. Kemball has suggested that π-bonded intermediates result in a greater amount of isomerization vs. exchange than σ-bonded species during reactions of polymethylcyclopentanes with deuterium on nickel films.[218] The isomerizations in these reactions result from methyl groups changing sides of the cyclopentane plane and are aided by π-bonded intermediates which bring methyl groups into the ring plane.

Hydrogenation of olefins on metal films has been studied extensively for ethylene and propylene; however, higher olefins have not been studied in depth. The more recent studies of olefin hydrogenation, isomerization, and D_2 exchange reactions have used π-bonded intermediates in mechanistic interpretations of results. Kemball found an activation energy of 7 kcal mol^{-1} for ethylene hydrogenation on a nickel film at −120 °C, and similar activation energies have been reported for the reaction on Ni powder, wire, and supported catalysts at various temperatures.[208] The important point to be brought out is that the nondissociative form of the olefin is believed to be an intermediate in hydrogenation reactions. The intermediate may be a σ-diadsorbed, π-adsorbed, or π-allyl-adsorbed species.

Due to discrepancies in results by different workers detailed mechanisms of D_2/olefin exchange cannot be given. Anderson and Baker gave a general mechanism which supports most of the data obtained for reactions on nickel films.[208] This mechanism is shown in reaction 5 where D and H represent active "hydrogen" species,

$$\underset{A}{\left. \begin{matrix} \underset{M}{H_2C} - \underset{M}{CH_2} \\ \text{or} \\ \underset{M}{H_2C} = \underset{M}{CH_2} \end{matrix} \right\}} \xrightarrow{+D} \underset{B}{\left. \begin{matrix} \overset{CH_2D}{\diagup} \\ \underset{M}{CH_2} \\ \underset{+D}{\downarrow} \\ DH_2C - CH_2D \end{matrix} \right\}} \xrightarrow{-H} \underset{C}{\left. \begin{matrix} \underset{M}{H_2C} - \underset{M}{CHD} \\ \text{or} \\ \underset{M}{H_2C} = CHD \end{matrix} \right\}} \quad (5)$$

the source of which is not perfectly clear and, therefore, not indicated. Nickel films catalyze multiple olefin exchange readily even at −100 °C. The multiple exchange presumably arises from a rapid rate for A → B and B → C processes creating half-hydrogenated species containing different amounts of deuterium.

Deuterium exchange with alkylbenzenes has been studied on many transition-metal films.[208] Apparently two different mechanisms operate for exchange of ring hydrogens and exchange of side group hydrogens. The ring hydrogens are exchanged at a much lower rate than alkyl group hydrogens on nickel films that have been sintered at 200 °C for 30 min after deposition at 0 °C. However, no such differences were found when unsintered films were used. It seems that certain structural sites on the surface are needed for exchange of the ring hydrogens. For side chain exchange, hydrogens on carbons α to the ring are by far the most reactive probably due to the lower C–H bond energies of the former. Proposed mechanisms for ring and side group hydrogen exchange with deuterium are shown in Figures 16 and 17.[208] For exchange of ring hydrogens, as shown in Figure 16, dissociative (A) and nondissociative (B) bonding modes of surface complexes can be visualized. It has been proposed that π bonding of the
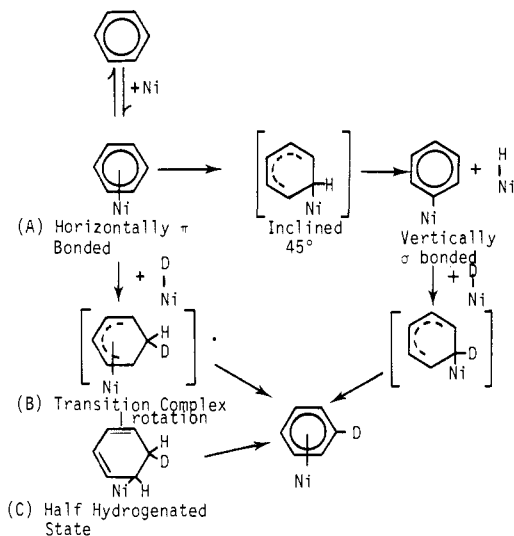
**Figure 16.** H-D exchange of benzene ring hydrogens on Ni films.[208]
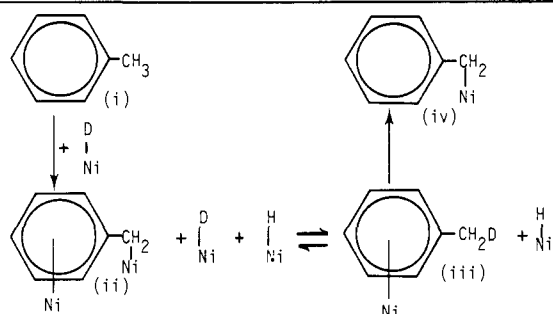
Figure 17. H-D exchange of α-carbon hydrogens on alkylbenzenes over Ni films.[208]

benzene ring to a nickel surface may be important in order to hold the ring flat on the surface so that bonding to the side chain carbons can be achieved (Figure 17).

Hydrogenation of benzene on nickel films at 20 °C has been found to proceed with an activation energy of 8.7 kcal mol⁻¹. Vapor phase hydrogenation of benzene and toluene over evaporated nickel films at 90 °C was found to be accompanied by some poisoning of the catalyst surface by "hydrocarbon residues".[208]

Studies of hydrogenation of benzene from -34 to 50 °C have shown that the slow step in the process is the formation of a $C_6H_{8(ads)}$ species. This intermediate can rapidly hydrogenate to cyclohexane. In fact, it was observed that hydrogenation of cyclohexene is 200 times faster than that of benzene at -34 °C on nickel films. The poisoning previously mentioned was proposed, in 1968, to be due to C–H bond cleavages resulting in formation of a carbonaceous residue consisting of multiply bonded C_6H_x rings.[208]

$$C_6H_{6(g)} \rightleftharpoons C_6H_{6-n(ads)} + nH_{(ads)}$$
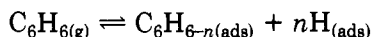
At elevated temperatures (~ 200 °C) the reaction is accompanied by hydrogenolysis to C_1–C_6 alkanes.

Hydrogenolysis will be considered, from this point on, to be any reaction involving C–C bond cleavage on a metal surface in the presence of hydrogen to yield products containing fewer carbon atoms than the parent molecule. The source of hydrogen can be from dehydrogenation of hydrocarbons or an external source. In most instances hydrogenolysis is accompanied by skeletal isomerization and cyclization processes.
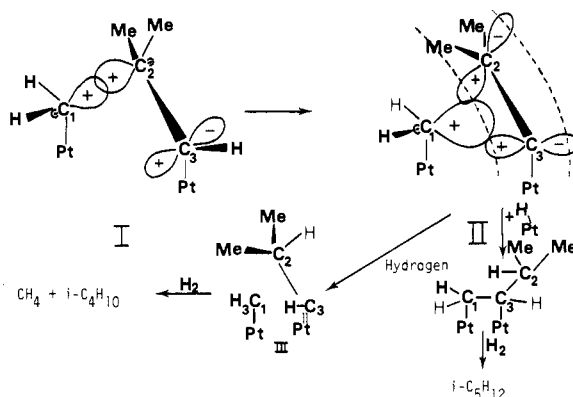

Figure 18. Bond shift mechanism.[208]

Therefore all three reaction paths will be considered. Anderson and Baker presented a review of these reactions on metal films in 1971, results of which will make up a large portion of the following discussion.[208]

When a normal, branched, or cyclic alkane is exposed to a metal surface in the presence of hydrogen, three major processes can occur: (1) isomerization, (2) cyclization (or dehydrocyclization), and (3) hydrogenolysis. Processes 1 and 3 involve the rupture of C–C bonds. From analysis of reaction products obtained for many alkanes on many metals two distinct mechanisms for skeletal isomerizations have become apparent. The first is a bond shift mechanism that usually seems to occur via a 1,3-diadsorbed intermediate. The second involves a carbocyclic intermediate that becomes important when a five- or six-membered ring can be formed. These two types of processes can occur simultaneously or consecutively, giving rise to a large diversity of products. Hydrogenolysis is a competitive process which leads to products containing a fewer number of carbon atoms than the parent compound. Cyclization processes can be considered as specific cases of skeletal isomerization since the number of carbon atoms in the products is the same as that in the parent alkane.

The most prominent mechanism used to interpret distributions of isomerization products from the reaction of butanes and neopentane on transition-metal films is the bond shift process. The skeletal isomerization of these alkanes on transition-metal films (Pt) was first demonstrated by Anderson and Avery in 1963.[220] These authors later proposed a bond shift mechanism for neopentane isomerization which involves a 1,3-diadsorbed intermediate.[221,222]
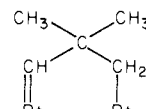
1,3-diadsorbed species

The formation of this species was proposed to be via a process as shown in Figure 18 (I and II) which follows dissociative adsorption of the alkane on the metal surface.[208] Additional interaction of hydrogen with the intermediate (II) was proposed to lead to adsorbed hydrogenolysis products (III). In Figure 18 (I) C_1 and C_2 are sp³ hybridized but C_3 is sp² hybridized and bound to the Pt surface via a double bond. Surface species I then rehybridizes at C_2 from sp³ to sp², and a π system is formed that extends from C_2 to C_3 to the metal surface (II) (dotted lines). The probability that isom-

TABLE XVlll. Reaction of Neopentane and H_2 over a Pt Film[221]

activation energy, kcal mol⁻¹	log A	product distribution, %								% conversion
		CH_4	C_2H_6	C_3H_8	$i\text{-}C_4H_{10}$	$n\text{-}C_4H_{10}$	$i\text{-}C_5H_{12}$	$n\text{-}C_5H_{12}$		
21 (<270 C)	21.2 (<270 °C)	14	5	4	10	3	59	5		78

Table XIX. Isomerization Products from Hexanes over Pt and Ni Films

metal	temp, °C	initial C_6 products, mol %								total convn, %
		$(CH_3)_2CH\text{-}(CH_2)_2CH_3$	$CH_3CH_2CH(CH_3)\text{-}CH_2CH_3$	$(CH_3)_2CHCH(CH_3)_2$, $c\text{-}C_6H_{10}$, $n\text{-}C_6H_{14}$	$(CH_3)_3C\text{-}CH_2CH_3$	$c\text{-}C_5H_9CH_3$	$c\text{-}C_6H_{12}$	C_6H_6		
Pt^a	281		23.2	0	0.1	58.2	0	0		
Pt^a	274	28.4	14.5	0	0	43.6	5.0	8.5	9.5^c	
Pt^b	273	12.5	5.6	0	0	72.4				3.3
Ni^b	273	11.6	26.6	0	0	0	61.8			0.6

^{a} Reference 208. ^{b} Reference 224. ^{c} Cyclohexane + benzene.

erization will occur via this mechanism is thought to be governed by the relative energy of II as compared with I. The bridged surface species II is stabilized by a partial electron transfer from the organic residue to the metal surface atom. The fact that platinum stands out among the transition metals in its selectivity for isomerization can be used to support this mechanism. An isolated platinum atom has an electronegativity of 2.2, and an sp^2-hybridized carbon atom has a value of 1.7. This difference is enough to cause a stabilization of the bridged structure and allow isomerization to proceed favorably. In contrast, nickel is much poorer for isomerization of alkanes, and this may be due to the much lower electronegativity of isolated nickel atoms (1.8). In addition to the influence of the metal, the structure of the alkane plays a role in isomerization activity. The activity of isomerization on platinum films is neopentane > isobutane > n-butane. This is due, in part, to the influence of hyperconjugation in the methyl groups.

In addition to the effect of the metal used and the alkane structure on isomerization activity, there is evidence that structural criteria of the metal surface may be important. Anderson and Avery showed that the rate of isobutane isomerization on platinum films was greatly enhanced when carried out on an epitaxially grown film exposing [111] planes as compared with a polycrystalline film.[221] Also, this enhancement was not observed when a [100] surface was used. It was suggested that for isoalkane isomerization on platinum (111) surfaces a triadsorbed species is the intermediate.
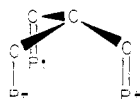
This structure happens to fit very well on a triangular array of atoms in a Pt[111] plane. The enhanced activity that results from such an intermediate is apparent from a statistical standpoint and by the extent to which electron removal from the π system of the bridged structure is facilitated.

It must be noted that interpretation of initial product distributions from these isomerization reactions often requires the proposal of two or more consecutive bond shifts. This is illustrated in Table XVIII by the formation of n-pentane from neopentane.[221] Since the products listed are initial distributions, it is assumed

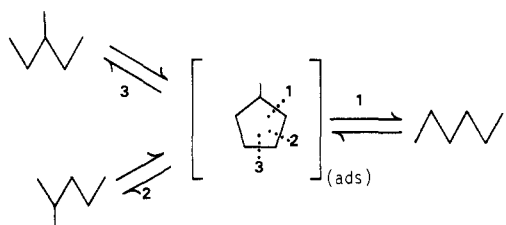Table XX. $(CH_3)_2C^*H(CH_2)_2CH_3$ + H_2 over Pt Films[208]

initial distribution of ^{13}C labels (*) in Hexane products

that they are the result of reactions occurring during a single visit to the surface.

In 1976, Taylor and Clarke suggested that a different mechanism may be operating for isomerization of neopentane than for that of isobutane.[223] This conclusion resulted from the observations that catalytic activity for isomerization of isobutane is general among transition-metal films, with only Mn, Fe, and Co showing negligible activity. In contrast, neopentane isomerization only occurs to a large extent on platinum films. Platinum, therefore, stands out as unique in its activity in isomerization at quaternary carbon centers. While a 1,3-diadsorbed species may be a common intermediate to both reactions as discussed, it was also suggested that on platinum a carbenium ion type mechanism may operate since increased branching of the alkane increases the rate of isomerization. A carbenium ion type intermediate can be visualized as an extreme case of electron withdrawal by platinum from the hydrocarbon residue II of Figure 18.

No support was given by Taylor and Clarke for a carbenium ion type mechanism other than the observation of an increased reaction rate with increased alkane branching. This dependence on alkane structure was not observed on any other metal employed. They did not think that this type of mechanism was likely; however, it could not be ruled out.

Higher alkanes, containing five or more carbons in a chain, can isomerize to products by way of a cyclic intermediate. This is apparent from Table XIX, which shows the formation of methylcyclopentane to be the major process in isomerization of n-hexane and 2-
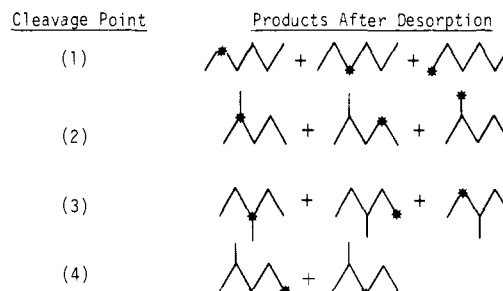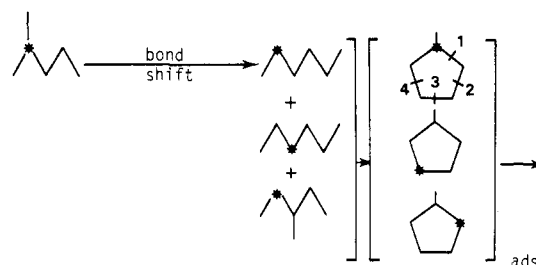
Figure 19. Isomerization of hexanes via a carbocyclic mechanism.[208]

Figure 20. Bond shift–carbocyclic combination mechanism for isomerization of 2-methylpentane-2-^{13}C over a Pt film.[208] (*) = ^{13}C.

methylpentane over Pt and Ni films. Normal hexane can cyclize to a six-membered ring, which it does to some extent, whereas the hexane isomers cannot directly form C_6 cyclic intermediates. It should be pointed out that the C_6 products from the reaction of n-hexane and H_2 over the nickel film shown in Table XX are minor products, with hydrogenolysis to CH_4 consisting of 70% of the total reaction products. The results, shown in Table XIX, indicate that carbocyclic intermediates consisting of four membered rings are unimportant and C_5 carbocyclic intermediates are dominant.

Products resulting from isomerization of hexanes via a carbocyclic mechanism can be visualized as in Figure 19.[208] It was suspected that the bond shift mechanism could be operating concomitantly with the carbocyclic mechanism. This was shown to be the case in 1969 by a study using isotopically labeled hexanes.[208] The distribution of products from isomerization of 2 methylpentane-2-^{13}C over platinum films as shown in Table XX confirms the hypothesis. In order to account for the products produced, combinations of bond shift and carbocyclic mechanisms were used. All of the products except 2-methylpentane-1-^{13}C can be formed by two consecutive bond shifts only. However, since methylcyclopentane is a major product, cyclic intermediates are probably dominant. With two consecutive carbocyclic processes all but five of the products can be accounted for. A combination of bond shift–carbocyclic, or carbocyclic–bond shift can account for all of the products except 3-methylpentane-x-^{13}C which is minor and of doubtful existence. A few examples of these combination mechanisms are given in Figure 20. The major products 2-methylpentane-3-^{13}C can be formed from a single carbocyclic intermediate formed by cyclization of the parent hexane.

The relative contributions that the bond shift and carbocyclic processes make depends on the nature of the catalyst as well as hydrocarbon geometry.[208] Anderson and co-workers observed in 1971 that ultrathin platinum films favored the formation of cyclic products and products resulting from carbocyclic intermediates rather than products formed by bond shift processes.[225] This was not the case for thick films. It was suggested that the presence of many surface metal atoms of low coordination on the smaller crystallites of ultrathin films facilitates the formation of adsorbed carbocyclic reaction intermediates. On the other hand, hydrogenolysis and isomerization by a bond shift mechanism are not favored by low coordination atoms but require two adjacent Pt atoms which is favored by a [111] face. It is interesting to note the contrast between this 1971 hpothesis and the conclusions drawn concerning hydrogenolysis on kinked step surfaces of single crystals as previously described.

Differences in isomerization product distributions have been reported for platinum films as compared with supported platinum catalysts.[208] In 1966 it was reported that isomerization of n-hexane to 2,3-dimethylbutane occurred with a 25% yield over Pt films while only 1–2% of this product was formed over a Pt/Al_2O_3 catalyst. A study in 1969 employing UHV conditions revealed no 2,3-dimethylbutane formation. Anderson and Baker suggested that the large amount of 2,3-dimethylbutane observed in the original study was due to a contaminant affecting the properties of active sites.[208] The role of contaminations, especially in the form of carbonaceous residues, on product formation of isomerization, cyclization, and hydrogenolysis reactions is very significant, yet poorly understood. The following discussion of hydrogenolysis reactions on metal films includes several examples of the influence of contamination on product distributions.

The hydrogenolysis of ethane to form methane is the simplest reaction of a saturated hydrocarbon involving C–C bond cleavage. Kemball and co-workers reported activation energies of 222 kJ mol^{-1} for reaction 6 over

$$H_2 + C_2H_6 \xrightarrow{\text{cat.}} 2CH_4 \qquad (6)$$
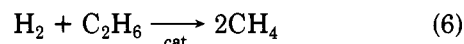
Pd films at 683 K, 226 kJ mol^{-1} over Pt films, and 239 kJ mol^{-1} over Ni/SiO_2 catalysts.[226] The close agreement of these activation energies (initial) indicates that the hydrogenolysis of ethane is rather structure insensitive.
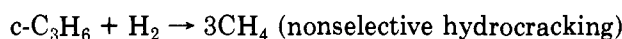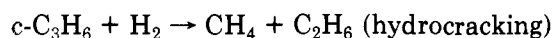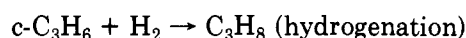
Chemisorption and hydrogenolysis of cyclopropane over nickel films were reported by Merta and Ponec.[227] At 273 K cyclopropane underwent self-hydrogenation at high coverages to yield propane. Some cracking to methane and ethane accompanied the self-hydrogenation. In the presence of H_2 cyclopropane underwent selective hydrocracking to yield constant percentages of CH_4 and C_2H_6 in the overall product mixture from 195 to 500 K. Above 500 K CH_4 formation was favored over C_2H_6. The low temperature fragmentations were proposed to occur via a simultaneous splitting of two

TABLE XXI. Kinetic Parameters for Some
Hydrogenolysis Reactions over Nickel Catalysts[208]

alkane	catalyst	$E_{act}{}^a$	$\log A^b$	temp range, °C
C_2H_6	Ni film	58	35.8	254-273
	Ni/Kieselguhr	52	-	181-214
	Ni/Al$_2$O$_3$ and Ni/SiO$_2$	28-42	-	175-335
C_3H_8	Ni film	31	26.4	217-267
n-C_4H_{10}	Ni film	34	28.5	188-209
i-C_4H_{10}	Ni film	30	26.8	201-221
neo-C_5H_{12}	Ni film	32	26.3	222-265
neo-C_6H_{12}	Ni film	>25		181-200

^{a} kcal mol^{-1}. ^{b} Molecules cm^{-2} s^{-1}.

bonds in the chemisorbed cyclopropane ring. Three competing processes were proposed:

$$c\text{-}C_3H_6 + H_2 \rightarrow C_3H_8 \text{ (hydrogenation)}$$

$$c\text{-}C_3H_6 + H_2 \rightarrow CH_4 + C_2H_6 \text{ (hydrocracking)}$$

$$c\text{-}C_3H_6 + H_2 \rightarrow 3CH_4 \text{ (nonselective hydrocracking)}$$

It has been shown that the fraction of CH_4 in the product mixture from propane hydrogenolysis over nickel films increases linearly with increasing reaction temperature from 475 to 550 K.[203]

After studying data from hydrogenolysis reactions over various films and supported catalysts, Anderson and Baker arrived at the conclusion that it is probable that extensive dehydrogenative adsorption will readily occur on clean metal surfaces, leading to extensive fragmentation. This extensive fragmentation causes methane to be the major cleavage product and also produces strongly adsorbed residues which can act as a poison. Kemball and co-workers observed a decelerating rate for hydrogenolysis of alkanes with more than four carbons.[226] In this case Pd films were used, and it was suspected that the hydrogenolysis of branched alkanes occurred by a carbenium ion type of mechanism. The poisoning was attributed to dimeric or polymeric olefinic material, formed by the carbenium ion species, which blocks active sites. It is not unlikely that the same type of residues can be formed by a radial type of mechanism as mentioned for olefin chemisorption.
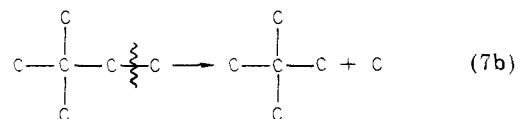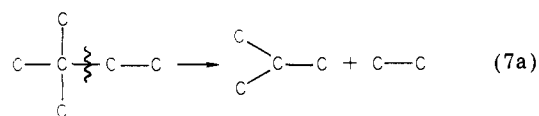
Anderson and Baker have compiled kinetic parameters for hydrogenolysis reactions of alkanes on metal films and some supported metal catalysts.[208] Data for hydrogenolysis reactions over nickel catalysts are summarized in Table XXI.

It can be seen from Table XXI that there is a wide variation in activation energies for ethane hydrogenolysis on various types of nickel catalysts. The lowest value of 28 kcal mol^{-1} was obtained for a 1% Ni supported catalyst, the lowest metal concentration studied. The Ni/kieselguhr catalyst contained 15 wt % Ni. These variations are probably due in part to the variation of electronic as well as structural properties of the metal surface with particle size.[208] Anderson and Baker believe that the variations in activities are mainly due to the effect of the chemical composition of the catalyst surface. It was further noted that clean metal films are very easily self-poisoned while supported metal catalysts are much less susceptible. These authors concluded, without supporting data, that the initial surfaces of

most supported metal catalysts are not clean as compared with metal films.

From Table XXI it is also apparent that hydrogenolysis of ethane is more difficult, energetically, than that of higher aliphatics. Mechanistic implications arise from these results. If a 1,2-diadsorbed species is a common intermediate for C_2 and >C_2 alkane hydrogenolysis, differences in activation energies should be small. Instead, ethane hydrogenolysis has a much higher activation energy. A 1,3-diadsorbed intermediate as illustrated for neopentane in Figure 18 is likely to occur for alkanes greater than two carbons. In fact neopentane cannot adsorb by a 1,2-diadsorbed species. The high activation energy for ethane hydrogenolysis shows that 1,2-diadsorption can occur, although it has a higher energy requirement. Hydrogenolysis of cyclopentane occurs readily even though a 1,3-diadsorption mode is sterically unlikely. It has been suggested that π-allylic type of adsorption may be important in such cases.[208] Therefore, three bonding modes may be competitive in the adsorption of nonquaternary alkanes larger than ethane: (1) a 1,2-diadsorbed intermediate, (2) a 1,3-diadsorbed intermediate, and (3) a π-allylic intermediate. Since extensive fragmentation to methane results from hydrogenolysis of alkanes over nickel catalysts, it is likely that more than one of the above processes occurs to form the observed products. There is convincing evidence from deuterium exchange studies that extensively dehydrogenated species are formed on Ni and Rh films. The 1,2-diadsorption mode is a most likely intermediate in the formation of such dehydrogenated species. These extensively dehydrogenated species favor C–C bond cleavage since they are strongly bound to the surface. The result is a large amount of methane formation.

Twenty years ago Anderson and Baker indicated that 1,2- and 1,3-diadsorption processes can occur.[228] From product distributions of neohexane hydrogenolysis over various metal films two processes were observed as shown in reactions 7a and 7b. The importance of re-

action 7a on the metals studied was in the order Pt > W ≫ Ni > Rh. Over Rh reaction 7b predominated. This is in agreement with later observations of extensive fragmentation, presumably through 1,2-diadsorbed intermediates, of alkanes over Rh and Ni as mentioned. This work was supported by Yoneda and co-workers.[229]

It is not clear at this time what the rate-controlling step(s) is (are) for hydrogenolysis reactions. It may be the adsorption of the alkane (in competition with hydrogen adsorption), the rate of C–C bond rupture, or the rate of cleavage product desorption. Due to the complexity of these reactions many mechanisms have been proposed, all of which may be valid under different circumstances. A very recent study of ethane hydrogenolysis on a nickel catalyst summarizes the mechanistic beliefs of the leaders in this field.[230] It should be

emphasized, however, that it is very dangerous to place much faith in the identification of the rate-controlling step!

C. Metal Powders

Metal powders have been used to a much lesser extent than metal films in the elucidation of mechanisms of catalytic processes. Catalytic studies of a particular reaction such as alkane hydrogenolysis often employ various supported catalysts as well as the pure metal powders. The use of the pure metal powders is generally included to provide an indication of the role of the metal in the catalytic process when dual functionality of the metal and support is suspected. Supported catalysts are used when effects of high metallic dispersion or small metal particle size are to be determined. Metal films prepared under UHV conditions are very easily poisoned or contaminated during their initial use. Metal powders, however, are not quite as easily poisoned initially. This may be due to two factors: (1) they are never as clean originally as metal films,[201] or (2) they are more slowly contaminated due to their porosity which causes a retarded Knudsen diffusion of contaminant molecules.[231] Since the metal particles in powders are easily able to make contact with each other, once contamination or poisoning occurs it is often irreversible since conditions necessary to remove the contaminants may lead to coalescence or sintering.

Hayward pointed out that the earliest chemisorption studies in metal surfaces were performed in the mid-1920s.[13] Conclusions drawn from these early studies are very questionable due to the unknown factor of degree of contamination. Although quantitative data on heats of adsorption of molecules on metal powders is difficult to reproduce, qualitative and semiqualitative conclusions can be obtained. The main advantage that metal powders have over single crystals and films is their much larger surface areas. The relatively large surface areas of metal powders (0.1–20 m^2/g) enable much larger amounts of reactants or higher pressures to be used. This reduces the importance of adsorption on reactor walls, electrodes, and other interfering surfaces in the reaction vessel. The large surface areas of powders enable large amounts of reaction products to be formed and thus eliminate the need for highly sensitive detection equipment, such as mass spectrometers, which are needed in thin film studies. Powders can easily be transferred from one system to another, such as a BET surface area apparatus or to a batch or flow reactor. This manipulation is not readily performed with thin films. Therefore, studies of metal powders can be used in systems much more closely resembling those utilized in industry than can metal films. A review of catalytic studies performed during the last 20 years utilizing metal powders will be discussed with primary emphasis on their poisoning by carbonaceous deposits.
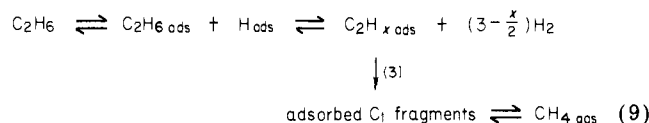
The methanation reaction (eq 8) was studied in 1967 over Pt, Rh, Ir, and Ru unsupported metals at reaction temperatures of 100–200 °C.[232] The catalysts employed

$$3H_2 + CO \rightarrow CH_4 + H_2O \qquad (8)$$
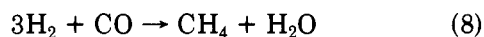
had surface areas of 20–50 $m^2 \, g^{-1}$. It was found that the order of decreasing specific activity for this reaction was Ru $\gg$ Rh, Ir > Pt, Pd. It was pointed out that Ni was also a very active methanation catalyst.

Ethylene decomposition on the surfaces of nickel powders was reported in 1967 by McKee.[23] High-purity carbonyl powders were used in these catalytic decompositions which were carried out at −30 to 200 °C. Below 60 °C ethane and hydrogen were produced and released to the gas phase. About 10% ethane was formed in 4 h at −30 °C. This self-hydrogenation of ethylene occurred at a measurable rate even at −78 °C. At these low temperatures no C_3, higher hydrocarbons, or polymerization products were detected. Adsorbed carbonaceous residues were left on the surface, the composition of which varied with temperature. At 0 °C the residue had an average composition of $(CH_{1.5})_x$. At 200 °C the average composition corresponded to $(C)_x$. Above 60 °C CH_4 appeared in the gas phase, the amount of which increased rapidly with temperature. A later report by McKee indicated that cracking products from ethylene on nickel powders did not appear until 105 °C.[233] However, chemisorption at lower temperatures was rapid and irreversible. Cracking products from propane adsorption first appeared at 65 °C, a much lower temperature than that of ethylene or ethane. Ethane cracking products were first observed at 95 °C. Methane was evolved at higher temperatures such that there was a zero order dependence on propane pressure.

Similar results were obtained for propane cracking over platinum blacks.[19] However, the specific activity of platinum was much less than that of nickel. Both the platinum blacks and nickel powders were easily sintered at temperatures above 100 °C. By comparing surface areas determined by N_2 adsorption and propane monolayer values, it was shown that loss of activity was due to the elimination of active sites rather than a "molecular sieve" effect. Poisoning of the catalysts by carbonaceous deposits also reduced the activity of the powders. These residues were not desorbed by evacuation at the reaction temperature but required reduction with hydrogen at 150 °C or above for several hours to regenerate the activity. The activity was not completely regenerated, due to sintering. A mechanistic investigation of ethane hydrogenolysis was reported in 1974.[234] A review of data obtained by several workers for hydrogenolysis and deuterium exchange of ethane over Ni, Ru, Rh, Co, Re, Fe, Cu, Pt, Pd, and W both supported and unsupported was compiled and analyzed. The reaction scheme shown in reaction 9 was obtained.

$$C_2H_6 \; \rightleftharpoons \; C_2H_{6\,ads} \; + \; H_{ads} \; \rightleftharpoons \; C_2H_{x\,ads} \; + \; (3 - \tfrac{x}{2})H_2$$
$$\downarrow (3)$$
$$\text{adsorbed } C_1 \text{ fragments} \; \rightleftharpoons \; CH_{4\,gas} \qquad (9)$$

These workers proposed that the rate-determining step for ethane hydrogenolysis is the formation of gaseous methane (step 4). The reaction over nickel powder was investigated in the temperature range 174–328 °C.

An interesting study of the effect of macroscopic aggregation of palladium blacks on surface area and catalytic activity of olefin isomerization/hydrogenation was reported by Sermon in 1975.[33] Sermon proposed a theoretical model for the aggregation of particles in Pd blacks in which loss of surface area due to aggregation was attributed to a close packing of particles. Surface area decreases with (1) an increase in interparticle contacts, (2) a decrease in particle size, and (3)

TABLE XXII. Products of Hydrogenation of Butadiene in 95% Ethanol[219]

catalyst	temp, °C	products, %		
		1-butene	trans-2-butene	cis-2-butene
Pt	-12	72.1	18.4	9.5
Pd	-12	48.5	40.1	11.4
Pd/BaSO$_4$	-8	6.0	75.0	19.0
Raney Ni	28	21.5	61.0	17.5

an increase in size of adsorbate molecules on the surface. Loss of surface area which occurred following reduction of air-exposed samples was due not to sintering but to rather close packing of macroscopic aggregates with an average of 12 interparticle contacts per particle. The model was supported by experimental investigations of the titration of preadsorbed hydrogen with 1-pentene. Formation of pentane was taken as an indication of the availability of adsorbed hydrogen on the catalysts. When samples of widely varying degrees of aggregation were used, it was shown that the availability of adsorbed hydrogen was nearly the same. The only effect of aggregation is a decrease in the specific surface area available for adsorption. The isomerization and hydrogenation of the alkene were not affected by aggregation or particle size. Upon addition of 1-pentene to Pd blacks containing adsorbed hydrogen, pentane is produced first. As the adsorbed hydrogen is consumed, cis- and trans-2-pentene appear. Once nearly all of the adsorbed hydrogen is consumed (no pentane product formed), 1-pentene appears as the sole product. It seems that a low concentration of adsorbed hydrogen favors the isomerization reaction. The possibility of poisoning by carbonaceous deposits was not indicated.

A study of isomerization and hydrogenation of 1,3-butadiene was reported in 1947.[219] It was shown that during hydrogenation of the diene over Pd, Pt, or Ni powders monoolefin intermediates were formed by dihydro-addition. The composition of the monoolefin product mixture obtained was strongly dependent upon the catalyst employed, as shown in Table XXII. It was found that two simultaneous hydrogenation reactions could occur. The first is the formation of butane by hydrogenation of 1,3-butadiene in one step. The second reaction involves the hydrogenation of the diene to butene products. Hydrogenation of the butenes was found to be very slow in the presence of butadiene, due to the selective adsorption of butadiene over the monoolefins. Isomerization of the butenes on the catalysts was observed only in the presence of adsorbed hydrogen. In the absence of hydrogen 1-butene did not isomerize over Pd/BaSO$_4$ after 24 h. This was suggested to support the following mechanism for butene isomerization:
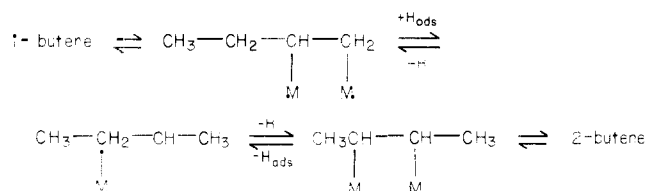

As was mentioned in a previous section, many reactions seem to be unaffected by particle size changes other than a single reduction or increase in available surface area. Boudart was the first to point this out.[163]

TABLE XXIII. Reaction of n-Heptane + H$_2$ over Various Group 8B Metal Powders[19]

metal	temp, °C	rate[a]	% hydro-genol-ysis	% isom-eriza-tion	% dehydro-cycliza-tion	total convn, %
Pd	300	0.010	5.8	0.5	0.2	6.4
Rh	113	0.010	2.7	0.2		2.9
Ru	88	0.010	3.7	0.3		4.0
Pt	275	0.010	8.0	10.0	3.4	21.4
Ir	125	0.010	1.3	0.2		1.5

[a] mol of n-heptane h^{-1} g^{-1} of catalyst.

He showed that certain reactions (demanding) were highly sensitive to catalyst preparation conditions and particle size while others (facile) were not. It was shown that the selectivity for the reaction of neopentane to isopentane over the hydrogenolysis pathway is a "very sensitive probe of special surface configurations". Selectivity was defined as the ratio of isomerization rate to hydrogenolysis rate for the pathways shown in reaction 10, that is, s = rate a/rate b. It was suggested
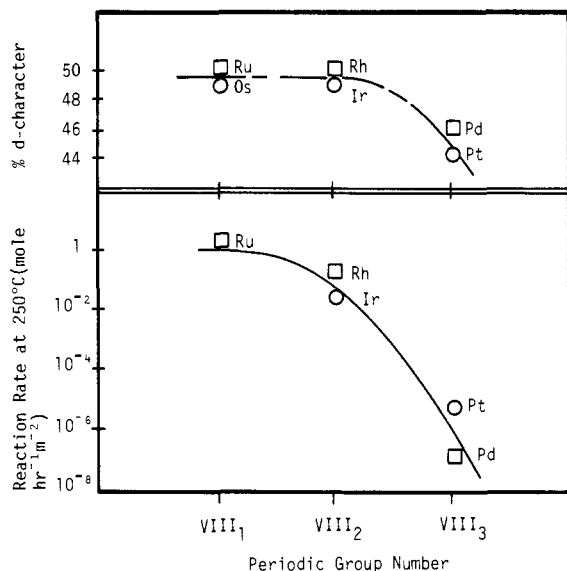

(10)
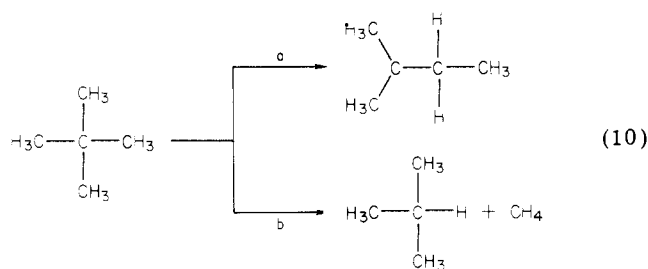
that the isomerization was favored by the presence of Pt atom triplets (sites for triadsorbed species) such as occur on (111) faces and at point defects, edges, and steps on Pt surfaces. The highest values of selectivity[2] were measured for Pt powders (compared with supported Pt catalysts). The explanation advanced for this observation was that a "roughening" of the metal surface in such powder produces a high surface concentration of triplets. These proposals assumed that a triadsorption of neopentane was necessary for isomerization, in contrast to conclusions obtained from metal film studies. It was also found that cleaning Pt powders by H$_2$/O$_2$/H$_2$ cycles at 500 °C led to a large increase in catalytic activity without a change in selectivity. It was therefore concluded that the reaction was contamination insensitive. This can be compared to the results of overlayer sensitivity of reactions on Pt single crystals reported by Somorjai.[206]

Carter, Sinfelt, and Cusamano reported a study of n-heptane hydrogenolysis over several group 8B metal powders.[19] Table XXIII lists the general activity and selectivity results from the studies, and Table XXIV lists the product distributions for the hydrogenolysis reaction. A wide range of reaction temperatures was used due to the wide variation in activities. Temperatures were used such as to give the same initial reaction rates for all metals. From these tables the order of activity for hydrogenolysis of n-heptane is seen to be Pd < Pt ≪ Rh < Ir < Ru. A wide variation in product distributions can be seen over the various metals (Table XXIV). It can be seen that Pd and Rh crack terminal C–C bonds almost exclusively while other metals exhibit much less selective cracking. As found in metal film studies Pt stands out in its ability for isomerization
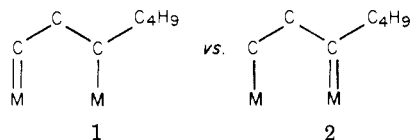
TABLE XXIV. Distribution of Products from Hydrogenolysis of n-Heptane[19]

metal	temp, °C	total convn, %	mol % product distribution (alkanes)					
			C_1	C_2	C_3	n-C_4	n-C_5	n-C_6
Pd	300	6.4	46	4	-	.	4	46
Rh	113	2.9	42	5	4	3	5	41
Ru	88	4.0	28	12	13	12	10	25
Pt	275	2.3	31	13	17	16	9	14
Ir	125	1.5	21	21	15	14	14	15

Figure 21. Correlations of % d character vs. periodic group number and rate of n-heptane hydrogenolysis vs. periodic group number.[19]

(Table XXIII). Smooth correlations were made between % d character of the metallic bond vs. periodic group number and reaction rate vs. periodic group number as shown in Figure 21. This type of correlation was observed for ethane hydrogenolysis by Carter and Sinfelt[235] and for hydrogenation of ethylene over metal films as described earlier.[213] It can be seen that the rate of hydrogenolysis of n-heptane decreases as the % d character of the metallic bond decreases. The selective terminal C–C bond cracking exhibited by Pd and Rh (Table XXIV) may be explained by assuming a 1,3-diadsorbed intermediate, as discussed in the metal film section, if it is further assumed that the C–C bond adjacent to a M=C bond is preferentially cleaved, such as


where structure 1 represents the surface species on Pd and Rh.[19] It was suggested that metals such as Pt and Ir can readily undergo changes in valency of surface atoms that would readily allow a shift of the metal–carbon double bond from a terminal carbon to other carbon atoms in the hydrocarbon chain. The easy shift of surface valencies in Pt and Ir is believed to be a result of easy promotion of d electrons to empty s levels. Support for this hypothesis was weak. It was pointed out that Au behaved similarly to Pt and Ir in its ability to isomerize neopentane to isopentane. This process was thought to be related to changes in surface valencies

Figure 22. Surface species proposed for n-pentane hydrogenolysis on Ni powder.[236]

occurring on these metals. Gold surfaces were observed by LEED to undergo surface rearrangements which would result in valency changes. Therefore, extrapolation of surface valency changes observed in gold studies was made to Pt and Ir to explain their similar isomerization abilities. Better support was provided by Carter and Sinfelt in a reference to studies made by Rhodin and co-workers. Carter and Sinfelt pointed out that Rhodin's FIM studies of the binding of metal atoms to tungsten crystals provided evidence for variable surface valency for Pt and Ir. The behavior of Rh and Pd was suggested to be related to their lack of abilities to undergo surface valency changes.

Nickel also prefers to cleave terminal C–C bonds of paraffins as pointed out by Taheri and Ollis in 1976.[236] These authors proposed triadsorbed surface structures as intermediates in n-pentane hydrogenolysis based on kinetic parameters. This intermediate, shown in Figure 22, was proposed to account for the easy degradation of n-butane, formed by terminal C–C cleavage of n-pentane, to propane and lower homologues.

The highly dehydrogenated state of the intermediate was proposed in light of an evaluation of kinetic parameters which yielded a value of $X_{max} = 5$ for the surface species $(C_5H_x)_{ads}$ (cf. Figure 22). This slow step in the reaction was proposed to be

$$C_5H_{x(ads)} \rightarrow CH_{y(ads)} + C_4H_{z(ads)}$$
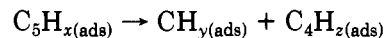
Surface species on Pt powders were found to be less dehydrogenated ($X_{max} = 6$) than those on Ni. A general observation in these studies of higher paraffin hydrogenolysis is that the rate has a negative hydrogen order and a positive paraffin order.

Further evidence that multiply bonded surface species are easily formed during hydrogenolysis of paraffins on certain metal powders was presented in 1977.[21] After a study of C_2, C_4, and C_5 alkane hydrogenolysis, isomerization, and deuterium exchange reactions over Ru, Rh, Ir, and Ni blacks, it was concluded that surface transformations of hydrocarbons into strongly multiply bonded species easily takes place. Furthermore it seemed that product desorption was rate determining. It was shown that Ru, Rh, and Ir blacks were 10^4–10^3 times more active than Co or Ni for hydrogenolysis of ethane and n-butane. As was observed for other hydrogenolysis reactions over Ni, these studies revealed an increase in methane formation with an increase in temperature. Irreversibly bonded residues remained on the blacks used for these reactions. The

TABLE XXV. Reactions of 3-Methylpentane and Methylcyclopentane over Various Metals[237] d

metal	T, K	3-MP $C_6{}^c$	F	$C_6{}^c$	2-MP n-H	MCP $C_6{}^c$	F	$C_6{}^c$	2-MP n-H
Co^a	573	1107	4.99	0		3060	4.98	130	1.9
Ni^a	543	463	3.13	0		380	3.11	120	2.8
Ru^a	513	545	3.76	0		1070	3.82	130	0.2
Ru^b	543	544	3.71	3.3	~2	520	3.46	40	1.7
Rh^a	513	591	1.86	34		75	2	655	1.6
Rh^b	453	1100	1.80	0		550	1.78	6600	6.5
Pd^a	588	813	2.01	578	6.5				
Pd^b	648	610	2.08	1080	3.4	280	2.48	1630	2.9
Re^a	633	805	3.45	0		690	3.37	120	0
Re^b	573	782	3.35	0		1070	3.12	110	0
Os^a	513	455	5.91	0		2070	5.97	90	0.5
Ir^a	543	1000	1.92	410	6.4	1000	1.81	5900	5.7
Ir^b	468	1060	1.76	430		1300	1.70	23600	32.4
Pt^b	603	482	1.89	2420	5.7	320	2.14	9600	9.8

^{a} Commercial powder. ^{b} Precipitated black. ^{c} 10^{15} C_6 molecules reacted per m² of metal. ^{d} See text for explanation of symbols.

species that remained on the metal surfaces after heat treatment at 673 K for 2 h could only be removed to an extent of about 5–10% by hydrogenation. This suggested that there was formation of a "superficial graphite-like carbon". Very rough calculations of the composition of the carbonaceous residue on Ni black from C_2H_6 and CH_4 decomposition yielded the following values for the species $(CH_x)_{ads}$: C_2H_6 at 234 °C, x = 0.36; CH_4 at 255 °C, x = 0.53; CH_4 at 128 °C, x = 0.87. These general results illustrate that dehydrogenation of surface residues is more extensive at higher temperatures.

An extensive investigation of hydrogenolysis of 3-methylpentane and methylcyclopentane over many unsupported transition-metal powders was reported by Paal and Tétényi in 1977.[237] These authors studied a wide variety of commercial metal powders and precipitated blacks and classified them according to their selectivity for hydrogenolysis. Table XXV shows some of their results. The data in Table XXV are related to temperatures (τ) at which nearly equal rates of 3-methylpentane (3-MP) hydrogenolysis were obtained. The activity for hydrogenolysis is inversely proportional to the τ values. These authors state that the difference in crystallite sizes of "powders" and "blacks" are reflected in the higher τ values of the former. The data do not support that conclusion. The depth of hydrogenolysis is indicated by a fragmentation factor F, which is defined as the number of fragment molecules produced per molecule of hydrocarbon hydrogenolyzed. It can be seen that the value of F appears to be independent of the hydrocarbon structure, the nature of the metal (powder or black), or the actual τ values for a given conversion. The formation of C_6 alkane isomer products is characterized by the ratio of the isomers 2-methylpentane (2-MP) to n-hexane (n-H).

F values near 2 indicate that single bond rupture of the hydrocarbon predominates while values greater than 2 indicate multiple cracking. When these values are used as criteria for classifications the metals studied can be grouped into two categories: group A—Rh, Pd, Ir, Pt ($F \sim 2$); group B—Co, Ni, Ru, Re, Os ($F \sim 3$–6). Group A is characterized by hydrogenolysis reactions involving only a single C–C bond cleavage of the reactant hydrocarbon. Group B is characterized by multiple C–C bond cleavage leading to extensive fragmentation

of the reactant hydrocarbon. In this latter group C_6 alkanes represent a minor portion of the product mixture. The high values for the amount of C_6 isomer products from the 3-MP reaction over platinum reflect the high selectivity for isomerization so often observed for this metal. The group A metals also show very high activities for ring-opening reactions as indicated by the very high values of C_6 isomer amounts for methylcyclopentane (MCP) compared with that from the 3-MP reactions. It was suggested that flatly chemisorbed C_5 cyclic intermediates are important for reactions over the group A metals.

D. Supported Metals

In this subsection discussions are limited to interactions and reactions on supported metal catalysts in which no dual functionality of metal and support is indicated. Primary emphasis is placed on the effect of the variation of dispersion and, hence, particle sizes on reactivities and mechanisms of surface reactions. The nature and properties of carbonaceous surface species on metal particles are also stressed. Reactions involving C–C bond cleavage make up the bulk of this section. Miscellaneous reactions and adsorption studies on supported metal surface are presented first.

An early report concerning the effect of special surface structural features of metal particles on adsorption properties appeared in the literature in 1966.[238] Prior to 1966 it was shown that N_2 does not adsorb, chemically or physically, or nickel at room temperature. However, in 1966 an infrared active adsorbed nitrogen species was observed on Ni, Pd, and Pt supported on SiO_2 and Al_2O_3 at room temperature. When electron microscopy was used in conjunction with infrared spectroscopy, it was shown that this IR active N_2 species was formed only on metal crystallites between ~15 and ~70 Å in diameter. The presence of the adsorbed species was dependent only on crystallite size, the nature of the metal having no effect. By use of models (marbles and mathematical) it was shown that N_2 adsorption occurred only at special sites in which five nearest neighbors existed. These sites of five nearest neighbors were termed B_5 sites, as shown in Figures 23 and 24. Since the appearance of the IR active species was not dependent upon the metal used, it was assumed
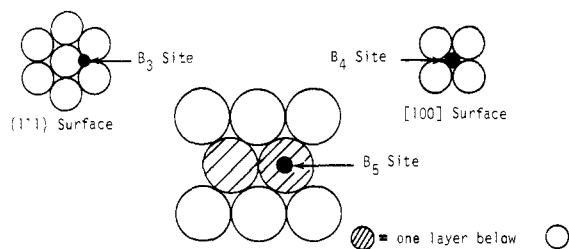
Figure 23. Adsorption sites on various metal surfaces.[238]
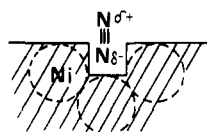
Figure 24. Cross sectional side view of N_2 in a B_5 site.[238]

that the adsorption was purely physical in nature. This report was the first attempt at relating a directly observable parameter (IR adsorption activity) to a specific structural feature of a small metal particle. It was concluded that N_2 adsorption must occur at a B_5 site and, conversely, if N_2 adsorption produces an IR active species, then B_5 sites are present.
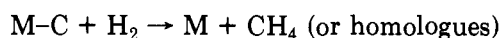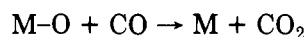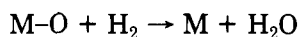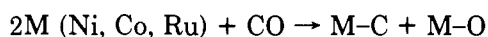
Adsorption of CO on supported metal surfaces has been studied in depth due to its importance in methanation reactions. Recent studies have been directed toward determining the role of surface carbon in the catalytic methanation reaction:[239,240]

$$CO + 3H_2 \rightarrow CH_4 + H_2O$$
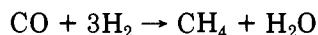
Results of such studies have revealed that CO adsorbs nondissociatively at temperatures below about 500 K on Ni/Al_2O_3 and on single nickel surfaces. This non-dissociated adsorbed CO is inert to H_2. However, at temperatures above about 500 K CO adsorbs dissociatively, forming adsorbed carbon in forms dependent upon the temperature. This is shown in reaction 11.

$$2CO \rightleftharpoons C_{(s)} + CO_{2(g)} \tag{11}$$
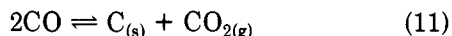
This disproportionation reaction produces CO_2 in the gas phase. At temperatures in which reaction 11 occurs, an active carbon species is formed that will readily react with hydrogen to form methane or higher homologues. At higher temperatures (e.g., 700 K) the active carbon is converted to a nonreactive form (presumably graphitic in nature). The current mechanism for methanation is believed to be the same as originally proposed by Fischer over 40 years ago. This mechanism is thought to proceed as follows:

$$2M \text{ (Ni, Co, Ru)} + CO \rightarrow M\text{-}C + M\text{-}O$$

$$M\text{-}O + H_2 \rightarrow M + H_2O$$

$$M\text{-}O + CO \rightarrow M + CO_2$$

$$M\text{-}C + H_2 \rightarrow M + CH_4 \text{ (or homologues)}$$

The active carbon, once formed, is reactive to hydrogen even at room temperature. An example of products obtained by the reaction between the active carbon and H_2 is shown in Table XXVI.[240] At higher temperatures than those shown in Table XXVI there is a greater fraction of CH_4 in the product mixture.

TABLE XXVI. Products Obtained by Pulsing H_2 over 7% Ni/SiO_2 Pretreated with CO at 300 °C[240]

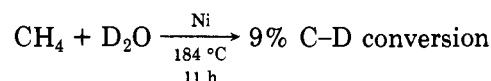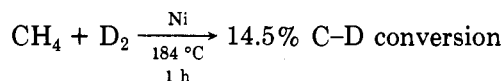| pulse temp, °C	convn,[a] %	carbon efficiencies,[b] %				
		CH_4	C_2H_6	C_3H_8	C_4H_{10}	C_5H_{12}
23	3.5	42	46	11	1	
80	9	72	16.5	7.5	4	trace
115	12	69.7	19.5	8.6	2.2	

[a] Fraction of surface layer converted to hydrocarbons.
[b] Calculated by multiplying moles of each product by number of carbons in that product.

TABLE XXVII. Observed Bond Numbers for Adsorption of Hydrocarbons on Ni/SiO_2 Compared with Bond Numbers Corresponding to Complete Cracking[242]

hydrocarbon	N_{calcd}	N_{obsd}	T_c, °C
methane	7	6.9	300
ethane	12	12.5	50
propane	17	18.0	90
butane	22	18.5	100
ethylene	10	10.2	75
propene	12	14.5	90
1-butene	20	17.0	125
2-butene	20	18.0	150
acetylene	8	7.8	150
cyclohexane	30	30.0	210
benzene	24	25.0	160

A study of the exchange reaction between CH_4 and D_2O on Ni/kieselguhr was reported in the early literature (1955).[214] Compared with CH_4/D_2 exchange, CH_4/D_2O exchange is very slow.

$$CH_4 + D_2 \xrightarrow[\substack{184 \text{ °C} \\ 1 \text{ h}}]{Ni} 14.5\% \text{ C–D conversion}$$

$$CH_4 + D_2O \xrightarrow[\substack{184 \text{ °C} \\ 11 \text{ h}}]{Ni} 9\% \text{ C–D conversion}$$

The slow reaction of CH_4 with D_2O was attributed to the strong adsorption of water vapor on the nickel surface, leaving little free surface for the activated adsorption of CH_4. No studies of the interaction of D_2O vapor with active carbon species on metal surfaces have been reported.

Adsorption of hydrocarbons on Ni/SiO_2 catalysts was reported in 1974 by Martin and Imelik.[242] By use of high-field magnetic measurements to monitor changes in the saturation magnetization of nickel upon hydrocarbon, adsorption information was obtained concerning the extent of dissociation of the adsorbed hydrocarbons. The slope of a magnetization vs. adsorbed volume plot is proportional to the number of single covalent bonds to the metal surface from the adsorbate. With this approach it was shown that, at low coverages, on "clean" metal surfaces (Ni), alkanes, alkenes, cycloalkanes, and benzene are strongly dehydrogenated upon adsorption. Sudden changes in the magnetization isotherms upon increasing the temperature of a hydrocarbon adsorbed on Ni/SiO_2 were attributed to cracking of the adsorbate. The temperature at which the cracking occurred is T_c, and values are shown in Table XXVII. Analysis of the data reveals that T_c alkane $< T_c$ alkene $< T_c$ alkyne for hydrocarbons containing the same number of carbon atoms. Also shown in Table XXVII are the bond numbers N observed and calculated with the assumption of complete cracking, as in reaction 12. It is im-
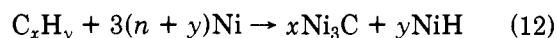
$$C_xH_y + 3(n + y)Ni \rightarrow xNi_3C + yNiH \tag{12}$$

TABLE XXVIII. Effect of Particle Size on Specific
Activity of Rh Catalysts for Ethane Hydrogenolysis[246]

Rh conc,[a] wt %	crystallite size, Å	spec act.[b]
100 (unsupported)	2560	0.79
10	23	13.5
5	20	12.2
5 (sintered at 800 °C)	127	0.41
1	12	16.0
0.3	11	4.3
0.1	11	4.4

[a] Supported on SiO_2. [b] Mmol of ethane converted h^{-1} m^{-2} of Rh at 253 °C. H_2 pressure = 0.20 atm, ethane pressure = 0.030 atm.

TABLE XXIX. Specific Activity of Pt Catalysts of
Various Dispersions for Cyclopropane
Hydrogenation at 0 °C[90]

wt % Pt on support	spec act.[a]	dispersion,[b] %
0.3% on η-alumina	8.1	44
0.3% on γ-alumina	7.4	59
0.6% on γ-alumina	5.6	73
1.96% on η-alumina	6.6	64

[a] Activity/specific area; activity = μmol of cyclopropane reacted min^{-1} g^{-1} of sample; specific area = μmol of H_2 g^{-1} of sample. [b] Dispersion = [(number of Pt atoms titrated by H_2)/(total number of Pt atoms in sample)] × 100%.
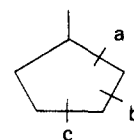

Figure 25. Positions of cleavage of MCP.

portant to note that these observations were made on initially "clean" nickel surfaces after only partial coverage by the adsorbate. Therefore, these data indicate interactions that occur between the hydrocarbons and the most energetic sites of the nickel surface.

Early studies of hydrogenolysis reactions on supported nickel catalysts were limited to ethane and propane.[243-245] Studies of hydrogenolysis of ethane on Ni/kieselguhr catalysts showed that in the presence of excess hydrogen, ethane undergoes dissociation to adsorbed methyl groups that are converted to methane. Without enough hydrogen, further dissociation occurs with the formation of CH_2, CH, and ultimately adsorbed C. Adsorbed atomic hydrogen is simultaneously formed. It was further indicated that C–C bond breakage is the slow reaction while an equilibrium between methane, adsorbed methyl, and methylene groups, etc., on the surface is quickly established. Activation energies for C–C and C–H bond cleavages on nickel were calculated as ~19 and ~15 kcal, respectively.

Later studies of ethane hydrogenolysis on supported Ni and Rh catalysts revealed a particle size effect on the catalytic activity of a given metal.[246,247] The first report of a particle size effect on catalytic activity for hydrogenolysis over supported nickel (SiO_2 and Al_2O_3) was an observation that catalytic activity per unit surface area of nickel decreased with an increase in crystallite size. Studies of ethane hydrogenolysis over Rh/SiO_2 catalysts revealed that there is an optimum crystallite size associated with a maximum activity. This optimum size is of an intermediate value, with smaller and larger sized crystallites having lower specific activities. Table XXVIII illustrates these particle size effects. In these studies extensive dehydrogenation of ethane upon chemisorption was indicated for Rh as well as Ni.

In contrast to the above sensitivity of catalytic activity on particle size, Boudart and co-workers showed that hydrogenolysis of cyclopropane over supported Pt catalysts was insensitive to particle size changes.[164] This insensitivity of a reaction to particle size variations led Boudart to term such reactions as "facile". Facile reactions are those for which the majority of sites on the catalyst surface possess ample activity such that surface heterogeneity is not noticed. The insensitivity to dispersion of cyclopropane hydrogenolysis over Pt at 0 °C is illustrated in Table XXIX.

While mechanistic studies of ethane hydrogenolysis on supported metals are still being pursued (e.g., see ref 230), many recent studies have been concerned with higher aliphatic hydrocarbons. Hydrogenolysis of *n*-

pentane over various metals supported on silica was studied over 20 years ago.[248] By comparison of specific activities for the reaction over various transition metals the following sequence of decreasing activity was obtained: Ru > Rh > Pt > Ni > Co > Ir > Pd ~ Fe. This sequence is in agreement with the previously described results of *n*-heptane hydrogenolysis over unsupported metal powders.[19] In contrast, however, this early report indicated that Ru, Rh, and Ir were characterized by multiple bond breakage and Ni was characterized by selective cleavage of terminal C–C bonds.[248] In this study, as observed for metal films and powders, Pt was found to be unique in its activity for isomerization of *n*-pentane to isopentane.

A series of reports by Corolleur, Gault, and co-workers in 1972 demonstrated the importance of particle size effects on mechanisms and product distributions of hydrogenolysis reactions over various platinum catalysts.[249-251] The mechanisms of isomerization and hydrogenolysis of aliphatic hydrocarbons as previously discussed consist of two distinct processes: (1) the bond shift mechanism and (2) the carbocyclic mechanism (cf. Figures 18–20). Using ^{13}C labeled hexanes Corolleur and Gault showed that interconversions between methylpentanes and *n*-hexane occurred 90% of the time by a cyclic mechanism except on very large Pt crystallites ($d > 150$ Å). Interconversions between methylpentanes occurred only by a cyclic mechanism on highly dispersed Pt catalysts ($d < 50$ Å). However, Pt catalysts with average crystallite sizes larger than ~50 Å catalyzed the interconversions by a bond-shift mechanism predominantly. When a 0.2 wt % Pt/Al_2O_3 (20-Å crystallites) catalyst is used, hexane isomerization products could be accounted for by a cyclic mechanism only. With a 10 wt % Pt/Al_2O_3 (200-Å crystallites) catalyst, hexane isomerization products could be accounted for only by including both cyclic and bond shift mechanisms. The selectivity in hydrogenolysis products of methylcyclopentane over various Pt catalysts in relation to metal particle size was also studied.[249] The selectivities for cleavage at the a, b, and c bonds of MCP shown in Figure 25 are definitely affected by the Pt particle size as shown in Table XXX. In Table XXX r_2 relates the relative rates of cleavage at bond c to cleavage at bond a and r_1 corresponds to b/c. No effect

TABLE XXX. Selectivity in Hydrogenolysis of MCP at 260 °C as a Function of Metal Particle Size[249]

catalyst	10% Pt/ Al$_2$O$_3$	10% Pt/ SiO$_2$	10% Pt/ Al$_2$O$_3$	10% Pt/ SiO$_2$
d_N,[a] A	185	44.5	23.5	15
r_2 = 3-MP/n-H	4.6	1.46	0.80	0.55
r_2 = 2-MP/3·MP	3.30	2.79	2.70	2.52

[a] d_H determined by the ratio of number of H atoms adsorbed to number of Pt atoms deposited on support. 3-MP = 3-methylpentane; n-H = n-hexane; 2·MP = 2-methylpentane.

TABLE XXXI. Relative Rates of Hydrogenolysis of C-C Bonds at 300 °C[252]

C$\overset{1}{-}$C$\overset{2}{-}$C$-$C	1	0.9
	2	1.2
C$\overset{1}{-}$C$\overset{2}{-}$C$\overset{3}{-}$C | C	1	0.8
	2	0.5
	3	1.9
C$\overset{1}{-}$C$\overset{2}{-}$C$\overset{3}{-}$C$\overset{4}{-}$C | C	1	0.85
	2	0.9
	3	1.2
	4	1.15
C$\overset{1}{-}$C$\overset{2}{-}$C$-$C | | C C	1	1.15
	2	0.45
C$\overset{1}{\underset{|}{-}}C\overset{2}{-}C\overset{3}{-}$C | C	1	0.8
	2	2.2
	3	0.35

[a] See text.

of support used was observed other than the particle size that could be obtained. Particle size effects were considered to be due to the influence of particle size on the formation of special defects which are responsible for various reaction mechanisms. It was presumed that these defects are formed during early stages of growth of the reactive metal surface during catalyst preparation.

A detailed study of many straight chain and branched alkane hydrogenolysis reactions over Pt/Al$_2$O$_3$ was reported in 1977.[252] In addition to surface intermediates consisting of 1,2- and 1,3-diadsorbed species, as previously discussed, 1,4- and 1,5-diadsorbed species were postulated as possible important hydrogenolysis intermediates. Evidence was given that whenever a 1,5-diadsorbed species can form, rates of isomerization and dehydrocyclization are increased relative to hydrogenolysis. Under the conditions (300 °C) used for the alkane/H$_2$ reactions over Pt in these studies, hydrogenolysis was the main reaction. The structure of the alkanes had an important effect on the distribution of products. Different bonds were shown to have different reactivities toward cleavage. In general, bonds β to tertiary carbons were extensively broken. Bonds α to a quaternary carbon were also extensively broken (more easily than bonds β to a quaternary carbon). These trends are illustrated in Table XXXI which shows a reactivity factor ω defined as

$$\omega = \frac{\text{actual rate of bond rupture}}{\text{statistical rupture rate}}$$

where statistical rupture rate = [(total hydrogenolysis rate) × (number of identical bonds under considera-
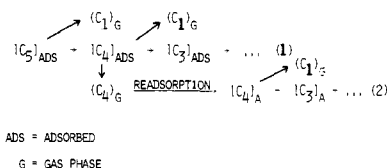
Figure 26. Primary (1) and secondary (2) cracking processes in hydrogenolysis reactions.[253]

tion)]/(total number of bonds).

The interpretation of hydrogenolysis product distributions is only valid if it is known that primary processes are being observed. Kuleli and Cecen defined primary processes as those that occur without desorption and readsorption onto the catalyst surface.[253] Primary processes are indicated by little effect of space velocity on product distributions. Two general processes leading to observable product distributions are possible, as shown in Figure 26. By varying the flow rates and temperatures, it was shown that CH$_4$ production from n-pentane and n-octane hydrogenolysis over Ni/Al$_2$O$_3$ was mainly due to primary multicracking (Figure 26 (1)). This multicracking was so rapid that not less than 50% of the methane formed was due to this process regardless of feed rate and reaction temperature (150–200 °C). Higher temperatures favored more extensive multicracking and hence CH$_4$ production. At lower temperatures ($\sim$150 °C) a significant amount of primary single cracking occurred (31%), producing CH$_4$ and n-butane from n-pentane. This single cracking was almost absent above 200 °C.

All of the hydrogenolysis product distributions covered thus far have been initial distributions (<10% conversion) so that secondary processes of adsorption-readsorption were not likely. The most recent studies of alkane hydrogenolysis have included changes in product distributions as a function of conversion.[254,255] Machiels and Anderson performed these studies by comparing product distributions observed at different levels of conversion (0–80%) to mathematical models which accounted for reversible adsorption and desorption of the hydrocarbons. Good agreement between experimental and theoretical distributions was obtained using assumptions such as (1) no isomerization, (2) irreversible splitting steps (i.e., no chain growth), (3) first-order splitting and desorption, (4) sequential splitting of C–C bonds, and (5) no assumed rate determining step. The good agreement indicated that these were valid assumptions. With this method 2,3-dimethylbutane, 2,2-dimethylbutane, and n-hexane hydrogenolysis over supported Ni, Ru, Co, and Fe were studied. A trend in product distributions was observed such that in going from Ru to Ni to Co to Fe the distributions were shifted toward smaller hydrocarbons, with CH$_4$ being the main product on Fe. On Ru tertiary carbon atoms were found to be relatively stable toward cleavage while on Ni and Co they were no more stable than secondary carbon atoms. Large amounts of CH$_4$ production on Fe suggested that the adsorbed species were very strongly adsorbed and cracking was much faster than desorption. Activity toward hydrogenolysis followed the sequence Ru > Co > Ni > Fe under the conditions employed. Selectivities for the various hydrogenolysis products remained fairly constant at low conversions (<20%) with an increasing selectivity for CH$_4$ production at higher conversions. This trend was

TABLE XXXII. Hydrocarbons Produced by Heating Metal Cluster Compounds Supported on Al_2O_3 under 600 torr of CO[258]

cluster	temp, °C	products, %					
		CH_4	C_2H_6	C_3H_8	C_3H_6	C_4H_{10}	C_5H_{12}
$Ru_3(CO)_{12}$	200	69^a	8	6	9	4	4
$Rh_4(CO)_{12}$	250	56^b	18	17	5	3	1
$Rh_6(CO)_{16}$	235	52^b	17	20	7	3	1
$Ir_4(CO)_{12}$	250	93^a	6	1			
$Os_3(CO)_{12}$	250	100					
$Os_6(CO)_{18}$	250	100					

^{a} 100% at 300 °C. ^{b} 100% at 400 °C.

predicted by the model used.

E. Metal Clusters: Supported, Ligand Stabilized, Solvated, and Matrix Isolated

This subsection deals with reactions involving H–H, C–H, and C–O bond-breaking on small metal clusters. In some cases they are structurally well-defined. This section is not intended to serve as a review of homogeneous catalysis but rather to point out some specific examples in which the above bond cleavage processes have been observed. This area is a zone of transition from heterogeneous catalysis to homogeneous catalysis the literature of which will, hopefully, be much larger 10 years from now.

It was pointed out in the section on the structure and stability of small metal particles that current research is being pursued in the direction of the synthesis of metal clusters which can be characterized in a homogeneous state and then deposited on a support without geometric changes in a reversible manner. Unfortunately little success has been achieved along these lines. However, Ichikawa reported the depositions of Ni_3 clusters on SiO_2 substrates by thermal decomposition of $[Cp_3Ni_3(CO)_2]$ complexes.[124a] The very highly dispersed catalyst that resulted from this preparation was believed to contain intact Ni_3 clusters. No detailed catalytic studies were made, but the activity of the catalyst for facile reactions was indicated. Ethylene and benzene were both readily hydrogenated at room temperature, and H_2–D_2 exchange was also easy. This shows that H–H bond cleavage and C–H bond formation are highly activated by two or three nickel atoms.

The first direct evidence of a "complex" between an alkane and a metal ion was reported in 1975.[256] Ni^{2+} and Co^{2+} ions (from nitrate salts) were adsorbed on Aerosil. Upon adsorption of saturated hydrocarbons, such as n-hexane, on the surface large paramagnetic shifts in the powder NMR spectra were observed. On Co^{2+} there was a nonlinear inverse relation between the shift and amount of hydrocarbon adsorbed which was taken to indicate the formation of a rather weak complex between the hydrocarbon and Co^{2+}. The heat of complexation was 2–2.5 kcal mol^{-1} larger than the value for heat of physical adsorption. Spectral assignments showed that Co^{2+} was tetrahedrally or trigonally coordinated. From spin density calculations the bonding model in Figure 27 was postulated. Ni^{2+} formed no such complex.

Very recently Ugo, Basset, and co-workers deposited Rh_6 clusters on SiO_2, Al_2O_3, and MgO supports maintaining the integrity of the clusters.[257] By reaction of the supported clusters with excess CO the original $Rh_6(CO)_{16}$ cluster was regenerated. During the thermal
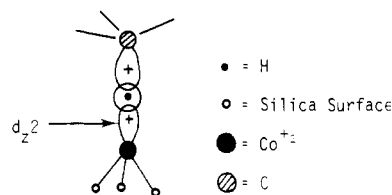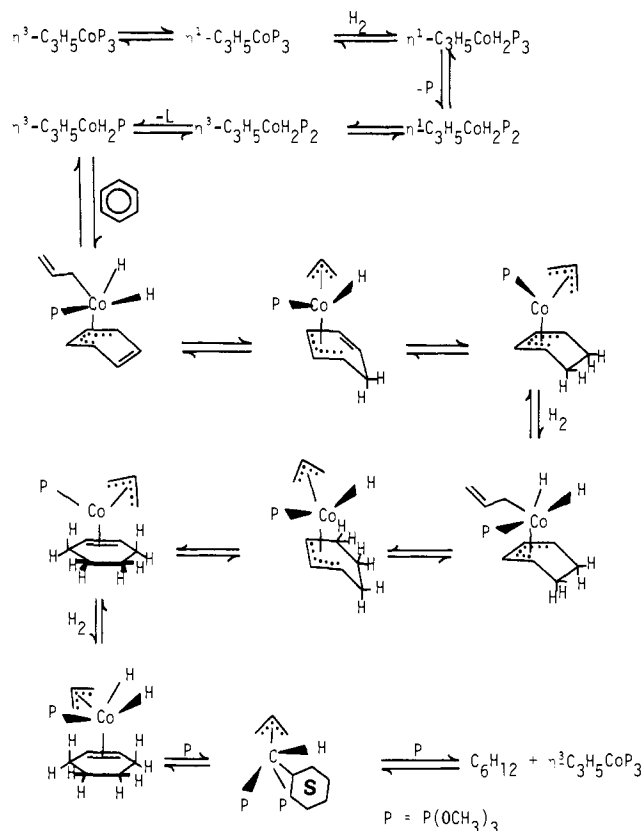

Figure 27. Alkane–Co^{2+} "complex".[256]

decomposition of $Rh_6(CO)_{16}$ on Al_2O_3, CO_2, H_2, and small amounts of hydrocarbons were evolved as products from a water-gas shift reaction. Therefore, Rh_6 clusters seem to catalyze C–O and O–H bond cleavages and C–O, C–H, and C–C bond formations to a limited extent. This formation of hydrocarbons was observed at temperatures as low as 150 °C.[258] A study of other metals revealed the following order of activity towards the water-gas shift reaction: $Ru_3(CO)_2 > Os_6(CO)_{18} > Rh_4(CO)_{12} \sim Rh_6(CO)_{16} \sim Ir_4(CO)_{12} \sim Os_3(CO)_{12}$. This reactivity sequence is comparable to that determined for the methanation reaction (reaction 8) on metal powders. Product distributions of hydrocarbons formed upon heating the supported carbonyl clusters under a CO atmosphere are shown in Table XXXII.

Transition-metal complexes have been intensively studied by researchers in the field of homogeneous catalysis. The main goals sought by these workers are control of product selectivity, stereochemistry, and the use of mild conditions (such as low temperature). Tailoring of selectivity by variations of ligands and solvent has been achieved to some extent.[259] Many advances have been made in the synthesis and understanding of monometallic and homonuclear cluster compounds for "easy" catalytic reactions such as olefin and arene hydrogenations and hydrocarbon/deuterium exchange reactions.[260-262] Catalysis of more difficult reactions such as those involving C–C bond cleavage or C–H bond activation in saturated hydrocarbons by homogeneous transition-metal complexes has been much less studied and with little success.[260] A report of alkane C–H bond activation by a monometallic transition-metal complex (Ir) has appeared in the literature.[263] This alkane activation is discussed later in this subsection. No monometallic complex has been found to be active for C–C bond cleavages. Cleavage of C–C bond by a ruthenium cluster compound was reported and will be discussed shortly.[264] Comparisons of processes occurring at the metal centers of homogeneous catalysts with those postulated on heterogeneous catalysts have been made frequently (e.g., ref 260, 262, 266). As a result, the "art" of heterogeneous catalysis is rapidly developing into a "science".

A recent review by Muetterties has revealed the flexibility of a metal complex during the process of

Figure 28. Proposed mechanism for arene hydrogenation by η^3-$C_2H_5Co[P(OCH_3)_3]_3$.[262]

Figure 29. Benzene/D_2 exchange catalyzed by metal polyhydrides.[267]

arene hydrogenation.[262] Allylcobalt complexes were demonstrated to catalyze, stereoselectively, the hydrogenation of various arenes. Mechanistic studies were performed that showed that two apparent criteria were required in order for these complexes to be catalytically active for hydrogenation. First, the allyl ligand seemed to be needed so that $\eta^1 \rightleftharpoons \eta^3$ changes could create open coordination sites on the metal center. Second, the metal needed to be able to easily, and reversibly, change between two oxidation states, +1 and +3 ($d^8 \rightleftharpoons d^6$). The latter criteria appear to be general since some complexes without allyl ligands have been found to be catalytically active. Muetterties and co-workers found high stereoselectivity in hydrogenations of arenes using η^3-$C_3H_5Co[P(OCH_3)_3]_3$ as a catalyst. This stereoselectivity was thought to be a result of continuous complexation of the arene during a reduction process. A mechanistic scheme proposed and supported for benzene hydrogenation is shown in Figure 28. According to this scheme, ligand dissociation from the metal center is necessary to generate enough open coordination sites for initial arene complexation (η^4-arene ligand). Hydrogen becomes attached to the metal center by oxidative addition, changing the metal from Co(I) d^8 to Co(II) d^6. It appeared as though a η^4-bound arene is a favorable first step in the hydrogenation sequence due to loss of aromatic delocalized energy. However, some η^6-arene complexes have been shown to be catalytically active. Two such complexes were studied in our laboratories, η^6-$C_6H_5CH_3Ni(C_6F_5)_2$ and η^6-$C_6H_5CH_3Co(C_6F_5)_2$.[265]

It has been presumed that dihydride complexes are important intermediates in homogeneous olefin or arene hydrogenations. Crabtree and co-workers isolated the
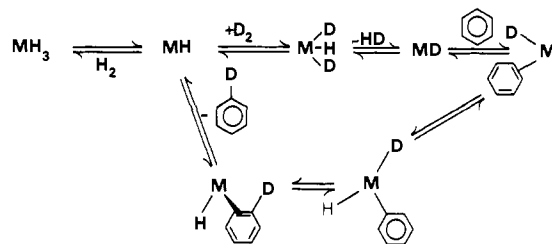
first dihydride olefin complex, cis-[IrH_2(COD)L_2]PF_6, prepared as in reaction 13.[261] This hydrogen addition

$$[Ir(COD)L_2]PF_6 \ + \ H_2 \ \longrightarrow \ \left[\begin{array}{c} \end{array} \right] PF_6 \qquad (13)$$
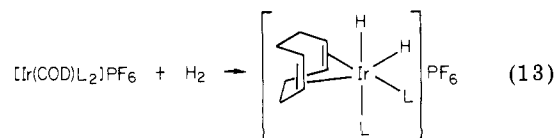
was suggested to be performed by a reductive addition of H_2.

Activation of C–H bonds by transition-metal complexes is illustrated by deuterium exchange reactions (which occur readily over heterogeneous catalysts). A review of studies on C–H bond activation by mononuclear metal complexes appeared in the literature in 1975.[266] There appears to be a close analogy between the process of D/H exchange with hydrocarbons that occur at the central metal atoms of a soluble complex and those that occur at the active sites of a metal surface. Metal hydrides are the most active of homogeneous catalysts for the exchange of deuterium with benzene. The C–H bond activation is believed to involve cleavage of the C–H bond by the metal, forming a C–M bond which subsequently undergoes reaction with a reagent such as D_2.

$$C-H \ + \ M-D \ \rightleftharpoons \ C\cdots M \overset{H}{\underset{D}{<}} \ \rightleftharpoons \ C-D \ + \ M-H$$
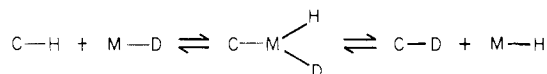
Some hydride complexes that were active toward D_2/benzene exchange reactions are $TaH_3(C_5H_5)_2$, Ir-$H_5[P(CH_3)_3]_2$, $NbH_3(C_5H_5)_2$, and $TaH_5[(CH_3)_2PCH_2C$-$H_2P(CH_3)_2]_2$; the latter two were the most active. With these catalysts only aryl C–H bonds were found to exchange with deuterium and only one C–H bond exchanges per collision. This is in contrast to the multiple exchange of aliphatic C–H bonds that occurs over heterogeneous catalysts. A mechanism for aromatic C–H/D_2 exchange by polyhydride metal catalysts was proposed in 1972 by Klabunde and Parshall.[267] This is illustrated in Figure 29. The key intermediate in the exchange reaction is the coordinatively unsaturated metal hydride formed by dissociation of H_2 from the trihydride. Two main processes occur in the reaction: (1) coordination of the arene and (2) oxidative addition of the aromatic C–H bond to the metal center. Either (1) or (2) may be the rate-determining process.[266] Some complexes have shown activity for benzene/D_2 exchange which initially contain no hydrides, for example, $Cp_2Nb(C_2H_5)(C_2H_4)$ and $CpRh(C_2H_4)_2$. In these complexes exchange is observed between D_2 and the ethylene and cyclopentadienyl ligands. These studies suggest that on a metal surface three adjacent metal atoms may not be required for deuterium exchange but rather three adjacent orbitals on a single metal atom, as shown in Figure 30. Some complexes catalyze D_2
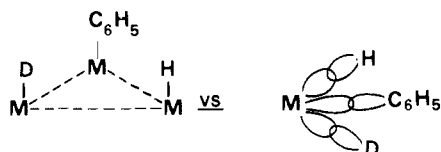
Figure 30. Benzene/D_2 exchange intermediates on a transition-metal surface.[266]

exchange with alkyl C–H bonds as well as multiple exchange. One such complex is the $(PtCl_4)^-$ salt, which acts like a heterogeneous catalyst in the aforementioned aspects.[266]

Activation of C–H bonds in alkanes was very recently reported.[263] In a noncoordinating solvent such as $C_2H_4Cl_2$, cyclopentane was found to react with $[IrH_2(Me_2CO)_2L_2]BF_4$ (L = PPh_3) to give $[CpIrHL_2]^+$ in 30% yield at 80 °C. Cyclooctane reacted similarly, giving $[Ir(COD)L_2]^+$ as a product. In both reactions a nonallylic hydrogen containing olefin, 3,3-dimethyl-1-butene, was added as a hydrogen acceptor. Smaller olefins or those containing allylic hydrogens completely inhibited the alkane dehydrogenations. The presence of the hydrogen acceptor was a necessity. Presumably an unstable olefin complex with the butene was formed that readily dissociated to allow access of the alkane to the metal center.

Other examples of activation of alkane C–H bonds can be found in the literature, mainly by platinum group complexes in low, nonzero, oxidation states.[268-270]

As mentioned earlier, no monometallic transition metal complexes have been reported to be active in C–C bond activation except for strained cyclic compounds such as cyclopropane.[270] However, $Ru_3(CO)_{12}$ has been shown to react with cyclohexadiene to give the μ-allylruthenium hydride shown in reaction 14.[264] The reaction was carried out at 98 °C with a 30% yield of product. This was the first reported cleavage of an

$$M = Ru(CO)_3$$
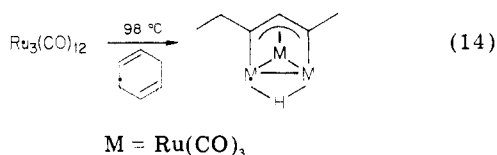
unstrained C–C bond by a transition-metal complex. A trinuclear complex seemed to be most reasonable as the catalyst for the cleavage.

The iron cluster, $(\eta^5-C_5H_5)_4Fe_4(\mu_3-CO)_4$, was shown by Pittman and co-workers to be active for alkyne hydrogenation.[260] Furthermore, this cluster was shown to selectively reduce terminal alkynes to olefins.

A recent comprehensive review of the metal cluster-surface analogy was given by Muetterties, Rhodin, and co-workers.[271] By comparison of the structural information of metal clusters containing hydrocarbon ligands (e.g., alkyl radical ligands) with the limited data obtained from studies of hydrocarbon chemisorption on metal surfaces, the following extrapolations to metal surface chemisorption intermediates were made: (1) Saturated hydrocarbons chemisorb dissociatively on metal surfaces with a minimum of one C–H or C–C bond cleavage to produce an adsorbed radical. (2) Multicenter bonds between the surface and an alkyl ligand are likely. (3) Two to six carbons of the benzene ring of aromatic hydrocarbons may be involved in their chemisorption. Aromatic C–H bond cleavage may occur
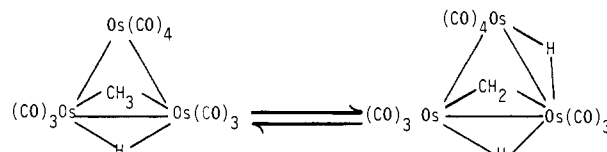

Figure 31. Methyl $\rightleftharpoons$ methylene transformation in $HOs_3(CO)_{10}CH_3$.[271]

to allow the C_6 ring to be bound in a complex manner to the metal surface. (4) CR or CR_2 fragments interact with a minimum of two surface metal atoms. The alkyl "fragments" in molecular clusters are all bound to an edge of the cluster, as exemplified by $HOs_3(CO)_{10}CH_3$ shown in Figure 31. This Os_3 cluster demonstrates three bonding concepts that may be applicable to surface chemistry: (1) multicenter bonding to metal atoms, (2) bonding of an alkyl fragment to an edge site on a metal surface, and (3) mobility of methyl, methylene, and hydrogen species on a metal surface through a unique bridging state.
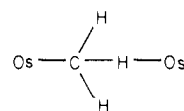
There are very few cluster compounds containing alkyl ligands that could serve as examples of chemisorbed hydrocarbon species on a metal surface.[271] Much future work is required before any reasonably sound correlations can be made. As the chemistry of the many cluster compounds now available is investigated, processes occurring on metal surfaces will be made more clear.

The final topic discussed in this section deals with reactions that occur with "naked" metal atoms and clusters. Due to the limited amount of work done in this area that can be applied toward an understanding of reactions with metal surfaces, only simple cases of chemisorption and specific examples of C–H bond cleavages of hydrocarbons are considered.

As described in the section on low temperature clustering of metal atoms in inert matrices, naked metal atoms and small clusters can be isolated and characterized by spectroscopic methods. A few studies of interactions between these naked clusters and molecules have been reported.[272-276]

A study of the bonding between simple molecules such as CO and N_2 and isolated nickel, platinum, and palladium atoms was reported in 1975.[272,273,276] $M(N_2)_x$ (x = 1, 2, 3, 4) complexes were isolated in inert gas matrices at 10–20 K. The changes in N–N stretching frequencies between free N_2 and N_2 complexes with metal atoms were compared with those changes due to chemisorption on metal surfaces as reported in the literature for the platinum group metals (Ni, Pd, Pt). The ratios of N–N stretching frequencies, $\Delta\nu_{MN_2}/\Delta\nu_{chemisorbed\ N_2}$, were found to be 1.9, 1.7, 1.6, and 1.9 for Ni, Pd, Pt, and Rh, respectively. This indicates, for all metals studied, that there is a weakening of the interaction with the N_2 molecule upon going from a single metal atom, MN_2, to N_2 adsorbed on a metal surface. N–N stretching force constants for $Ni(N_2)_4$, NiN_2, and N_2 adsorbed on a Ni surface were calculated as 19.65, 17.74, and 19.99 mdyn/Å, respectively. Values for $Ni(CO)_4$, NiCO, and CO adsorbed on a Ni surface were found to be 17.23, 16.09, and 17.38 mdyn/Å, respec-

tively. These data indicate that the bonding between these ligands and metal atoms in ordinary complexes such as $Ni(CO)_4$ is very similar in both strength and character to those on a metal surface.[273] In addition it was shown that there is a decrease in σ donation from the ligands and π back-bonding to the ligand upon going from a complex to chemisorption on a metal surface.

Moskovits pointed out in a recent review that N_2 interaction with Fe atoms and Fe metal surfaces is physical in nature.[276] However, small clusters of Fe were found to chemisorb N_2. It was cautioned that conclusions obtained from studies of mononuclear species are not necessarily applicable to small clusters and results from small cluster studies are not necessarily applicable to bulk metals. Matrix isolation studies of CO on Pd atoms and aggregates forming Pd_xCO ($x \leq 4$) in frozen Ar matrices revealed IR bands corresponding to linearly bonded, μ_2-bridged and μ_3-bridged carbonyls. It was also pointed out by Moskovits that broadening of peaks and shifts to higher frequencies in the IR with increasing coverage of CO on Pd single crystal planes has been observed. This was explained by a rather strong "communication" between adsorbate molecules, presumably a result of vibrational coupling between the admolecules via conduction electrons of the metal. These nonlocal interactions are much stronger between adsorbate molecules on a metal surface than between ligands in cluster carbonyls.

Reactions of ethylene with metal atoms and small clusters (M_2) in inert matrices were studied by Ozin and Power.[274,275] A study of the complexes $Ni_2(C_2H_4)_m$ (m = 1, 2) and $Ni(C_2H_4)_m$ (m = 1, 2, 3) revealed that addition of a second metal atom increases the $M-C_2H_4$ binding energy.[275] Thus, the binding energy increased from 14.2 kcal for $Ni(C_2H_4)$ to 16.8 kcal for $Ni_2(C_2H_4)$. Also, in the $Ni_2(C_2H_4)$ complex the ethylene was thought to be mainly interacting with only one of the two nickel atoms so the other nickel atom displays the effect of a neighboring atom. A study of C_2H_4 interaction with Pd atoms and a Pd metal surface showed a strengthening of C=C and C—H bonds upon going from $(C_2H_4)Pd$ to $(C_2H_4)_{ads}Pd_{metal}$ (Pd/Al_2O_3). There appears to be an optimal size of cluster between M_{atom} and M_{bulk} for maximum interaction with C_2H_4. One must be careful in placing much faith in these correlations due to other factors such as support–metal interactions and surface cleanliness.

Interactions of metal atoms with arenes have been utilized to a large extent in preparative metal atom chemistry.[277] Chromium atoms react with benzene to form bis(benzene)chromium; however, complexes of benzene and Fe, Co, and Ni appear to have a 1:1 benzene:metal stoichiometry when formed at low temperature (77 and 10 K).[278,279] It should be noted that the existence of a formal 1:1 stoichiometry in these low temperature complexes is the subject of much controversy.[277] The strength of interaction between arenes and metal atoms is of the order Cr > Fe > Co > Ni as determined by relative C=C stretching and C—H bending modes of benzene in the complexes by use of matrix isolation techniques.[278] Decomposition of Ni–(toluene) complexes in toluene matrices by matrix meltdown and warmup leads to metal particle formation and fragmentation of the arene ligands as indicated

by high carbon and hydrogen content in the metal powders produced.[280,281] Even cleavage of saturated hydrocarbons by clusters of nickel atoms has been indicated.[281] Nickel particles formed by Ni toluene decomposition at low temperatures were shown to have very interesting magnetic properties.[280] X-ray diffraction patterns and interference functions revealed nickel crystallite sizes of 16 Å diameter and a normal fccub packing. These small metal particles would be expected to exhibit superparamagnetism; however, this was not observed in magnetization vs. H/T curves. Furthermore, sample magnetization increased with increasing temperature in the 450–500 K range. These results indicated that the small crystallites were not isolated, but nearly in contact with each other such that magnetic coupling interactions between crystallites occurred. Organic surface layers were shown to be present on the crystallites, preventing their direct contact. Heating in the 450–500 K range caused a loss of some organic layers, allowing enhancement in interparticle coupling. The nature of the organic layers was not investigated.

At low temperatures, Ozin and co-workers showed that vanadium atoms isolated in alkane matrices did not react with the matrix molecules up to one-half the melting point of the alkane.[89]

A possible example of C–H activation by a single metal atom can be found in an early report of Skell and co-workers.[282] Cocondensation of iron atoms and 1,3-cyclohexadiene at 77 K followed by reaction at 97 K for 1 h led to formation of cyclohexene (33%), benzene (36%), and cyclohexadiene (30%). It appeared as though this disproportionation reaction involved only a single iron atom.

A recent report by Skell and co-workers suggested that Zr atoms can react with alkanes (isobutane and neopentane) at cryogenic temperatures (77 K).[283] Cocondensation of Zr atoms with neopentane followed by warmup and solvent removal produced a black powder. During matrix warmup H_2 and small amounts of CH_4 were produced; they evolved for about 1 h after the matrix reached room temperature. Hydrolysis of the dried black powder with D_2O produced HD (80%) and D_2 (20%) as well as C_2, C_3, and C_4 hydrocarbons that were highly deuterated. Neopentane was also released but was exclusively monodeuterated. The lack of polydeuterated neopentane and the presence of hydrogen and olefinic products were taken to indicate a lack of an active metal surface catalyzing H/D exchange between D_2O and the hydrocarbon products. In light of Ozin's work on vanadium atom clustering in alkane matrices it was suggested that Zr atoms reacted with the alkane matrix upon impact to form species a and b of Figure 32. The black solid obtained was suggested to be a three-dimensional structure formed by agglomeration of organozirconium species. Muetterties has cautioned chemists to be wary of results obtained from "black" reaction mixtures when attempting to attribute reactions to monometallic species.[262] No X-ray studies were performed on Skell's black powders, which were believed to contain only monozirconium species. Such studies would clearly show if crystallites were indeed present.

A recent report by Ridge and co-workers has shown that Fe^+, Co^+, and Ni^+ ions, generated by electron im-
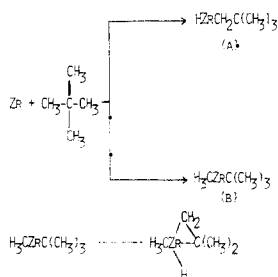
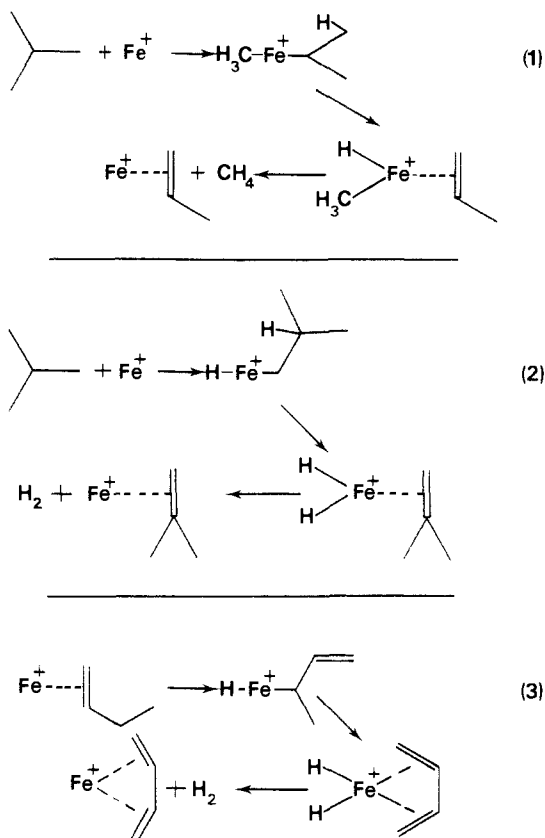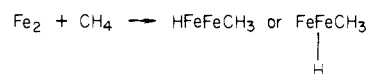**Figure 32.** Organozirconium species formed by reaction of Zr atoms with neopentane.[283]

Figure 33. Proposed reaction mechanisms for Fe⁺ + isobutane and Fe⁺ + n-butane.[284]

pact on the corresponding carbonyl complexes, react with alkanes by insertion into C–H or C–C bonds.[284] With monodeuterated isobutane and n-butane the mechanisms shown in Figure 33 were suggested to account for products. Either initial C–C insertion or C–H insertion can account for the cleavage products of n-C_4H_{10} by the metal ions. Thus, reaction 3 of Figure 33 could follow the reaction 2 analogue for n-butane to cause H_2 evolution and formation of $FeC_4H_6^+$. Evolution of CH_4 is believed to be caused by an initial Fe⁺ insertion into a C–C bond of isobutane as shown in reaction 1 of Figure 33. This reaction accounts for 85% of the reaction products while reaction 2 accounts for only 15%.

Pearson and co-workers recently reported oxidative cleavage of C–H bonds of an alkane (CH_4) by iron dimers (Fe_2) in a low temperature matrix.[285] These workers used Mössbauer spectroscopy of Fe/CH_4 matrices to obtain evidence of reaction between Fe_2 and CH_4. In contrast, Fe atoms showed no reaction with the methane matrix. Bands in the 2000-cm⁻¹ region of the infrared gave indications of Fe–H presence. The

reaction sequences suggested are

$$Fe_2 + CH_4 \longrightarrow HFeFeCH_3 \text{ or } FeFeCH_3$$

and possibly

$$FeFeCH_3 \longrightarrow Fe\text{---}Fe\text{==}CH_2$$
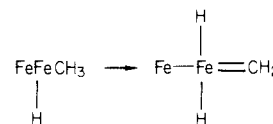
due to the expected change of oxidation state from Fe(0) to Fe(II). None of the above structures have been rigorously characterized, but the Mössbauer spectra provide strong evidence for the reaction.

Current studies by Billups and co-workers have demonstrated, by IR spectroscopy, that Fe atoms can insert into C–H bonds of methane in low temperature matrices when subjected to photolysis by a Hg arc lamp.[286] No insertion occurs without the photoexcitation.

$$M + CH_4 + \underset{\text{(excess)}}{\text{argon}} \xrightarrow[15\text{ K}]{h\nu} CH_3\text{-}M\text{-}H$$
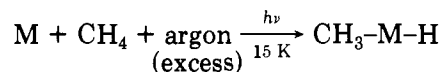
A summary of recent matrix metal atom/cluster reactions would be in order since several remarkable hydrocarbon reactions have been observed. These findings are enumerated chronologically as follows: (1) Small Ni clusters react with alkanes and arenes by C–C and C–H cleavages as low as –130 °C.[73,74,281] (2) Diiron (Fe_2) reacts with CH_4 by C–H insertion as low as 15 K.[285] (3) Zr atoms react with alkanes by C–C and C–H cleavage as low as –196 °C.[283] (4) Several metal atoms react with CH_4 by C–H insertion upon photolytic excitation of the metal atom as low as 15 K.[286] The weight of all this evidence is very convincing, and indicates that bare atoms and clusters exhibit astonishing reactivities with hydrocarbons. Further studies are certainly warranted since these recent reports set the scene for possibly gaining fundamental knowledge about atom vs. cluster reactions with hydrocarbons.

VII. Methods for the Characterization of Metal Particles, Metal Surfaces, and Adsorbed Species

This section deals with experimental methods used to study the topography and chemical composition of metal surfaces. It is intended to be a "broad brush" introduction to the many new techniques and methods made available in recent years. Main emphasis is placed on methods suitable for studying dispersed metal catalysts containing small metal crystallites (<100 Å). Many surface analysis techniques applicable to massive metal surfaces and thin films are summarized briefly. The reader who is interested in these techniques is referred to more exhaustive recent reviews by Madix and by Nieuwenhuys as well as other reviews cited in previous sections of this review.[287,288] Methods covered in this section that are suitable for studies of dispersed metals are used to provide information concerning (1) surface area, (2) crystallite size, and (3) chemical composition (nature of adsorbed species).

Extensive research has been carried out for the last 30 years in the development of techniques to study solid surfaces. Today the list of such techniques is quite extensive. A complete description of all the available

techniques used to study surfaces would be voluminous; therefore, those most commonly employed will be summarized.

The counterpart of X-ray crystallography in surface chemistry is low energy electron diffraction (LEED). LEED involves the irradiation of a specimen surface with low energy electrons (10–200 eV) and records the elastically back-reflected electron beams. The picture obtained consists of spots, the geometric arrangement of which can be used to determine the two-dimensional unit cell vectors of the surface lattice. Long-range order must be present on the surface (≥200 Å laterally)[172] in order to get sharp spots. It is this requirement of LEED that limits its applicability to single metal crystals and thin films. Nieuwenhuys pointed out that information on the atomic structure of thin film surfaces is limited due to the lack of ordered domains of 200 Å in these specimens.[288]

LEED is very useful for the study of single metal crystals. Analysis of diffraction spots intensities (I) as a function of incident beam energy (V) yields I–V profiles that can be used to determine the location of adsorbed atoms or simple molecules on the surface.

The measurement of the work function, which is the energy required to remove an electron from the top of the Fermi sea to a point outside the metal, is suitable for massive metals and thin polycrystalline films. The work function is highly dependent upon the structure of a film since it is closely related to the electron distribution in the surface region. The work function of tungsten crystals has been related to the density of steps on the surface.[287] Work functions can also be used to provide compositional information since adsorbed species change its value.

A final technique commonly employed to determine surface topography of massive metals and thin films is transmission electron microscopy (TEM). The surfaces of massive metal samples are studied by making replicas of the surfaces and looking at these by TEM. Replication is performed by coating the metal surface with a thin film of plastic, which is subsequently removed. In a one-step process, the plastic impression is shadowed with a metal such as platinum and also with carbon by evaporative deposition. In a two-step process, the plastic impression is coated with a thin layer of evaporated carbon. The plastic is removed by a suitable solvent and the carbon replica is then shadowed. With the two-step process resolutions of about 20 Å can be obtained.[3]

Thin films are best observed by TEM when they are deposited on mica. A thin top layer of the mica is peeled off using "Cellotape". The "Cellotape" is then dissolved and the film on mica is recovered on a TEM grid for observation.

Surface composition of massive metals and thin films can be obtained by a wide variety of techniques. Many electron spectroscopy techniques have been developed for the study of metal surfaces. These techniques fall into two general categories: (1) core-level electron spectroscopy and (2) valence electron spectroscopy. The first category includes methods such as X-ray photoemission spectroscopy (XPS), electron energy loss spectroscopy (ELS), photoelectron spectroscopy (PES), Auger electron spectroscopy (AES), and appearance potential spectroscopy (APS). The second category includes methods such as ultraviolet photoemission spectroscopy (UPS).

In XPS incident X-rays excite electrons from a core level to the vacuum level and the energy distribution of the emitted electrons is observed. This technique provides information concerning the oxidation state of atoms and elemental composition of the surface. This method is used for electron spectroscopy for chemical analysis (ESCA).

ELS and HRELS (high resolution electron energy loss spectroscopy) involve excitation of core level electrons by incident electrons to a final level above the Fermi level of the metal. In making this transition the incident electrons reflected back in an inelastic manner suffer energy losses. This loss of energy can be analyzed to obtain vibrational spectra of adsorbed atoms and molecules.

A core level electron of a surface or near surface atom can be excited by an electron or photon of higher energy. Deexcitation follows by removal of an electron from a higher energy level to the hole created by excitation of the core level electron. During this process energy is released which is compensated for by release of an electron from another level, called an Auger electron in AES. An X-ray photon may also be emitted. In AES the energy distribution of emitted Auger electrons is measured. Since AES involves excitation of core level electrons it is good for determinations of surface elemental composition and distribution mapping. In APS the derivative of the intensity of emitted X-rays or Auger electrons is measured as a function of incident electron energy. When the incident electron energy is increased, a threshold value is reached that is just sufficient in magnitude to excite a core electron to vacant levels above the Fermi level (E_F). When this threshold potential is reached, there is a sudden increase in the intensity of emission that is recorded as a peak in the derivative curve of the emission intensity. Core level electrons are excited by high energy photons in PES. The kinetic energy of a photoelectron ejected from the surface by the incident photon is given by the photon energy minus the work function and the difference in energy between the electron level and the Fermi level. These transitions are element dependent, which makes APS and PES well suited for compositional analysis.

AES and related methods have the advantage of being fast and accurate for analysis of surface composition. However, chemical or structural changes in the surface may be induced by impact of the high energy electron beam.[288] XPS has the advantage of being suitable for surfaces that are easily damaged by electron bombardment. However, poor spacial resolution is obtained due to the inability to focus an intense X-ray beam.

The major valence electron spectroscopy technique is UPS. This method involves the adsorption of an ultraviolet photon by a valence electron whose energy is then increased by $h\nu$ of the photon. The final energy state (E_2) of the excited electron is measured. With knowledge of the value of E_2, the energy of the excited electron before excitement (E_1) can easily by determined by $E_1 = E_2 - h\nu$. In UPS incident photons with energies in the range 10–45 eV are used. Since this technique produces photoelectrons originating from the valence band of the solid, it is used primarily in the

elucidation of band structure rather than chemical analysis. In XPS band states as well as core states can be analyzed.

In addition to the various electron spectroscopic techniques, ion spectroscopic methods are also used. The two main techniques are secondary ion mass spectrometry (SIMS) and ion scattering spectroscopy (ISS). In SIMS a specimen surface is bombarded by high energy ions (keV range); this causes ejection of positive and negative ions. The masses of the secondary ions are measured. This method is a very sensitive one for surface composition analysis. ISS is somewhat less sensitive than SIMS. ISS involves bombardment of a surface with a monoenergetic beam of inert gas ions, which are back-scattered from the surface with an accompanying loss of energy. The energy loss of the ions due to their inelastic collision is a function of the mass of the surface atoms with which they collide. The major problem with these methods (SIMS and ISS) is that surface etching of the surface occurs during the analysis.

The above techniques require that the electrons or ions emitted from the surface under study are able to reach the detector without interference from collisions with other surfaces. It is for this reason that these methods are best suited for thin film or massive metal surfaces studies. Metal powders must be pressed into pellets which may cause morphological changes such as sintering. Supported metals need to be used that have rather high metal loadings so that sufficient intensities of electrons or ions can be obtained to give good signal to noise ratios. It is for this reason that electron-stimulated Auger electron spectroscopy of highly dispersed supported metal catalysts has not been rewarding.[3]

Methods of characterization which are commonly used for dispersed metal catalysts include (1) physical and chemical adsorption of gases, (2) X-ray diffraction and scattering, (3) electron microscopy, (4) magnetic measurements, (5) infrared spectroscopy, and (6) temperature programmed desorption. Of the above methods, (5) and (6) are used for characterization of adsorbed species such as hydrocarbons. These latter two methods are much less commonly used than the former four.

The most commonly measured characteristic of dispersed metal catalysts is surface area. The importance of this parameter is obvious. The higher the surface area of a catalyst that is exposed to reactants, the higher is the total conversion to products. Metal atoms that are not present on the surfaces of particles are in effect "wasted" and increase the expense of a catalyst. It is, therefore, most desirable to obtain the highest surface to volume ratios of catalytic metal particles possible. The surface area is inversely proportional to particle size so very small particles of metals are desirable. Surface areas are normally expressed as specific areas (area per unit mass).

In 1938 Brunauer, Emmett, and Teller reported a technique for rapidly and accurately determining surface areas using gas adsorption.[289] The technique, referred to as the BET method, is used routinely today. Brunauer, Emmett, and Teller obtained low temperature van der Waals adsorption isotherms for various gases (N_2, O_2, Ar, CO, CO_2, and SO_2) on various catalysts. In all cases S-shaped isotherms were obtained (e.g., see Figure 34) that were concave with respect to the pressure axis at low pressures and convex at high
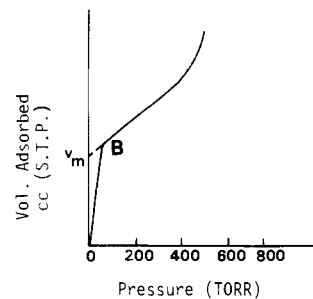

Figure 34. Typical adsorption isotherm for surface area determination by N_2 adsorption at 77 K.

pressures. The Langmuir theory of multimolecular adsorption was used to interpret the results. Two equations emerged, 15 and 16, which predicted S-shaped isotherms. Equation 16 related the total vol-

$$\frac{p}{v(p_0 - p)} = \frac{1}{v_m c} + \left(\frac{c - 1}{v_m c}\right)\frac{p}{p_0} \qquad (15)$$

$$v = \left(\frac{v_m c x}{(1 - x)}\right)\frac{1 - (n + 1)x^n + nx^{n+1}}{1 + (c - 1)x - cx^{n+1}} \qquad (16)$$

ume of gas adsorbed (v) at various pressurs (x) to the number of layers of gas molecules formed on the surface (n). In the equations p_0 is the saturation pressure of the gas above which no further adsorption occurs. Constant c is approximately equal to $e^{(E_1-E_L)/RT}$, where E_1 is the heat of adsorption of a monolayer of the gas and E_L is the heat of liquefaction of the gas; $x = P/P_0$, where P is the gas pressure above the sample. The most important value which is a constant for a given sample is v_m. v_m is the volume of gas adsorbed when the entire adsorbent surface is covered with a complete unimolecular layer. It was demonstrated that v_m can be readily obtained by plotting volume of gas adsorbed (STP) vs. pressure (torr) from experimental measurements. The point (B) at which the curve begins to become linear corresponds to v_m, as shown in Figure 34. Once v_m is known, the value can be used to determine surface area. This is done by multiplication of the number of molecules corresonding to v_m by the average area occupied by each adsorbed molecule or atom. A general criterion for this method is that the experiment is carried out at a temperature that is close to the condensation temperature of the adsorbate gas employed.

Another very useful gas adsorption technique is that of chemisorption. This method is particularly useful for determining the surface area of a metal in a supported catalyst. This is achieved by using hydrogen which chemisorbs selectively on the metal (e.g., nickel) and not the support (e.g., alumina). Hydrogen adsorption isotherms are obtained in an entirely analogous manner as the BET isotherms. However, there is a sharp change in slope once a complete monolayer of hydrogen is chemisorbed to the metal. This monolayer consists of one hydrogen atom per surface metal atom (in the case of nickel) since hydrogen chemisorbs dissociatively.[3] The surface area is then easily determined by multiplication of the number of hydrogen atoms in a complete monolayer by the cross-sectional area of the metal atom (e.g., nickel).

Anderson points out that contamination of unsupported nickel catalysts can create problems with hy-

drogen chemisorption.[3] It has been observed that there is a substantial slow hydrogen uptake which could be caused by carbonaceous contamination. Chemisorption of hydrogen on clean polycrystalline films of nickel is very rapid, with a monolayer being formed in a few seconds to a minute. Slow uptake is characterized by adsorption that may take as long as several hours to reach monolayer capacity. The reasons for slow hydrogen uptake are not clear. However, it is assumed that chemisorption stoichiometry for the slow component is the same value as the fast component.[3]

Surface area determination can be used to calculate average metal particle sizes of catalysts.[3] Once the total surface area, A, is known, the average particle size can be found after determination of the total metal volume. This latter value is obtained from the mass of metal present and its density. The average diameter, assuming spherical particles, is given by

$$\bar{d}_{VA} = 6V/A$$

Sermon reported an equation for the determination of average particle diameters, which is

$$D_{calcd} = \frac{6 \times 10^3}{\rho \, S_{avg}}$$

where D_{calcd} is average particle diameter (nm), ρ is metal density (g cm^{-3}), and S_{avg} is average surface area (m^2 g^{-1}).[111]

Another method used to determine crystallite sizes is X-ray diffraction line broadening.[79,290] In this method the Scherrer equation is used which is commonly in the form

$$L = K\lambda/(\beta \cos \theta)$$

where L is crystallite size (Å), λ is the X-ray wavelength (Å), K is a constant, usually taken as 0.9, β is the observed peak width at one-half maximum intensity for any given reflection, and θ is the Bragg angle for the reflection.

The reason this method works is that peaks observed from the diffraction of X-rays become broadened as the sample becomes less crystalline, which occurs as the crystallite sizes decrease. Thus, the broadening of diffraction peaks is related to crystallite size by the Scherrer equation. Other factors that contribute to line broadening are (1) the geometry of the specimen, (2) X-ray adsorption and scattering effects in the specimen, and (3) instrumental effects.[70] Broadening due to the system setup is determined by using a crystalline material (such as quartz powder), that should have no broadening. The true broadening of the sample is then found by the relationship:

$$\beta^2_{true} = \beta^2_{obsd} - \beta^2_{instr}$$

This is called the Warren's relationship after its 1941 founder.[291] It has been found that greater accuracy is obtained if β_{corr} is used in the Scherrer equation, where

$$\beta_{corr} = (\beta_{obsd} - \beta_{instr})(\beta^2_{means} - \beta^2_{instr})^{1/2}$$

Whyte pointed out that the best accuracy that can be obtained with this method is 50% due to the different shapes of particles present in the specimen.[125]

In 1977 DeAngelis and co-workers reported a method that enables one to determine a particle size distribution

function from a single X-ray diffraction profile.[119] The calcualtions necessary are quite involved but have been computerized by this group. The main advantage of this method is that lattice strains which may be appreciable in very small crystallites are taken into account. Knowledge of crystallite size distributions in catalysts has been realized to be very important in determining structural effects on catalytic reactions and in sintering studies.[125,130]

The main advantage of X-ray diffraction over gas adsorption measurements for particle size determination is the insensitivity of the former to catalyst contamination.[125] In gas adsorption techniques much of the metal surface may be inaccessible to the adsorbate, resulting in too large of a particle diameter as measured. This lack of adsorbate accessibility may be due to surface contamination or the presence of micropores too small to allow adsorbate entrance.

X-ray diffraction line broadening is most useful for the determination of crystallites in the 30–500 Å diameter range.[3] Smaller crystallite sizes than 30 Å result in lines so broad and diffuse that they are difficult to measure. Smaller crystallite sizes than 30 Å have, however, been reported using the X-ray diffraction technique.[130]

Small angle X-ray scattering has been used to determine crystallite sizes down to 10-Å diameter.[3] This method involves analysis of X-radiation scattered within a few degrees of the incident beam. This technique, called SAXS, is most commonly used for highly dispersed supported catalyst particle size determinations. The main difficulty encountered in the technique is scattering that occurs in support pores. For alleviation of this problem, the support pores are filled with a liquid that has the same electron density as the support. This leaves the metal particles as the only scattering centers.

Electron microscopy is widely used for average particle size and particle size distribution determinations. The method is very straightforward but has the disadvantage of being time consuming since many samples must be observed to obtain representative measurements. The main advantage is that particle shapes can be observed.[125] The lower size limit of particles observable is dependent on the power and resolution of the microscope. Particle sizes as small as 10 Å have been observed by this method using TEM.

When a bulk ferromagnetic metal such as nickel is subdivided into very small particles, there is a drastic change in the magnetic properties. If a particle of a normally ferromagnetic metal has a size that is smaller than a ferromagnetic domain (100–300 Å), it will no longer be attracted to an ordinary bar magnet. If subjected to a large external field, it will act like a paramagnetic atom with a very large magnetic moment. This phenomenon is termed "collective paramagnetism" or "superparamagnetism".[3,142] This unique property of small particles of ferromagnetic metals has been applied in a technique to determine particle size and distribution profiles.

The basis for such determinations is that an assembly of the small particles can be treated as though it is an assembly of paramagnetic atoms. If there are n_i particles each having a volume of v_i, the magnetic moment m_i is expressed as

$$m_i = M_{sp}n_iv_i \left[\coth\left(\frac{M_{sp}v_iH}{kT}\right) - \left(\frac{kT}{M_{sp}v_iH}\right) \right] \quad (17)$$

where M_{sp} is spontaneous magnetization and H is field strength.[3] There are two types of approximations used for eq 17. The high field approach uses a high field strength (10 kOe) and low temperature ($\leq$4.2 K). The smallest particles are affected most by the high fields. The second approximation is the low field approach, which uses field strengths of 5 kOe or less at room temperature. The low field approach determines the sizes of the larger particles.

Under the low field approximation eq 17 reduces to

$$M = M_{sp}V \frac{M_{sp}vH}{3kT} \quad (18)$$

for particles that have the same size.[142] Since not all particles are the same size

$$M = \frac{M_{sp}^2H}{3kT} \sum_i n_iv_i^2 \quad (19)$$

where $v_in_i = V$ in eq 18, n_i is the number of particles with volume v_i. M_s is approximately equal to $M_{sp}\sum n_iv_i$, and if relative magnetizations are used, then

$$\frac{M}{M_s} = \frac{M_{sp}H}{3kT} \frac{\sum\limits_i n_iv_i^2}{\sum\limits_i n_iv_i} \quad (20)$$

where M_s is the saturation magnetization (maximum field strength after which the magnetization becomes field independent). The average particle volume under the low field approximation is $\bar{v}^2/\bar{v}$, which may be represented as

$$\frac{\bar{v}^2}{\bar{v}} = \frac{3kT}{M_{sp}H}(M/M_s) \quad (21)$$

$\bar{v}^2/\bar{v}$ is obtained by plotting M vs. H/T and taking the slope at very low values of H.

In practice M_s is first determined by using high field strengths and very low temperatures or by use of an empirical relation at higher temperatures and lower field strengths as discussed later. Once M_s is determined, M is measured at a known field strength (e.g., 1 kOe). An assumption is that M_{sp} for small metal particles is the same as the bulk M_{sp} value (e.g., 485 G for nickel at 296 K). Since all terms of eq 21 are now known, $\bar{v}^2/\bar{v}$ can be readily calculated. It has been shown that $\bar{v}^2/\bar{v}$ is an upper limit for the average particle volume.[142] In order to obtain an accurate value for M_s, very high field strengths and extremely low temperatures are needed. However, a rather close approximation can be used which is an empirical relation of Heukelom modified by Trzebiatowski in the form of

$$\frac{1}{M} = \frac{1}{M_s} + \frac{1}{M_s(\alpha H)^{0.9}}$$

where α is a constant and an assumption of no residual magnetization is made.[292,293] A plot of $1/M$ vs. $1/(\alpha H)^{0.9}$ should give a straight line with an intercept of the vertical axis at M_s.

Average particle diameters ($\bar{d}$) are easily found from $\bar{v}^2/\bar{v}$ by

$$\bar{d} = [(6\bar{v}^2/\bar{v})/\pi]^{1/3}$$

Variations of the magnetic method calculations have been reported in the literature.[109,146] However, the low field approximation is most commonly employed.

The most fundamental criteria that must be established is that superparamagnetism does exist in the sample. This is determined by plotting M vs. H/T for various field strengths. Superimposition of the curves occurs when superparamagnetism is present. As mentioned previously in this review, Scott did not observe superimposition of M vs. H/T curves for nickel powders produced by cocondensation of nickel atoms and toluene vapors at 77 K followed by warmup and solvent removal.[280] This was very unexpected since SAXS and TEM studies showed average crystallite sizes of 16-Å diameter, which is well within the range for superparamagnetism to occur. This lack of superparamagnetism was suggested to be due to magnetic coupling between the 16-Å crystallites through a carbonaceous layer of 2–5.5 Å.

The validity of the assumption that saturation magnetization values for small particles and bulk metal are equal has recently been demonstrated.[146] Furthermore, it was shown that the Curie temperature of a metallic sample is independent of particle size but strongly dependent on the degree of reduction of the metal. Variations in magnetic properties due to chemisorption of hydrocarbons was exploited by Martin and Imelik.[242] These workers used magnetic measurements to determine the number of covalent bonds between the adsorbed hydrocarbon and the metal for adsorption studies on Ni/SiO_2 catalysts. The results of this study have already been discussed.

Methods for direct observation of catalytic reaction intermediates or chemisorbed molecules on dispersed transition-metal catalysts are limited, and few reports can be found in the literature. Of the spectroscopic techniques available, only infrared spectroscopy has been fruitful. Most IR absorption studies have been made with highly dispersed supported metal catalysts in which the support material is rather transparent to IR radiation (e.g., SiO_2 and Al_2O_3). This dispersion is necessary since metal particles or agglomerates larger than about 100 Å create severe energy dispersion by scattering.[294] An example of IR spectroscopy for the study of chemisorbed species can be found in a 1975 report by Erkelens.[295] Erkelens used a dual cell to compensate for the gas phase spectra of various gases over Ni/SiO_2 catalysts. The IR spectra of C_2H_4, C_3H_6, 1-butene, and butadiene were monitored during their hydrogenations over Ni/SiO_2 catalysts. In the case of ethylene, a band at 3012 cm^{-1} was attributed to the species $NiCH=CHNi$. If the spectral assignment was correct, direct evidence for dissociative chemisorption has been made. The major problem encountered in the study of hydrocarbon adsorption by IR is the weak absorptions by the IR active species. This is probably the reason that most IR studies of chemisorption have been limited to strongly IR absorbing species such as carbon monoxide.

Samples that lack IR transparency, such as compacted powders or films, can be studied by using reflectance methods involving multiple reflections. The combination of this method with Fourier spectroscopy seems promising.[294]

Temperature programmed desorption is a widely used method for identification of adsorbed species.[3,13,296] Information concerning the binding energy of the adsorbed species on the metal surface can be obtained since the temperature at which a molecule desorbs depends upon the strengths of the chemisorptive bonds. A major disadvantage that this method suffers is that reactions of the adsorbed species such as dehydrogenation (for adsorbed hydrocarbons) may occur during heating, creating a more strongly chemisorbed species which will not desorb readily.

VIII. References

(1) D. W. Blakely and G. A. Somorjai, *J. Catal.*, **42**, 181 (1976).
(2) S. L. Bernasek, W. J. Siekhaus, and G. A. Somorjai, *Phys. Rev. Lett.*, **30**, 1202 (1973).
(3) J. R. Anderson, "Structure of Metallic Catalysts", Academic Press, New York, 1975.
(4) T. J. Coutts, "Electrical Conduction in Thin Metal Films", Elsevier, New York, 1974.
(5) K. L. Chopra, "Thin Film Phenomena", McGraw-Hill, New York, 1969.
(6) L. Royer, *Bull. Soc. Fr. Mineral.*, **51**, 7 (1928).
(7) J. R. Anderson and N. R. Avery, *J. Catal.*, **5**, 446 (1966).
(8) S. Kishimoto, *J. Phys. Chem.*, **77**, 1719 (1973).
(9) J. A. Venables, *Thin Solid Films*, **50**, 357 (1978).
(10) R. Shrader, W. Staedter and H. Oettel, *Chem. Tech. (Leipzig)*, **23**, 363 (1971).
(11) G. C. Bond, "Catalysis by Metals", Academic Press, New York, 1962.
(12) K. C. Campbell and S. J. Thomson, *Trans. Faraday Soc.*, **55**, 306 (1959).
(13) D. O. Hayward, "Chemisorption and Reactions on Metallic Films", Vol. 1, J. R. Anderson, Ed., Academic Press, New York, 1971, p 225.
(14) O. Beeck, A. E. Smith and A. Wheeler, *Proc. R. Soc., Ser. A*, **177**, 62 (1940).
(15) G. C. Granqvist and R. A. Burhman, *J. Appl. Phys.*, **47**, 2200 (1976).
(16) J. V. Sanders, "Chemisorption and Reactions on Metallic Films", Vol. 1, J. R. Anderson, Ed., Academic Press, New York, 1971, p 1.
(17) S. R. Logan and C. Kemball, "Structure and Properties of Thin Films", C. A. Neugebauer, J. B. Newkirk, and D. A. Vermilyea, Eds., Wiley, New York, 1959, p 495.
(18) A. H. Pfund, *Phys. Rev.*, **35**, 1434 (1930).
(19) J. L. Carter, J. A. Cusumano, and J. H. Sinfelt, *J. Catal.*, **20**, 223 (1971).
(20) M. Kobayashi and T. Shirasaki, *J. Catal.* **28**, 289 (1973).
(21) A. Sárkány, K. Matusek, and P. Tétényi, *J. Chem. Soc., Faraday Trans. 1*, **73**, 1699 (1977).
(22) R. Willstätter and E. Waldschmidt-Leitz, *Chem. Ber.*, **54**, 121 (1921).
(23) D. W. McKee, *Nature (London)* **192**, 654 (1961).
(24) R. Adams and R. L. Shriner, *J. Am. Chem. Soc.*, **45**, 2171 (1923).
(25) M. S. Borisova, V. A. Pzis'ko, S. P. Noskova, N. Z. Petrova, and L. M. Plyasova, *Kinet. Katal.*, **12**, 1034 (1971).
(26) P. H. Emmett and N. Skau, *J. Am. Chem. Soc.*, **65**, 1029 (1943).
(27) W. K. Hall and P. H. Emmett, *J. Phys. Chem.* **62**, 816 (1958).
(28) A. Y. Kipnis, K. A. Muravin and N. A. Nemoitin, *Poroshk. Metall.*, **11**, 8 (1971).
(29) K. Hata, "New Hydrogenating Catalysts: Urushibara Catalysts", Wiley, New York, 1971, p 88.
(30) P. Fouilloux, G. A. Martin, A. J. Renouprez, B. Moraweck, B. Imelik, and M. Prettre, *J. Catal.*, **25**, 212 (1972).
(31) Ichikawa, Masaru, Japan, Kokai 76,122,655 (1976); *Chem. Abstr.*, **86**, 77433b (1977).
(32) C. Moureau and G. Rodier, *C. R. Hebd. Seances Acad. Sci.*, **246**, 1861 (1958).
(33) P. A. Sermon, *J. Catal.*, **37**, 297 (1975).
(34) W. Strohmeier and H. Steigerwald, *Z. Naturforsch. B, Anorg. Chem., Org. Chem.*, **32B**, 111 (1977).
(35) B. D. Polkovnikov, N. N. Mal'tseva, G. O. Frangulyan, and Z. K. Strelyadkina, USSR Patent 416,083 (1974); *Chem. Abstr.*, **81**, 96800g (1974).
(36) Z. K. Sterlyadkina and N. N. Mal'tseva, *Izv. Akad. Nauk SSSR, Ser. Khim.*, **6**, 1240 (1972).
(37) A. G. Hinze and D. J. Frost, *J. Catal.*, **24**, 541 (1972).
(38) C. A. Brown and H. C. Brown, *J. Am. Chem. Soc.*, **85**, 1003 (1963).
(39) C. A. Brown, V. K. Ahnja and K. Jijay, *J. Org. Chem.*, **38**, 2226 (1973).

(40) T. W. Russell, D. M. Duncan, and S. C. Hansen, *J. Org. Chem.*, **42**, 551 (1977).
(41) F. Wodtcke, F. Wolf, K. Wenke, and G. Stanye, German Patent 1,144,696 (1963); *Chem. Abstr.*, **58**, 10776c (1963).
(42) A. A. Alchudzhan, and M. A. Melkumov, *Arm. Khim. Zh.*, **26**, 332 (1973).
(43) A. A. Alchudzhan, *Izv. Akad. Nauk. Arm. SSR, Ser. Khim. Nauk*, **14**, 89 (1961).
(44) F. Lihl and P. Zemsch, *Z. Elektrochem.*, **57**, 58 (1953).
(45) A. A. Alchudzhan, *Izv. Akad. Nauk. Arm. SSR, Ser. Khim. Nauk*, **14**, 101 (1961).
(46) A. A. Alchudzhan, *Izv. Akad. Nauk. Arm. SSR, Ser. Khim. Nauk*, **13**, 3 (1960).
(47) T. Yamanaka, K. Taya, and Y. Takag, *Rikagaku Kenkyusho Hokoku*, **37**, 276 (1961).
(48) J. Grant, R. B. Moyes, R. G. Oliver, and P. B. Wells, *J. Catal.*, **42**, 213 (1976).
(49) R. G. Oliver and P. B. Wells, "Proceedings: 5th International Congress on Catalysis", J. W. Hightower, Ed., North-Holland, Amsterdam, 1973, p 659.
(50) J. B. LePrince, *Bull. Soc. Chim. Fr.*, **3**, 367 (1976).
(51) G. Rienacker and G. Roloff, *Z. Anorg. Allg. Chem.*, **308**, 263 (1961).
(52) G. W. Watt and P. I. Mayfield, *J. Am. Chem. Soc.*, **75**, 1760 (1953).
(53) J. S. Botzold, French Patent 1,438, 140 (1966); *Chem. Abstr.*, **66**, 14430q (1967).
(54) N. Muruogesn and S. Sarkav, *J. Catal.*, **31**, 469 (1973).
(55) W. R. Kroll, U.S. Patent 3,323,902 (1967); *Chem. Abstr.*, **67**, 70113w (1967).
(56) M. Kajitani, Y. Susaki, and J. Okada, *Bull. Chem. Soc., Jpn.*, **47**, 1203 (1974).
(57) M. Kajitani and J. Okada, *Chem. Lett.*, **8**, 777 (1973).
(58) M. Shimizu and Y. Hirai, *Yuki Gosei Kagaku Kyokaishi*, **21**, 709 (1963).
(59) T. Tamanaka and Y. Takagi, *J. Sci. Res. Inst. Tokyo*, **51**, 168 (1957).
(60) K. Hata, K. Watanabe, and M. Tanaka, *Bull. Chem. Soc. Jpn.*, **31**, 775 (1958).
(61) T. Sasa, *Yuki Gasei Kagaku Kyokaishi*, **12**, 58 (1954).
(62) K. Hoizumi and T. Yamanakaj, *Kagaku Kenkyusho Kakoku*, **31**, 350 (1955).
(63) M. Krivanek, V. Danes, and V. Nikolajenkov, *Collect. Czech. Chem. Commun.*, **29**, 2736 (1964).
(64) M. Krivanek, V. Danes, and V. Nikolajenkov, *Collect. Czech. Chem. Commun.*, **31**, 1950 (1966).
(65) A. E. Agronomov, G. V. Lisichkin, and N. G. Yavkina, *Zh. Fiz. Khim.*, **46**, 1769 (1972).
(66) W. J. C. deKok and H. I. Waterman, *J. Appl. Chem.*, **1**, 196 (1951).
(67) M. Ichikawa, Japan, Kokai 76 122 655 (1976); *Chem. Abstr.*, **86**, 77433b (1977).
(68) K. Ackermann, German Patent 1 191 111 (1965); *Chem. Abstr.*, **63**, 9615b (1965).
(69) J. Freel, W. J. M. Pieters, and R. B. Anderson, *J. Catal.*, **16**, 281 (1970).
(70) S. D. Robertson and R. B. Anderson, *J. Catal.*, **23**, 286 (1971).
(71) P. Fouilloux, G. A. Martin, A. J. Renouprez, B. Moraweck, B. Imelik, and M. Prettre, *J. Catal.*, **25**, 212 (1972).
(72) J. I. MacNab and R. B. Anderson, *J. Catal.*, **29**, 328 (1973).
(73) S. C. Davis and K. J. Klabunde, *J. Am. Chem. Soc.*, **100**, 5973 (1978).
(74) (a) S. C. Davis, S. Severson, and K. J. Klabunde, *J. Am. Chem. Soc.*, **103**, 3024 (1981). (b) K. J. Klabunde, H. F. Efner, T. O. Murdock, and R. Ropple, *J. Am. Chem. Soc.*, **98**, 1021 (1976).
(75) K. J. Klabunde, S. C. Davis, H. Hattori, and Y. Tanaka, *J. Catal.*, **54**, 254 (1978).
(76) (a) K. Matsuo and K. J. Klabunde, *J. Catal.*, **73**, 216 (1982). (b) K. J. Klabunde, D. H. Ralston, R. Zoellner, H. Hattori, and Y. Tanaka, *J. Catal.*, **55**, 213 (1978).
(77) B. A. Scott, R. M. Plecenik, G. S. Cargill, III, T. R. McGuire, and S. R. Herd, *Inorg. Chem.*, **19**, 1252 (1980).
(78) M. Harsdoff, *Thin Solid Films*, **32**, 103 (1976).
(79) J. F. Hamilton, *J. Phys. Colloq. (Orsay, Fr.)*, C2, 181 (1977).
(80) M. E. Behrndt, *J. Vac. Sci. Technol.*, **8**, 724 (1971).
(81) H. Levinstein, *J. Appl. Phys.*, **20**, 306 (1949).
(82) R. G. Picard and O. S. Duffendack, *J. Appl. Phys.*, **14**, 291 (1943).
(83) J. J. Stowell and T. E. Hutchinson, *Thin Solid Films*, **8**, 41 (1971).
(84) J. F. Hamilton, P. C. Logel, and R. C. Baetzold, *Thin Solid Films*, **32**, 233 (1976).
(85) J. A. Venables, *Philos. Mag.*, **27**, 697 (1973).
(86) R. C. Baetzold, *J. Appl. Phys.*, **47**, 3799 (1976).
(87) J. W. Geus, "Chemisorption and Reactions on Metallic Films", J. R. Anderson, Ed., Academic Press, New York, 1971, p 129.
(88) J. R. Anderson, B. G. Baker, and J. V. Sanders, *J. Catal.*, **1**, 443 (1962).

(89) W. E. Klotzbucher, S. A. Mitchell, and G. A. Ozin, *Inorg. Chem.*, 16, 3063 (1977).
(90) G. A. Ozin, *Acc. Chem. Res.*, 16, 21 (1977).
(91) E. P. Kundig, M. Moskovits and G. A. Ozin, *Nature (London)*, 254, 503 (1975).
(92) M. Moskovits and J. E. Hulse, *J. Chem. Soc., Faraday Trans. 2*, 73, 471 (1977).
(93) W. Schulze, H. U. Becker, and H. Abe, *Ber. Bunsenges. Phys. Chem.*, 82, 138 (1978).
(94) R. Busby, W. Klotzbücher, and G. A. Ozin, *J. Am. Chem. Soc.*, 98, 4013 (1976).
(95) J. R. Anderson and B. G. Baker, *J. Phys. Chem.*, 66, 482 (1962).
(96) D. W. McKee, *J. Phys. Chem.*, 67, 841 (1963).
(97) J. W. E. Coenen and B. C. Linsen, "Physical and Chemical Aspects of Adsorbents and Catalysts", B. G. Linsen, Ed., Academic Press, London, 1970, p 471.
(98) H. A. Smith, "Catalysis", P. H. Emmett, Ed., Reinhold, New York, 1957, p 175.
(99) G. K. Boreskov and A. P. Karnaukhov, *Zh. Fiz. Khim.* 26, 1814 (1952).
(100) J. M. Thomas and W. J. Thomas, "Introduction to the Principles of Heterogeneous Catalysis", Academic Press, New York, 1967.
(101) H. F. Schaefer, *Acc. Chem. Res.*, 10, 287 (1977).
(102) J. M. Basset and R. Ugo, "Aspects of Homogeneous Catalysis", Vol. 3, R. Ugo, Ed., D. Reidel, Dordrecht, Holland, 1977, p 137.
(103) N. I. Kobozev, *Acta Physicochim. USSR*, 9, 1 (1938).
(104) J. G. Allpress and J. V. Sanders, *Aust. J. Phys.*, 23, 23 (1970).
(105) M. R. Hoare and P. Bal, *Adv. Phys.*, 20, 161 (1971).
(106) J. R. Gaspard, *J. Phys. Colloq. (Orsay, Fr.)*, 2, 63 (1977).
(107) J. Friedel, *J. Phys. Colloq. (Orsay, Fr.)*, 2, 1 (1977).
(108) C. L. Briant and J. J. Burton, *Surf. Sci.*, 51, 345 (1975).
(109) P. Desai and J. T. Richardson, *J. Catal.*, 42, 294 (1976).
(110) J. H. Sinfelt, *CRC Crit. Rev. Solid State Sci.*, 4, 311 (1974).
(111) P. A. Sermon, *J. Catal.*, 24, 467 (1972).
(112) S. Ino, *J. Phys. Soc. Jpn.*, 21, 346 (1966).
(113) T. Komoda, Jap., *J. Appl. Phys.*, 7, 27 (1968).
(114) L. Harris, D. Jefferies, and B. Siegel, *J. Appl. Phys.*, 19, 791 (1948).
(115) K. Kimoto and I. Nishida, *J. Phys. Soc. Jpn.*, 22, 940 (1967).
(116) A. Yokozeki and G. D. Stein, *J. Appl. Phys.*, 49, 2224 (1978).
(117) N. R. Avery and J. V. Sanders, *J. Catal.*, 18, 129 (1970).
(118) J. G. Allpress and J. V. Sanders, *Surf. Sci.*, 7, 1 (1967).
(119) (a) P. Ganesan, H. K. Kuo, A. Saavedra, and R. J. DeAngelis, *J. Catal.*, 52, 310 (1978). (b) E. B. Prestridge and D. J. C. Yates, *Nature (London)*, 234, 345 (1971).
(120) J. J. Burton, *Catal. Rev.*, 9, 209 (1974).
(121) D. M. Washecheck, E. J. Wucherer, L. F. Dahl, A. Ceriotti, G. Longoni, M. Manassero, M. Sansoni, and P. Chini, *J. Am. Chem. Soc.*, 101, 6110 (1979).
(122) R. L. Rawls, *Chem. Eng. News*, 57, 30 (Nov. 12, 1979).
(123) G. L. Smith, T. P. Chojnacki, S. R. Dasgupta, K. Iwatate, and K. L. Waters, *Inorg. Chem.*, 14, 1419 (1975).
(124) (a) M. Ichikawa, *J. Chem. Soc., Chem. Commun.*, 11 (1976). (b) K. J. Klabunde, S. C. Davis, H. Hattori, and Y. Tanaka, *J. Catal.*, 54, 254 (1978).
(125) T. E. Whyte, Jr., *Catal. Rev.*, 8, 117 (1973).
(126) J. T. Richardson and R. J. Dubus, *J. Catal.*, 54, 207 (1978).
(127) M. Riassian, D. L. Trimm, and P. M. Williams, *J. Catal.*, 44, 320 (1976).
(128) N. Wada and M. Ichikawa, *Jpn. J. Appl. Phys.*, 15, 755 (1976).
(129) N. Wada, *J. Phys. Colloq. (Orsay, Fr.)*, 2, 219 (1977).
(130) J. T. Richardson and J. G. Crump, *J. Catal.*, 57, 417 (1979).
(131) P. C. Flynn and S. E. Wanke, *J. Catal.*, 34, 390 (1974).
(132) E. Ruckenstein and B. Pulvermacher, *AIChE J.*, 19, 356 (1973).
(133) E. Ruckenstein and B. Pulvermacher, *J. Catal.*, 29, 224 (1973).
(134) W. Leick, *Wied. Ann.*, 58, 691 (1896).
(135) J. Frenkel and J. Dorfman, *Nature (London)*, 126, 274 (1930).
(136) W. C. Elmore, *Phys. Rev.*, 54, 1092 (1938).
(137) C. Kittel, *Phys. Rev.*, 70, 965 (1946).
(138) C. P. Bean and J. D. Livingston, *J. Appl. Phys.*, 30, 1205 (1959).
(139) R. E. Dietz and P. W. Selwood, *J. Chem. Phys.*, 35, 270 (1961).
(140) C. P. Bean, *J. Appl. Phys.*, 26, 1381 (1955).
(141) P. W. Selwood, S. Adler, and T. R. Phillips, *J. Am. Chem. Soc.*, 77, 1462 (1955).
(142) P. W. Selwood, "Adsorption and Collective Paramagnetism", Academic Press, New York, 1962.
(143) J. A. Sabatka and P. W. Selwood, *J. Am. Chem. Soc.*, 77, 5799 (1955).
(144) L. E. Moore and P. W. Selwood, *J. Am. Chem. Soc.* 78, 697 (1956).
(145) P. W. Selwood, *J. Am. Chem. Soc.*, 78, 3893 (1956).

(146) E. G. Derouane, A. Simoens, C. Colin, G. A. Martin, J. A. Dalmon, and J. C. Védrine, *J. Catal.*, 52, 50 (1978).
(147) J. L. Carter and J. H. Sinfelt, *J. Phys. Chem.*, 70, 3003 (1966).
(148) J. L. Carter and J. H. Sinfelt, *J. Catal.*, 10, 134 (1968).
(149) J. I. MacNab and R. B. Anderson, *J. Catal.*, 29, 338 (1975).
(150) R. Kubo, *J. Phys. Colloq. (Orsay, Fr.)*, 2, 69 (1977).
(151) R. F. Marzke, *Catal. Rev.-Sci. Eng.*, 19, 43 (1979).
(152) G. S. Painter, P. J. Jennings, and R. O. Jones, *J. Phys. C*, 8, L199 (1975).
(153) R. O. Jones, P. J. Jennings, and G. S. Painter, *Surf. Sci.*, 53, 409 (1975).
(154) F. Cyrot-Lackman, M. C. Desjonqueres, and M. B. Gordon, *J. Phys. Colloq. (Orsay, Fr.)*, 2, 203 (1977).
(155) M. G. Mason, C. J. Gerenser, and S.-T. Lee, *Phys. Rev. Lett.*, 39, 288 (1977).
(156) J. F. Hamilton and R. C. Baetzold, *Science (Washington, D.C.)*, 205, 1213 (1979).
(157) T. Rhodin and D. Adams, *NATO Adv. Study Inst. Ser., Ser. B*, B16, 163 (1976).
(158) T. Rhodin and D. Adams, *NATO Adv. Study Inst. Ser. Ser. B*, B16, 1 (1976).
(159) A. B. Anderson and R. Hoffmann, *J. Chem. Phys.*, 61, 4545 (1974).
(160) H. S. Taylor, *Proc. R. Soc. London, Ser. A*, 108, 105 (1925).
(161) H. E. Farnsworth and R. F. Woodcock, *Adv. Catal.*, 9, 123 (1957).
(162) A. Clark, "The Theory of Adsorption and Catalysis", Academic Press, London, 1970.
(163) M. Boudart, A. W. Aldag, L. D. Ptak, and J. E. Benson, *J. Catal.*, 11, 35 (1968).
(164) M. Boudart, A. W. Aldag, J. E. Benson, N. A. Dougharty, and C. G. Harkins, *J. Catal.*, 6, 92 (1966).
(165) T. A. Dorling and R. L. Moss, *J. Catal.*, 5, 111 (1966).
(166) G. C. Bond, *NATO Adv. Study Inst. Ser., Ser. B*, B16, 523 (1976).
(167) G. A. Somorjai, *Science (Washington, D.C.)*, 201, 489 (1978).
(168) G. A. Somorjai, *Catal. Rev.-Sci. Eng.*, 18, 173 (1978).
(169) G. A. Somorjai, *Acc. Chem. Res.*, 9, 248 (1976).
(170) J. C. Buchholz and G. A. Somorjai, *Acc. Chem. Res.*, 9, 333 (1976).
(171) L. L. Kesmodel and G. A. Somorjai, *Acc. Chem. Res.*, 9, 392 (1976).
(172) G. A. Somorjai, *Angew. Chem.*, 16, 92 (1977).
(173) I. Toyoshima and G. A. Somorjai, *Catal. Rev.-Sci. Eng.*, 19, 105 (1979).
(174) G. A. Somorjai, *Pure Appl. Chem.* 50, 963 (1978).
(175) H. Leidheiser, Jr., and A. T. Gwathmey, *J. Am. Chem. Soc.*, 70, 1206 (1948).
(176) R. E. Cunningham and A. T. Gwathmey, *Adv. Catal.*, 9, 25 (1957).
(177) G. Malre, J. R. Anderson, and B. B. Johnson, *Proc. R. Soc., Ser. A*, 320, 227 (1970).
(178) P. Legare and G. Maire, *J. Chim. Phys. Phys-chim. Biol.*, 68, 1206 (1971).
(179) R. P. H. Gasser, *Q. Rev., Chem. Soc.*, 25, 223 (1971).
(180) T. A. Clarke, R. Mason, and M. Tescari, *Proc. R. Soc. London, Ser. A*, 331, 321 (1972).
(181) R. W. Joyner, B. Lang, and G. A. Somorjai, *J. Catal.*, 27, 405 (1972).
(182) S. L. Bernasek, W. J. Siekhaus, and G. A. Somorjai, *Phys. Rev. Lett.*, 30, 1202 (1973).
(183) J. McAllister and R. S. Hansen, *J. Chem. Phys.*, 59, 414 (1973).
(184) J. Block, H. Thimm, and M. S. Zei, *Ind. Chim. Belge*, 38, 392 (1973).
(185) P. C. Cartier and R. R. Rye, *J. Catal.*, 32, 88 (1974).
(186) E. W. Plummer, B. J. Waclawski, and T. V. Vorburger, *Chem. Phys. Lett.*, 28, 510 (1974).
(187) J. E. Demuth and D. E. Eastman, *Phys. Rev. Lett.*, 32, 1123 (1974).
(188) J. E. Demuth and T. N. Rhodin, *Surf. Sci.*, 45, 249 (1974).
(189) H. Conrad, G. Ertl, J. Koch, and E. E. Latta, *Surf. Sci.*, 43, 462 (1974).
(190) Y. Iawasawa, R. Mason, M. Textor, and G. A. Somorjai, *Chem. Phys. Lett.*, 44, 468 (1976).
(191) S. P. Singh-Boparai, M. Bowker, and D. A. King, *Surf. Sci.*, 53, 55 (1975).
(192) R. W. McCabe and L. D. Schmidt, *Surf. Sci.*, 66, 101 (1977).
(193) K. Christmann, G. Ertl, and T. Pignet, *Surf. Sci.*, 54, 365 (1976).
(194) R. J. Gale, M. Salmeron, and G. A. Somorjai, *Phys. Rev. Lett.*, 38, 1027 (1977).
(195) M. Salmeron, R. J. Gale, and G. A. Somerjai, *J. Chem. Phys.*, 67, 5324 (1977).
(196) E. Ruckenstein and M. L. Malhotra, *J. Catal.*, 41, 303 (1976).
(197) K. Baron, D. W. Blakely, and G. A. Somorjai, *Surf. Sci.*, 41, 45 (1974).
(198) L. L. Kesmodel, P. C. Stair, R. C. Baetzold, and G. A. Somorjai, *Phys. Rev. Lett.*, 36, 1316 (1976).

(199) P. C. Stair and G. A. Somorjai, *Chem. Phys. Lett.*, **41**, 391 (1976).
(200) L. L. Kesmodel, L. H. Dubois, and G. A. Somorjai, *Chem. Phys. Lett.*, **56**, 267 (1978).
(201) J. E. Demuth and D. E. Eastman, *Phys. Rev. B*, **13**, 1523 (1976).
(202) C. Brucker and T. Rhodin, *J. Catal.*, **47**, 214 (1977).
(203) G. Casalone, M. G. Cattania, M. Simonetta, and M. Tescari, *Surf. Sci.*, **62**, 321 (1977).
(204) F. C. Schouten, E. W. Kaleveld, and G. A. Bootsma, *Surf. Sci.*, **63**, 460 (1977).
(205) D. R. Kahm, E. E. Petersen and G. A. Somorjai, *J. Catal.*, **34**, 294 (1974).
(206) D. W. Blakely and G. A. Somorjai, *J. Catal.*, **42**, 186 (1976).
(207) Y. W. Tsang and L. M. Falicov, *J. Phys. C*, **9**, 51 (1976).
(208) J. R. Anderson and B. G. Baker, "Chemisorption and Reactions on Metallic Films", Vol. 2, J. R. Anderson, Ed., Academic Press, New York, 1971, p 63.
(209) E. F. McCoy and R. St. C. Smart, *Surf. Sci.*, **39**, 109 (1973).
(210) B. A. Sexton and G. A. Somorjai, *J. Catal.*, **46**, 167 (1977).
(211) K. C. Campbell, J. R. Fryer and K. G. Gray, *Surf. Sci.*, **33**, 198 (1972).
(212) G. Blyholder and R. W. Sheets, *J. Catal.*, **39**, 152 (1975).
(213) O. Beeck, *Discuss. Faraday Soc.*, **8**, 118 (1950).
(214) G. I. Jenkins and S. E. Rideal, *J. Chem. Soc.*, 2490 (1955).
(215) J. Wojtczak, R. Queau, and R. Poilblanc, *J. Catal.*, **37**, 391 (1975).
(216) M. Araki and V. Ponec, *J. Catal.*, **44**, 439 (1976).
(217) C. Kemball, *Proc. R. Soc. London, Ser. A*, **223**, 377 (1954).
(218) F. G. Gault, J. J. Rooney, and C. Kemball, *J. Catal.*, **1**, 255 (1962).
(219) W. G. Young, R. L. Meier, J. Vinograd, H. Bollinger, L. Kaplan, and S. L. Linden, *J. Am. Chem. Soc.*, **69**, 2046 (1947).
(220) J. R. Anderson and N. R. Avery, *J. Catal.*, **2**, 542 (1963).
(221) J. R. Anderson and N. R. Avery, *J. Catal.*, **5**, 446 (1966).
(222) J. R. Anderson and N. R. Avery, *J. Catal.*, **7**, 315 (1967).
(223) J. F. Taylor and J. K. A. Clarke, *Z. Phys. Chem. (Wiesbaden)*, **103**, 216 (1976).
(224) J. R. Anderson and R. J. MacDonald, *J. Catal.*, **19**, 227 (1970).
(225) J. R. Anderson, R. J. MacDonald, and Y. Shimoyama, *J. Catal.*, **20**, 147 (1971).
(226) R. S. Dowie, D. A. Whan, and C. Kemball, *J. Chem. Soc., Faraday Trans. 1*, **68**, 2150 (1972).
(227) R. Merta and V. Ponec, *J. Catal.*, **17**, 79 (1970).
(228) J. R. Anderson and B. G. Baker, *Nature (London)*, **187**, 937 (1960).
(229) H. Matsumoto, Y. Saito and Y. Yoneda, *J. Catal.*, **22**, 182 (1971).
(230) G. A. Martin, *J. Catal.*, **60**, 345 (1979).
(231) F. Vander Heijden and J. J. F. Scholten, *Delft. Progr. Rep., Ser. A*, **1**, 45 (1974).
(232) D. W. McKee, *J. Catal.*, **8**, 240 (1967).
(233) D. W. McKee, *J. Am. Chem. Soc.*, **84**, 4427 (1962).
(234) A. Frennet, L. Degols, G. Lienard, and A. Crucq, *J. Catal.*, **35**, 18 (1974).
(235) J. H. Sinfelt, *Catal. Rev.-Sci. Eng.*, **3**, 175 (1969).
(236) D. F. Ollis and H. Taheri, *AIChE J.*, **22**, 1112 (1976).
(237) Z. Paal and P. Tétényi, *Nature (London)*, **267**, 234 (1977).
(238) R. Van Hardeveld and A. Van Montfoort, *Surf. Sci.*, **4**, 396 (1966).
(239) P. R. Wentrcek, B. J. Wood, and H. Wise, *J. Catal.*, **43**, 363 (1976).
(240) J. A. Rabo, A. P. Risch, and M. L. Poutsma, *J. Catal.*, **53**, 295 (1978).
(241) K. Morikawa, W. S. Benedict, and H. S. Taylor, *J. Am. Chem. Soc.*, **58**, 1445 (1936).
(242) G. A. Martin and B. Imelik, *Surf. Sci.*, **42**, 157 (1974).
(243) K. Morikawa, W. S. Benedict, and H. S. Taylor, *J. Am. Chem. Soc.*, **58**, 1795 (1936).
(244) K. Morikawa, N. R. Trenner, and H. S. Taylor, *J. Am. Chem. Soc.*, **59**, 1103 (1937).
(245) C. Kemball and H. S. Taylor, *J. Am. Chem. Soc.*, **70**, 345 (1948).
(246) J. L. Carter, J. A. Cusumano, and J. H. Sinfelt, *J. Phys. Chem.*, **70**, 2257 (1966).
(247) D. J. C. Yates and J. H. Sinfelt, *J. Catal.*, **8**, 348 (1967).
(248) E. Kikuchi, M. Tsurumi, and Y. Morita, *J. Catal.*, **22**, 226 (1961).
(249) C. Corolleur, F. G. Gault, D. Juttard, G. Maire, and J. M. Muller, *J. Catal.*, **27**, 466 (1972).
(250) C. Corolleur, S. Corolleur, and F. G. Gault, *J. Catal.*, **24**, 385 (1972).
(251) C. Corolleur, D. Tomanova, and F. G. Gault, *J. Catal.*, **24**, 401 (1972).
(252) G. Leclercq, L. Leclercq, and R. Maurel, *J. Catal.*, **50**, 87 (1977).
(253) O. Kuleli and F. Cecen, *Fuel*, **57**, 46 (1978).
(254) C. J. Machiels and R. B. Anderson, *J. Catal.*, **58**, 260 (1979).

(255) C. J. Machiels and R. B. Anderson, *J. Catal.*, **58**, 268 (1979).
(256) V. B. Kazansky, V. Yu. Borovkov, and G. M. Zhidominov, *J. Catal.*, **39**, 205 (1975).
(257) A. K. Smith, F. Hughes, A. Theolier, J. M. Basset, R. Ugo, G. M. Zanderighi, J. L. Bilhou, V. Bilhou-Bougnol, and W. F. Graydon, *Inorg. Chem.*, **18**, 3104 (1979).
(258) A. K. Smith, A. Theolier, J. M. Basset, R. Ugo, D. Commereuc, and Y. Chauvin, *J. Am. Chem. Soc.*, **100**, 2590 (1978).
(259) G. N. Schrauzer, "Transition Metals in Homogeneous Catalysis", Marcel-Dekker, New York, 1971.
(260) C. U. Pittman and R. C. Ryan, *CHEMTECH*, **8**, 170 (1978).
(261) R. Crabtree, *Acc. Chem. Res.*, **12**, 331 (1979).
(262) E. L. Muetterties and J. R. Bleeke, *Acc. Chem. Res.*, **12**, 324 (1979).
(263) (a) R. H. Crabtree, J. M. Mihelcic, and J. M. Quirk, *J. Am. Chem. Soc.*, **101**, 7738 (1979). (b) D. Baudry, M. Ephritikhine, and H. Felkin, *J. Chem. Soc., Chem. Commun.*, 1243 (1980).
(264) T. E. Whitesides and R. A. Budnik, *J. Chem. Soc., Chem. Commun.*, 87 (1973).
(265) K. J. Klabunde, B. B. Anderson, M. Bader, and L. J. Radonovich, *J. Am. Chem. Soc.*, **100**, 1313 (1978).
(266) G. W. Parshall, *Acc. Chem. Res.*, **8**, 113 (1975).
(267) U. Klabunde and G. W. Parshall, *J. Am. Chem. Soc.*, **94**, 9081 (1972).
(268) J. L. Garnett, M. A. Long, and K. B. Peterson, *Aust. J. Chem.*, **27**, 1823 (1974).
(269) D. E. Webster, *Adv. Organomet. Chem.*, **15**, 147 (1977).
(270) A. E. Shilov and A. A. Shteinman, *Coord. Chem. Rev.*, **24**, 97 (1977).
(271) (a) E. L. Muetterties, T. N. Rhodin, E. Band, C. F. Brucker, and W. R. Pretzer, *Chem. Rev.*, **79**, 91 (1979). (b) R. B. Calvert and J. R. Shapley, *J. Am. Chem. Soc.*, **99**, 5225 (1977).
(272) G. A. Ozin and A. Vander Voet, *Prog. Inorg. Chem.*, **19**, 105 (1975).
(273) M. Moskovits and G. A. Ozin, *Vib. Spectra Struct.*, **4**, 187 (1975).
(274) G. A. Ozin and W. J. Power, *Ber. Bunsenges. Phys. Chem.*, **82**, 105 (1978).
(275) G. A. Ozin and W. J. Power, *Ber. Bunsenges. Phys. Chem.*, **82**, 93 (1978).
(276) M. Moskovits, *Acc. Chem. Res.*, **12**, 229 (1979).
(277) R. G. Gastinger and K. J. Klabunde, *Transition Met. Chem. (Weinheim, Ger.)*, **4**, 1 (1979).
(278) H. F. Efner, W. B. Fox, R. R. Smardzewski, and D. E. Tevault, *Inorg. Chim. Acta*, **24**, L93 (1977).
(279) H. F. Efner, D. E. Tevault, W. B. Fox, and R. R. Smardzewski, *J. Organomet. Chem.*, **146**, 45 (1978).
(280) B. A. Scott, private communications. (Also see ref 77.)
(281) S. C. Davis Ph.D. Thesis, University of North Dakota, 1980 (also see ref 73 and 74).
(282) D. L. Williams-Smith, L. R. Wolf, and P. S. Skell, *J. Am. Chem. Soc.*, **94**, 4042 (1972).
(283) R. J. Remick, T. A. Asunta, and P. S. Skell, *J. Am. Chem. Soc.*, **101**, 1320 (1979).
(284) J. Allison, R. B. Freas, and D. P. Ridge, *J. Am. Chem. Soc.*, **101**, 1332 (1979).
(285) P. H. Barrett, M. Pasternak, and R. G. Pearson, *J. Am. Chem. Soc.*, **101**, 222 (1979).
(286) W. E. Billups, M. M. Konarski, R. H. Hauge, and J. L. Margrave, *J. Am. Chem. Soc.*, **102**, 7393 (1980).
(287) R. J. Madix, *Acc. Chem. Res.*, **12**, 265 (1979).
(288) B. E. Nieuwenhuys, *Thin Solid Films*, **50**, 257 (1978).
(289) (a) S. Brunauer, P. H. Emmett and E. Teller, *J. Am. Chem. Soc.*, **60**, 309 (1938). (b) For an excellent review and summary, see S. Lowell, "Introduction to Powder Surface Area", Wiley-Interscience; New York, 1979.
(290) J. I. Langford and A. J. C. Wilson, *J. Appl. Crystallogr.*, **11**, 102 (1978).
(291) B. E. Warren, *J. Appl. Phys.*, **12**, 375 (1941).
(292) W. Heukelom, J. J. Broeder, and L. L. van Reijen, *J. Chem. Phys.*, **54**, 474 (1957).
(293) W. Trzebiatowski and W. Romanowski, *Rocz. Chem.*, **31**, 1123 (1957).
(294) D. F. Klemperer, "Chemisorption and Reactions on Metallic Films", J. R. Anderson, Ed., Academic Press, New York, 1971, p 39.
(295) J. Erkelens, *J. Catal.*, **37**, 332 (1975).
(296) R. J. Cvetanovic, *Prepr., Div. Petrol. Chem., Am. Chem. Soc.*, **17**, C-77 (1972).
(297) K. J. Klabunde, H. F. Efner, T. O. Murdock, and R. Roppel, *J. Am. Chem. Soc.*, **98**, 1021 (1976).
(298) T. O. Murdock and K. J. Klabunde, *J. Org. Chem.*, **41**, 1076 (1976).
(299) K. J. Klabunde, S. C. Davis, H. Hattori, and Y. Tanaka, *J. Catal.*, **54**, 254 (1978).
(300) D. Schriver, "Manipulation of Air Sensitive Compounds", McGraw-Hill, New York, 1969.
(301) S. J. Severson, unpublished results.

(302) R. C. Weast, Ed., "Handbook of Chemistry and Physics", 56th ed., Chemical Rubber Co., Cleveland, OH, 1968, p E-120.
(303) G. C. Bond and P. B. Wells, *Adv. Catal.*, 15, 91 (1964).
(304) E. F. Meyer and R. L. Burwell, Jr., *J. Am. Chem. Soc.*, 85, 2881 (1963).
(305) K. J. Klabunde, *Acc. Chem. Res.*, 8, 393 (1975).
(306) F. Daniels, J. H. Mathews, J. W. Williams, P. Bender, and R.

A. Alberty, "Experimental Physical Chemistry", 5th ed., McGraw-Hill, New York, 1956, p 230.
(307) W. A. Dietz, *J. Gas Chromatography*, 5, 68 (1967).
(308) H. Hattori, Y. Tanaka and K. Tanabe, *J. Am. Chem. Soc.*, 98, 4652 (1976).
(309) J. W. Hastie, R. H. Hauge, and J. L. Margrave, *High Temp. Sci.*, 1, 76 (1969).